

**PARTIAL PURIFICATION AND CHARACTERIZATION OF
ARYLAMINE N-ACETYLTRANSFERASES FROM
HUMAN BREAST TUMOR TISSUES**

**A THESIS SUBMITTED TO
THE GRADUATE SCHOOL OF NATURAL AND APPLIED SCIENCES
OF
MIDDLE EAST TECHNICAL UNIVERSITY**

BY

YAŞASIN SENEM SU

**IN PARTIAL FULFILLMENT OF THE REQUIREMENTS
FOR
THE DEGREE OF DOCTOR OF PHILOSOPHY
IN
BIOCHEMISTRY**

JANUARY 2006

Approval of the Graduate School of Natural and Applied Sciences

Prof. Dr. Canan Özgen
Director

I certify that this thesis satisfies all the requirements as a thesis for the degree of Doctor of Philosophy.

Prof. Dr. Orhan Adalı
Head of the Department

This is to certify that we have read this thesis and that in our opinion it is fully adequate, in scope and quality, as a thesis for the degree of Doctor of Philosophy.

Prof. Dr. Tülin Güray
Supervisor

Examining Committee Members:

Prof. Dr. Meral Yücel (METU, BIO) _____

Prof. Dr. Tülin Güray (METU, BIO) _____

Prof. Dr. Zümrüt Ögel (METU, FDE) _____

Prof. Dr. Mesude İşcan (METU, BIO) _____

Prof. Dr. Kamer Kılınç (Hacettepe Univ., BIOCHEM) _____

I hereby declare that all information in this document has been obtained and presented in accordance with academic rules and ethical conduct. I also declare that, as required by these rules and conduct, I have fully cited and referenced all material and results that are not original to this work.

Name, Last name: YAŞASIN SENEM SU

Signature:

ABSTRACT

PARTIAL PURIFICATION AND CHARACTERIZATION OF ARYLAMINE N-ACETYLTRANSFERASES FROM HUMAN BREAST TUMOR TISSUES

Su, Yaşasın Senem

Ph.D., Department of Biochemistry

Supervisor: Prof. Dr. Tülin Güray

January 2006, 122 pages

Arylamine N-acetyltransferases (NATs) were partially purified from human breast tumor tissues with complete separation of the isoforms in DEAE-Cellulose ion-exchange step. NAT with activity towards p-aminobenzoic acid (PABA) was isolated and purified from human breast tumor with 77 % yield and a purification factor of 5-fold. NAT with activity towards sulfamethazine (SMZ) was isolated and purified from human breast tumor with 21 % yield and a purification factor of 3-fold. Further purification attempts by Blue Sepharose affinity column chromatography resulted in the complete loss of both enzyme activities. The NAT1 purified from human breast tumor tissues had a molecular weight (M_r) value of about 27600 and an isoelectric point (pI) around 4.8, as confirmed by SDS-PAGE, IEF and Western blotting analysis. With immunohistochemical analysis, level of intensity of NAT1 immunostaining was observed to be going from weak in reduction mammoplasty samples to strongest in malignant breast tissue.

The interindividual variation in the conjugation of p-aminobenzoic acid (PABA) and of sulfamethazine (SMZ) by cytosolic arylamine N-acetyltransferases (NATs) were investigated in 30 human breast tumor and matched samples. The average specific activity against PABA was calculated as 13 ± 2 pmole/min/mg protein for breast control NATs, and 20 ± 3 pmole/min/mg protein for breast tumor NATs. The average specific activity against SMZ was calculated as 12 ± 2 pmole/min/mg protein for breast control NATs, and 34 ± 6 pmole/min/mg protein for breast tumor NATs. Wilcoxon test revealed that the difference between the control and tumor groups is statistically significant with respect to the NAT1 activities as well as NAT2 activities. In three (3/30, 10%) patients tumor and tumor-free breast tissue NAT1 activity was not detectable. Among control tissues, the percentage of measurable NAT2 activity was 77% (23/30), while in tumor tissues it increased to 91%. Chemotherapy treatment was observed to have a slight inhibitory effect on mean NAT1 and NAT2 activities. There was an indication of a possible negative association with mean NAT1 activity and estrogen receptor status, while mean tumor NAT2 activity was observed to increase among estrogen receptor positive patients.

Grade of malignancy seems to be positively associated with NAT1, but no such association could be suggested for NAT2 enzyme. Menopausal state of the patient was suggested to have a significant effect on NAT2 activity.

Genotype determination of NATs revealed that NAT1*4 and NAT2*5A allele being most common among 10 breast cancer patients. NAT1*11 allele was prevalent among postmenopausal women. The putative rapid NAT1 genotypes was found to display lower control and tumor mean NAT1 activities compared to normal NAT1 genotypes. Among slow NAT2 acetylators, mean tumor NAT2 activities was found to be significantly higher than respective controls.

Key Words: N-acetyltransferases, Breast Cancer, Polymorphism, Purification, Western Blotting, Isoelectrofocusing

ÖZ

İNSAN MEME TÜMÖRÜ DOKULARINDAN ARILAMIN N-ASETİLTRANSFERAZLAR'IN KISMİ SAFLAŞTIRILMASI VE KARAKTERİZASYONU

Su, Yaşasın Senem

Doktora, Biyokimya Bölümü

Danışman: Prof. Dr. Tülin Güray

Ocak 2006, 122 Sayfa

Arilamin N-asetiltransferazlar (NATlar) insanda kanserli meme dokusundan, DEAE-selülöz iyon-değişim kolon kromatografisiyle birbirinden bağımsız izoformlar halinde kısmi olarak saflaştırılmıştır. p-Aminobenzoik asid'e (PABA) karşı aktivite gösteren NAT, insan tümörlü meme dokusundan % 77 verim ve 5-kat saflaştırma faktörü ile saflaştırılmıştır. Sulfametazin'e (SMZ) karşı aktivite gösteren NAT, insan tümörlü meme dokusundan % 21 verim ve 3-kat saflaştırma faktörü ile saflaştırılmıştır. İnsan tümörlü meme dokusundan saflaştırılmış NAT1 izoziminin molekül ağırlığı yaklaşık olarak 27600 ve izoelektrik noktasının da 4.8 civarında olduğu SDS-PAGE, IEF ve Western Blot analizleri ile gösterilmiştir. İmmunohistokimyasal analiz sonucunda, NAT1'in boyanma miktarının meme küçültme ameliyatlarından alınan örneklerde az, tümörlü meme dokusunda fazla olduğu gözlenmiştir.

PABA ve SMZ'nin sitozolik NATlar ile in vitro konjugasyonları 30 hastadan alınan tümörlü meme ve aynı hastalardan alınan normal dokularda incelendi. Kontrol meme dokularında PABA ve SMZ substratına karşı NAT özgül aktivitesi sırasıyla, 13 ± 2 ve 12 ± 2 pmole/dak/mg protein olarak, kanserli dokularda ise 20 ± 3 ve 34 ± 6 pmole/dak/mg protein olarak saptandı. Wilcoxon testi, kontrol ve tümör gruplarındaki NAT1 ve NAT2 aktiviteleri arasındaki farkın istatistiksel olarak anlamlı olduğunu göstermiştir. Üç hastanın (3/30, % 10) tümörlü ve normal meme dokusunda NAT1 aktivitesi tespit edilememiştir. Kontrol dokularının % 77'sinde, tümörlü meme dokularının ise % 91'inde NAT2 aktivitesi ölçülebilmektedir. Kemoterapi tedavisinin, ortalama NAT1 ve NAT2 aktivitelerini düşük miktarda inhibe ettiği gözlenmiştir. Östrojen reseptör statüsünün ortalama NAT1 aktivitesi ile muhtemel, negatif ve NAT2 aktivitesi ile de pozitif ilişkisi olduğu gösterilmiştir. Tümörün derecesi, NAT1 ile pozitif şekilde ilişkilendirilmiş fakat NAT2 ile böyle bir

baęlantı bulunamamıştır. Hastaların menopozal durumlarının NAT2 aktivitesi üzerinde önemli bir etkisi olduęu öne sürülmüştür.

On meme kanserli hastada yapılan genotip deęerlendirmesinde NAT1*4 ve NAT2*5A 'nın en sık rastlanan aleller olduęu görülmüştür. NAT1*11 aleline postmenopozal kadınlarda daha fazla rastlanmıştır. Hızlı olduęu düşünölen NAT1 genotiplerinin, kontrol ve tümörlü meme dokularındaki ortalama NAT1 aktivitelerinin, normal NAT1 genotiplerine göre daha düşük olduęu saptanmıştır. NAT2 yavaş asetilatör grubundaki tümör NAT2 ortalama aktivitesinin kontrole göre daha yüksek olduęu istatistiksel olarak gösterilmiştir.

Anahtar kelimeler: N-asetiltransferazlar, Meme Kanseri, Polimorfizm, Saflaştırma, Western Blot, İzoelektrik Fokuslama.

TO MY MOTHER, İLKİN

ACKNOWLEDGEMENTS

I would like to express my deepest gratitude to Prof. Dr. Tülin Güray. She has always been a great mentor with her encouragement, valuable advises and continued guidance throughout this study. She is a wonderful person encouraging you to achieve the best you can in any field by setting a good example herself.

I would like to thank Prof. Dr. Mesude İscan, she is also a wonderful scientist. Dr. Tülin Güray and Dr. Mesude İscan have been a second family to all of us. My thanks are also extended Prof. Dr. Zümrüt Ögel for her valuable advises. I wish to express my thanks to Prof. Dr. Meral Yücel and Prof. Dr. Kamer Kılınç for their valuable suggestions and corrections.

I am thankful to Prof. Dr. Ragıp Çam for providing the breast tissues, also Prof. Dr. Serpil Sak in helping about the classification of the tissues. My thanks are extended to wonderful pathologists, Dr. Sibel, Dr. Gülşah, Dr. Berna and many others working in the frozen section of İbni Sina Hospital who saved the breast tissues in the freezer and kept their records for me.

I am grateful to Dr. E. Sim for providing the polyclonal antibody for NAT1. It was a wonderful opportunity to work in her laboratory, Oxford University, UK. Fiona, Larissa Wakefield and Valerie Cornish have given valuable support during the experiments and have been very good friends.

I would like to thank Ebru Saatçi, Gökhan Sadi, Metin Konuş, Pembegül Uyar, Can Yılmaz, Belgin İşgör, Ayçin Atalay, Elif Güler, Ebru Özgür, Serpil Oğuztüzün and Awni Abuhijleh for making the long hours spent in the laboratory enjoyable, we had a great time together. I should mention that Metin, Gökhan and Can; besides becoming the valuable scientists of the future, they have the ability to fix and repair almost anything including a fraction collector. Gökhan even manages to locate the extra (!) nails in the fraction collector. Pembegül has been very helpful in getting the immunostained breast tissue section pictures from the computer. I want to thank Serpil who was so generous to share her knowledge on immunohistochemical analyses and for her valuable advises.

Finally, I would like to express my sincere gratitude to my family for their great support, patience and encouragement during the long period of my study. I guess without them, it could not have been possible. My lovely parents, İlkin-Muammer Geylan and Ali-Hesna Su, my dearest son, Emil and my life-long partner, Erkan; I love you all very much and would like to thank for always being there for me.

TABLE OF CONTENTS

PLAGIARISM.....	iii
ABSTRACT.....	iv
ÖZ.....	vi
DEDICATION.....	viii
ACKNOWLEDGEMENTS.....	ix
TABLE OF CONTENTS.....	xi
LIST OF TABLES.....	xiv
LIST OF FIGURES.....	xv
LIST OF ABBREVIATIONS.....	xvi
CHAPTERS	
1. INTRODUCTION.....	1
1.1. Acetyl Coenzyme A: arylamine N-acetyltransferases (NATs).....	1
1.1.1. Reaction mechanism of NATs.....	2
1.1.2. Structure of NATs.....	4
1.1.3. Substrates of NATs.....	7
1.1.4. Species and Tissue-specific Distribution of NATs.....	9
1.1.5. Purification and Biochemical Characteristics of NATs.....	10
1.2. Genetics of NATs.....	12
1.2.1. Gene Families Encoding Cytosolic NATs.....	12
1.2.2. Localization, Structure and Expression of NATs Genes.....	14
1.2.3. NAT1 Allelic Variants.....	15
1.2.4. NAT2 Allelic Variants.....	19
1.2.5 Nomenclature and Classification of NATs.....	22
1.3 Breast Cancer and NATs.....	23
1.3.1 General Anatomy of the Human Breast Tissue.....	23
1.3.2 Breast Cancer.....	23
1.3.2.1 Classification of Breast Cancers.....	23
1.3.2.2 Non-invasive Cancers of the Breast.....	24

1.3.2.3 Invasive Cancers of the Breast.....	24
1.3.2.3.1 Invasive Ductal Cancer (NST).....	25
1.3.2.3.2 Invasive Lobular Cancer.....	25
1.3.3 General Risk Factors for Breast Cancer.....	26
1.3.4 Role of NATs in Breast Cancer.....	28
1.4 Scope of the work.....	29
2. MATERIALS AND METHODS.....	30
2.1 Materials.....	30
2.2 Methods.....	31
2.2.1 Collection of Human Breast Tissue Specimens.....	31
2.2.2 Preparation of Human Breast Tissue Cytosols.....	31
2.2.3 Protein Determinations.....	32
2.2.4 Determination of Human Breast NATs Activities.....	32
2.2.5 Purification of NATs from Human Breast Tissues.....	33
2.2.5.1 Ion-Exchange Column Chromatography on DEAE-Cellulose...33	
2.2.5.2. Affinity Column Chromatography on Blue Sepharose.....34	
2.2.6 SDS-Polyacrylamide Gel Electrophoresis (SDS-PAGE).....	35
2.2.6.1 Electrophoresis Procedure.....	35
2.2.6.2 Electroblotting of SDS-PAGE Gels.....	38
2.2.6.3 Silver Staining of SDS-PAGE Gels.....	39
2.2.7 Isoelectric Focusing on Polyacrylamide Gels	41
2.2.7.1 Coomassie Blue Staining of IEF-PAGE Gels.....	43
2.2.7.2 Electroblotting of IEF-PAGE Gels.....	43
2.2.8 Immunostaining of Nitrocellulose Membranes.....	43
2.2.9 Immunohistochemical Detection of NAT1 in Human Breast Tissues.....	44
2.2.10 Preparation of Genomic DNA from Human Breast Tissues.....	46
2.2.11 Polymerase Chain Reaction for Genotype Determination of NATs...47	
2.2.11.1 Human NAT1* Alleles.....	48
2.2.11.2 Human NAT2* Alleles.....	53
2.2.12 Statistical Analysis.....	56
3. RESULTS.....	57
3.1 Purification of NATs.....	58

3.1.1 Ion-Exchange Column Chromatography on DEAE-Cellulose.....	58
3.1.2 Affinity Column Chromatography on Blue Sepharose.....	61
3.1.3 SDS-PAGE, Isoelectric Focusing (IEF) and Western Blotting.....	62
3.1.4 Immunohistochemical Detection of NAT1 in Human Breast Tissues.....	65
3.1.4.1 Optimization for Immunohistochemical Staining for Human Breast Tissues.....	65
3.1.4.2 Immunohistochemical Staining of NAT1 from Human Breast Tissue.....	65
3.2 Human Breast Tumor and Tumor-free NAT1 and NAT2 Activities.....	71
3.3 Genotype Determination of NATs.....	74
4. DISCUSSION.....	83
REFERENCES.....	90
APPENDICES	
A. Preparation of SDS-PAGE Solutions.....	103
B. Questionnaire on Breast Cancer Risk Factors.....	105
CURRICULUM VITAE.....	106

LIST OF TABLES

Table 1 Human NAT1 Alleles.....	16
Table 2 Human NAT2 Allelic Variants.....	20
Table 3 Molecular Weight Standards for SDS-PAGE.....	35
Table 4 Formulations for SDS-PAGE separating and stacking gels.....	37
Table 5 Rapid Silver Staining of Proteins in Polyacrylamide Gels.....	40
Table 6 Formulation of the IEF polyacrylamide gel.....	41
Table 7 Immunohistochemical staining protocol for NAT1 in human breast tissues.....	45
Table 8 Primers used for the amplification of the NAT1*gene.....	49
Table 9 Restriction fragments generated by MboII digestion.....	50
Table 10 NAT1* Alleles amplified with N769/ N1110a, and N769/ N1110b.....	51
Table 11 NAT1* Alleles amplified with N539 and N713.....	51
Table 12 NAT1* Alleles amplified with N-376 and N1176.....	52
Table 13 NAT1* Alleles amplified with N2 and N850.....	53
Table 14 Primers used to amplify the NAT2* gene for determination of NAT*genotype.....	54
Table 15 Purification of NATs from human breast tumor tissues.....	59
Table 16 Arylamine NATs activities in tumors and surrounding tumor-free breast tissues of 30 breast cancer patients with infiltrating ductal cancer.....	72
Table 17 Variables with the susceptibility of breast cancer among 10 breast cancer patients.....	75
Table 18 NAT1 and NAT2 allele distributions among 10 breast cancer patients.....	76
Table 19 Genotype distributions of NAT1 and NAT2 among 10 breast cancer patients	80
Table 20 Genotype and phenotype of NATs from 10 breast cancer patients.....	81
Table 21 Comparison of genotype and phenotype of NATs in breast cancer patients.....	82

LIST OF FIGURES

Figure 1 Reaction mechanism of arylamine N-acetyltransferases.....	3
Figure 2 Structure of the catalytic N-terminal domains of <i>Sr</i> NAT, human NAT1, and human NAT2.....	5
Figure 3 Structural alignment of the catalytic cores of human NAT1 and NAT2.....	6
Figure 4 Structural analysis of the active-site loop of NATs.....	8
Figure 5 Phylogenetic tree for the NATs.....	13
Figure 6 General anatomy of the breast.....	24
Figure 7 Stepwise genotyping procedure used in identification of the human NAT1* alleles.....	48
Figure 8 PCR Primers used in the amplification of the NAT1* gene to determine NAT1* genotype.....	49
Figure 9 Stepwise genotyping procedure used in identification of the human NAT2* alleles.....	54
Figure 10 PCR Primers used in the amplification of the NAT1* gene to determine NAT2* genotype.....	56
Figure 11 Purification Profile of Human Breast Cytosolic NATs on Ion Exchange Column (1.5 X 10 cm) of DEAE-Cellulose.....	60
Figure 12 Protein Profile of Human Breast Tumor Cytosolic NATs on Blue Sepharose Column Chromatography.....	61
Figure 13 SDS-PAGE stained with silver (12 %), of the breast tumor purification fractions and molecular weight markers.....	64
Figure 14 SDS-PAGE stained with silver (12 %), of the breast control purification fraction and molecular weight markers.....	65
Figure 15 Western blotting of the purification fraction.....	66
Figure 16 Typical molecular weight standard curve (12 % SDS-PAGE).....	67
Figure 17 Isoelectric focusing of the cytosolic fractions from breast control and tumor.....	68
Figure 18 Immunohistochemical staining for NAT1.....	69
Figure 19 Examples of PCR and RFLP used to determine NAT1* Genotype.....	77
Figure 20 Examples of PCR and RFLP used to determine NAT2* Genotype.....	78

LIST OF ABBREVIATIONS

AcCar	Acetylcarnitine
AcCoA	Acetyl Coenzyme A
AP	Alkaline phosphatase
APS	Ammonium persulfate
AS	Ammonium sulfate
BCIP	5-Bromo-4-chloro-3-indolyl phosphate
Bis	N,N'-methylene bisacrylamide
BSA	Bovine serum albumin
CAT	Carnitine acetyltransferase
DMAB	Dimethylaminobenzaldehyde
DTT	Dithiothreitol
EDTA	Ethylenediaminetetraacetic acid
gDNA	Genomic DNA
HRP	Horse-Radish peroxidase
INH	Isoniazid
Mes	2-Morpholinoethanesulfonic acid
MOPS	(N-morpholino) propane sulfonic acid
NAT	N-acetyltransferase
NO-MeIQ	N-OH-2-amino-3-methyl imidazo [4, 5-f] quinoline
NO-PhIP	N-OH-2-amino-1-methyl-6-phenylimidazo[4,5-b] pyridine
PABA	p-Aminobenzoic acid
PMSF	Phenylmethylsulfonylfluoride
SDS	Sodium dodecyl sulfate
SDS-PAGE	SDS-Polyacrylamide gel electrophoresis
SMZ	Sulfamethazine
TBS	Tris-buffered saline
TBST	Tris-buffered saline with Tween-20
TCA	Trichloroacetic acid
TE	Tris-EDTA
TEMED	N,N,N',N'-tetramethylethylenediamine
Tris	Tris(hydroxymethyl) aminomethane
TBST	Tris-buffered saline containing Tween-20

CHAPTER 1

INTRODUCTION

1.1 Acetyl Coenzyme A: arylamine N-acetyltransferases (NATs)

The arylamine N-acetyltransferases (NATs) are found nearly in all species from “bacteria to humans. They catalyse the acetyl transfer from acetyl coenzyme A (AcCoA) to an aromatic amine, heterocyclic amine or hydrazine compound. In humans, acetylation is a major route of biotransformation for many arylamine and hydrazine drugs, as well as for a number of carcinogens present in the diet, cigarette smoke and the environment (Minchin et al., 1992, Hein et al.,1993).

The reaction pathway is catalysed by two cytoplasmic acetyltransferases (NAT; EC 2.3.1.5), N-acetyltransferase 1 (NAT1) and N-acetyltransferase 2 (NAT2). The genes encoding both proteins were first isolated in 1989 by Grant et al. who showed that each consists of an intronless open reading frame of 870 base pairs. The two genes are 87% homologous and are located at 8p22 (Blum et al., 1990), a chromosomal region commonly deleted in human cancers (Bova et al., 1993, Maitra et al., 1999).

Ohsako and Deguchi isolated the transcript for each gene from a human cDNA library in 1990. Sequencing of NAT1 and NAT2 revealed a number of allelic variants that affect activity of both genes *in vivo*. This work provided an understanding for the long known functional polymorphism in NAT2 activity (Vatsis et al., 1995) and, more recently, in NAT1 activity (Butcher et al., 1998, Hughes et al., 1998). Genetic variation modulates the acetylator status of individuals and therefore may impact upon their predisposition to different types of cancer including the breast.

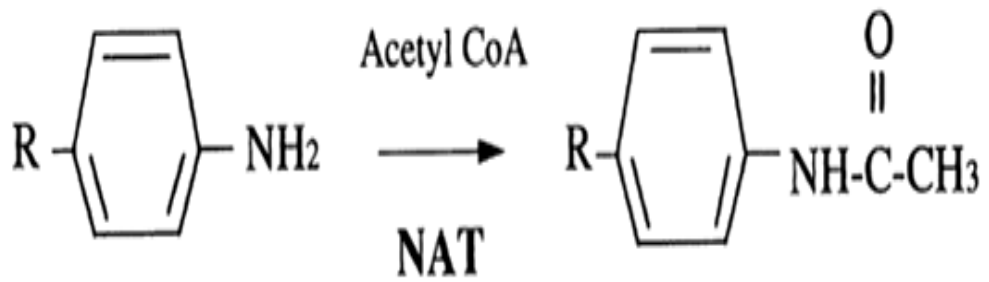
1.1.1 Reaction Mechanism of NATs

The mechanism of the acetyl transfer and the co-ordination of the substrate binding to the enzyme hold the key to understanding the variability in substrate specificities of the NATs and their pharmacogenetics. The reaction was determined to proceed via a 'ping pong' mechanism, involving first binding of the acetyl group to the enzyme followed by acetyl transfer onto the arylamine substrate (Weber et al., 1967) (Figure 1). Evidence showed that the transfer involved general base catalysis to form an acetyl-cysteinyl intermediate (Riddle and Jencks, 1971). The highly conserved Arg⁶⁴ in human NAT1 was suggested to be responsible for general base catalysis, but further mutation experiments suggested that it had a structural rather than a catalytic role (Delomenie et al., 1997).

A fragment of the first 204 amino acids of human NAT1 could perform the first step of the reaction, to form the acetyl-enzyme intermediate but could not transfer the acetyl group onto an arylamine substrate (Sinclair and Sim, 1997). The Cys⁶⁹ from *Salmonella typhimurium* had previously been shown to be important in the enzyme mechanism and substitution to an alanine with site-directed mutagenesis led to the inactivation of the enzyme as did the same mutation introduced into recombinant human NAT2 (Watanabe et al., 1992, Dupret et al., 1992). Previous studies on the human NATs had suggested a possible role for a histidine in catalysis, which was in agreement with the presence of the catalytic triad found in the structure of NAT from *S. typhimurium*.

NATs do not only possess N-acetylation activity, but also O-acetylation (OAT) and N,O-acetyltransfer (NOAT) activities (Grant et al., 1991, Minchin et al., 1992). With the first crystal structures becoming available, how allelic variants of NATs affect enzymic activity can be better understood by linking the kinetic and pharmacogenetic properties of human NATs to the structure. The four common slow acetylator alleles, NAT2*5, NAT2*6, NAT2*7 and NAT2*14 contain the substitutions Ile¹¹⁴Thr, Arg¹⁹⁷Gln, Gly²⁸⁶Glu and Arg⁶⁴Gln, respectively. Current opinion is that the first substitution could lead to a reduced rate of substrate turnover, but that the other three reduce the protein stability (Grant et al., 1997, Leff et al.,

Arylamine



Hydrazine

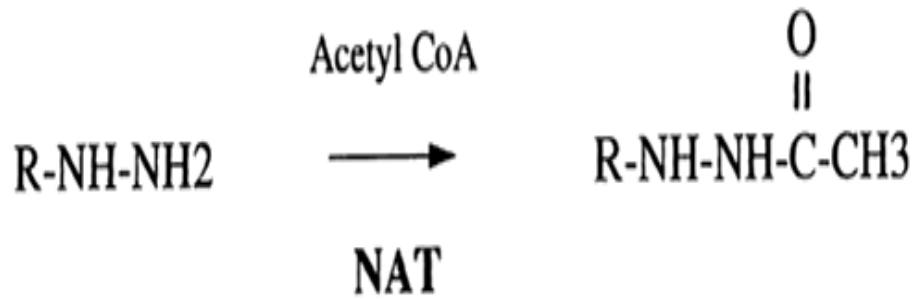


Figure 1. Reaction mechanism of arylamine N-acetyltransferases (Adapted from Trepanier et al., 1998)

1999, Hein et al., 1994). The slow acetylator phenotype may be linked to reduction of NAT2 levels in human liver (Grant et al., 1990), but it is suggested that this is due to the protein of some variants being less stable and being degraded more rapidly. Information to support this suggestion is compatible with the crystal structure albeit that no human crystal structure is available yet.

Arg⁶⁴ was found to correlate with Arg⁶⁵ of *S. typhimurium*, since both were four residues away from the active site cysteine. Arg⁶⁵ was found to form a salt bridge with the Glu³⁹ in *S. typhimurium* which was a highly conserved residue throughout NATs (Payton et al., 2001). Mutation of the arginine residue to a glutamine in the NAT2*14 cluster would be likely to break a potential salt-bridge within only hydrogen bonding being possible between Gln⁶⁴ and Glu³⁹. The substitution of a salt bridge for a hydrogen bond would be expected to diminish protein stability. The substituted residues in the other alleles do not have direct homologues in the *S. typhimurium* NAT structure. A full crystal structure of an eukaryotic NAT will be invaluable for determining genetic and structural relationships.

1.1.2 Structure of NATs

The first crystal structure of an arylamine N-acetyltransferase was of bacterial origin (Sinclair et al., 2000). It revealed a number of surprising features that provided novel structural and functional information about the enzyme. Specifically, a cysteine-histidine-aspartate catalytic triad was identified in the N-terminus of the protein. Based on structural analysis the protein was divided into three domains. The first consists of a helical bundle, located from amino acid 1 to approximately 90, which forms one side of a cleft in which the cysteine involved in acetyl transfer resides. All NATs were found to be highly homologous in this region. The second domain consists of residues from approximately 90 to 210 and is located on the other side of the cleft. It mostly consists of β -sheet structures. The last domain at the carboxyl terminus is a combination of β -sheets and α -helices, and this region shows the greatest diversity between species.

To date, the crystal structure of the human NATs has not been resolved. However, a preliminary model of human NAT2 based on *S. typhimurium* NAT N-terminal catalytic domain (*S. typhimurium* NAT N-terminal catalytic domain is 32% identical to human NAT2) suggests similar features will be present. Structural analysis of this NAT2 model showed that its backbone was extremely similar to that of crystal structure of StNAT (residues 35-131) and of the human NAT1 model (Figure 2).

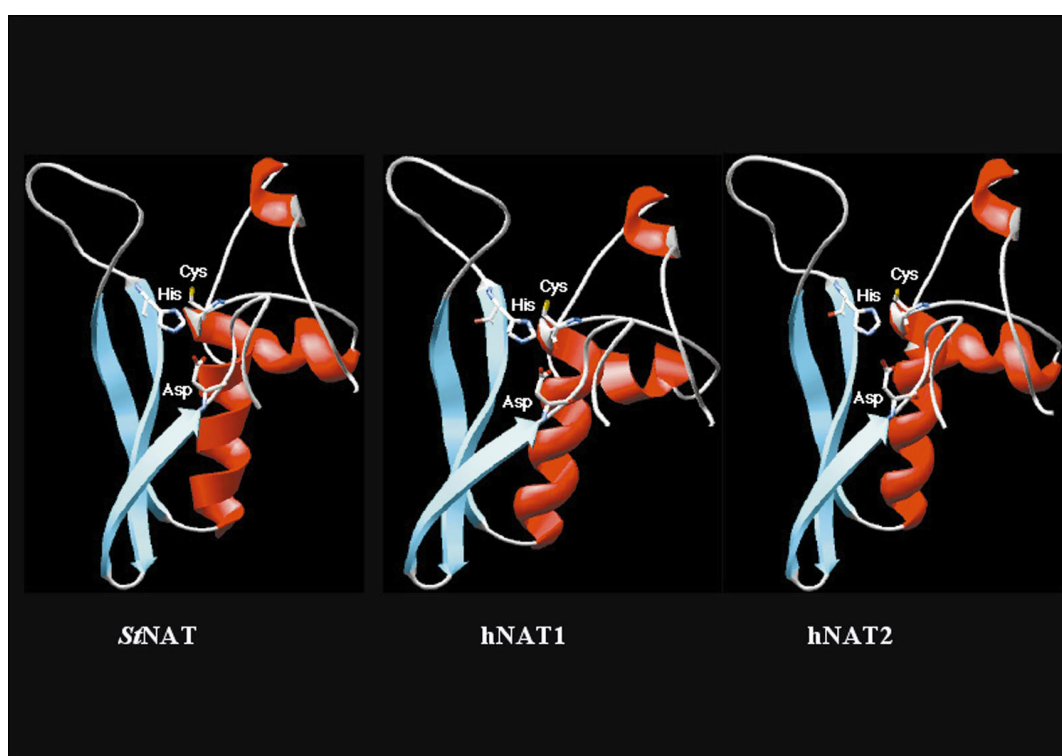


Figure 2: Structure of the catalytic N-terminal domains of *St*NAT, human NAT1, and human NAT2. Swiss-PdbViewer (ribbon images) representation of the three-dimensional structure of *St*NAT (residues 35–131) (PDB Entry 1e2t) and of the homology models of human NAT1 (residues 34–131) (14) and NAT2 (residues 34–131). Catalytic triad residues are shown as stick models (Rodrigues-Lima et al., 2002)

The location of the catalytic triad was found to be conserved in the structures of StNAT, NAT1 and NAT2 (Figure 2 and 3). The structural features surrounding the triad are similar to the cysteine-protease superfamily of proteins which includes the transglutaminases, cathepsins and caspases. While, these proteins traditionally catalyze the hydrolysis of the amide substrates, The NATs and transglutaminases catalyse an acyl transfer that results in amide bond formation.

This is also the case for the NAT homolog found in *A. Mediterreanei*. (Floss et al., 1999). This suggests that vertebrate and eubacterial NATs have adapted a mechanism commonly found in cysteine proteases for use in acetyl-transfer reactions.

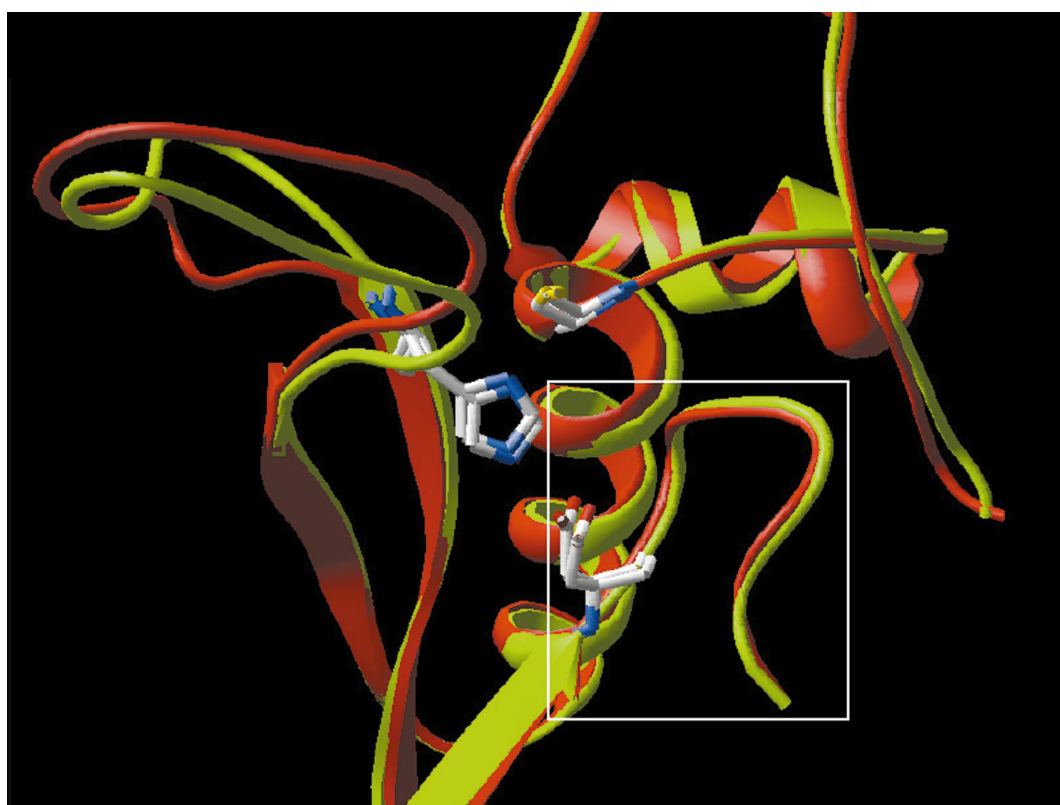


Figure 3 : Structural alignment of the catalytic cores of human NAT1 and NAT2. Swiss-PdbViewer representation of least squares alignment of the C_{α} atoms of NAT1 and NAT2 models. NAT1 is shown in green and NAT2 in red. Catalytic triad residues are shown as stick models. Active site loops are boxed. (Rodrigues-Lima et al., 2002).

Structural alignment in Figure 3 reveals the presence within the active site of human NATs of a loop of conserved structure spanning the residues Asp¹²² (catalytic triad residue) to Met¹³¹. Analysis of crystal structure of *Mycobacterium smegmatis* NAT showed the presence of its extremely conserved active site loop which is an indication of structural conservation of the active site loop from eubacteria to human NATs (Sandy et al., 2002). It has been reported that this active site loop may contain a P-loop motif (spanning residues Gly¹²⁶ to Ser¹²⁹ in NAT2), a nucleotide binding structural motif involved in AcCoA binding (Sinclair et al., 2000) and arylamine substrate specificity (Goodfellow et al., 2000). Site-directed mutagenesis experiments have shown that the residue at position 125 in the active-site loop of human NATs is involved in substrate recognition (Goodfellow et al., 2000).

The homology models of NAT1 and NAT2 aid in showing that the possible involvement of this active-site residue in arylamine substrate selectivity acting by a steric hinderance mechanism (Figure 4). The amino acid in position 125 (Phe¹²⁵ in NAT1 and Ser¹²⁵ in NAT2) was shown to be proximal to the catalytical triad and facing a passageway to the catalytical core (Rodrigues-Lima et al., 2001). The hydroxy group of Ser¹²⁵ residue of NAT2 took up less space than the bulky phenyl ring of the Phe¹²⁵ residue in NAT1. The presence of a smaller group at position 125 might facilitate the access of larger substrates such as SMZ, to the active site.

1.1.3 Substrates of NATs

NATs have broad and overlapping substrate specificity. Drugs or chemicals that possess NH₂ or NH-NH₂ attached directly or via a carbonyl group to an unsaturated ring, are substrates for acetyl-Coenzyme A (AcCoA) dependent arylamine N-acetyltransferases. Also compounds with NH₂ groups attached to ring systems via a short aliphatic carbon side chain can undergo acetylation reactions (Weber et al., 1990).

The examples of drugs that are biotransformed through N-acetylation are isoniazid (INH), antituberculosis agent, hydralazine, antihypertensive agent,

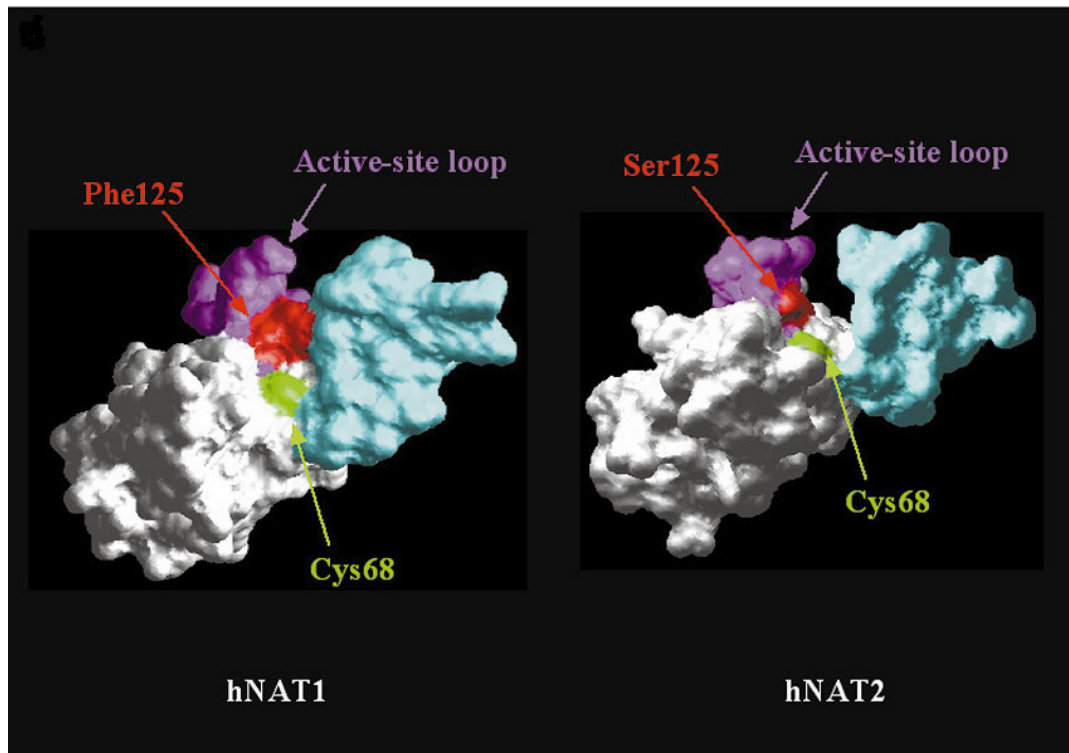


Figure 4. Structural analysis of the active-site loop of NATs. Van der Waals representations of human NAT1 and NAT2 are shown under similar angles. The active-site loops of NAT1 and NAT2 are shown in magenta. The residues at position 125 (Phe125 for NAT1 and Ser125 for NAT2), which are believed to be involved in steric restriction, are shown in red. The catalytic Cys residue is shown in green. The loop spanning residues Val93 to Ile106 in NAT1 and spanning residues Phe93 to Val106 in NAT2 is shown in turquoise. (Rodrigues-Lima et al., 2002)

procainamide, antiarrhythmic agent and dapsone, chemotherapeutic agent. Xenobiotics like PABA, p-amino benzoyl glutamate and p-aminosalicylic acid (PAS), caffeine and sulfamethazine (SMZ), biogenic amines such as serotonin, histamine and tyramines were also found to be substrates of this enzyme. Other substrates include potential carcinogens like 4-aminobiphenyl, β -naphthylamine, 2-aminofluorene found in cigarette smoke and various heterocyclic arylamine food pyrolysates like N-OH-2-amino-1-methyl-6-phenylimidazo [4, 5-b] pyridine (NO-PhIP), N-OH-2-amino-3-methylimidazo [4, 5-f] quinoline (NO-MeIQ) (Risch et al., 1995, Stone et al., 1998).

There is no clear structural motif that determines substrate specificity for different isoforms of NAT. In general, PABA, p-amino benzoyl glutamate and PAS are considered specific substrates for human NAT1 (or mouse NAT2). These substrates can be characterized by the presence of relatively small hydrophilic substitutions in the para position of the aromatic ring. By contrast, SMZ, procainamide and dapson are acetylated primarily by human NAT2. Some compounds, such as 2-aminofluorene, are excellent substrates for both human NAT1 and NAT2.

1.1.4 Species and Tissue-Specific Distribution of NATs

AcCoA-dependent arylamine N-acetyltransferase activity has been detected in many tissues of humans and animals. It is distributed to wide variety of species including monkey, human, rabbit, rat (Weber et al., 1968), hamster, (Ozawa et al., 1990), sheep (Guray and Guvenc, 1997), chicken (Deguchi et al., 1987), housefly (Whitaker et al., 1993) and pigeon (Andres, et al., 1983). Hamster and rabbit possess comparatively high N-acetylating capacities, while primates (including humans), mouse and rat have intermediate capacities. However, the dog has little or no appreciable N-acetylation activity (Weber, et al., 1990, Trepanier et al., 1997). Investigators have shown the activation of 2-aminofluorene (AF) by plant cells (Wagner et al., 1990); however, there is very little information on NATs activities in plants. A study investigating the NATs activities in plant tissues reported presence of AcCoA-dependent arylamine N-acetyltransferase activity in common foodstuffs like broccoli, garlic, hot pepper and bamboo sprout with the highest activity being detected in Balsam pear (Chung et al., 1997).

Biochemical studies have improved the knowledge on the tissue distribution of NATs. Major site of biological N-acetylation was the liver and the highest activity for the NAT enzyme was detected in this tissue (Weber et al., 1990).

Extrahepatically, N-acetyltransferases have been identified in urinary bladder (Hayes et al., 1993), colon (Minchin et al., 1993), gut, kidney, brain, testes, lung, thymus, spleen (Weber et al., 1973), ovary, intestinal mucosa, human placenta,

uterus, adrenal gland (Weber et al., 1990), leukocytes (Cribb et al., 1991), red blood cells (Ward et al., 1992), bone marrow, salivary gland, pancreas, pineal gland (Mannens et al., 1990), intestinal mucosa, human placenta, skin (Gaudet et al., 1993), mammary gland (Gaubatz et al., 1996), skeletal muscle (Rodrigues-Lima et al., 2003), but has not been detected in plasma and fat (Weber et al., 1990).

1.1.5 Purification and Biochemical Characteristics of NATs

The present understanding of AcCoA-dependent arylamine N-acetyltransferases relies largely upon the data gathered from many purification and characterization studies carried on different species and tissue types.

Andres and coworkers purified arylamine N-acetyltransferase from pigeon liver in 1983. Purification steps involved protamine sulfate precipitation, ion exchange chromatography on DEAE-25 Sephadex, gel filtration on Sephadex G-75, amethopterin-AH-Sepharose 4B affinity chromatography and gel filtration on Sephadex G-100. The enzyme was a monomer with a molecular weight determined to be 32,900 by high speed sedimentation equilibrium analysis, 33,000 by Sephadex G-100 gel filtration and 31,600 by SDS-PAGE gel electrophoresis. The isoelectric point was determined as 4.8.

Hepatic arylamine N-acetyltransferase was purified from homozygous rapid acetylator rabbit in 1987 (Andres et al., 1987). The enzyme preparation was homogeneous as judged by gel filtration, SDS-PAGE gel electrophoresis and isoelectrofocusing. The molecular weight was determined as 33,500 by SDS-PAGE disc gel electrophoresis and 33,000 by Sephacry S-200 gel filtration. The isoelectric point was determined as 5.2.

Later, in 1988, Deguchi and coworkers purified arylamine N-acetyltransferase from chicken liver by immunoaffinity purification procedures which included Protein A Sepharose column, usage of monoclonal antibodies immobilized to Sepharose 4B and SDS-PAGE disc gel electrophoresis. The molecular weight of the enzyme was determined to be between 33,000 and 34,000.

In 1989, arylamine N-acetyltransferases were purified from human liver. The purification steps followed were ammonium sulfate precipitation, chromatofocusing, DEAE-Sepharose ion-exchange, gel filtration on Sephadex G-25 and CoA-Sepharose affinity chromatography. This was the first study to report the successful separation of NATs isoforms with anion-exchange chromatography step. The molecular weight of both isoforms was determined as 31000 by SDS-PAGE. The isoelectric point was determined as 4.8 for NAT1 and 4.75 for NAT2.

In the same year, Mattano et al. (1989) purified the arylamine N-acetyltransferase from mice. The molecular weight was determined as 31,500. Biochemical studies on the purified enzyme from hamster revealed a molecular weight of 31,000 (Ozawa et al., 1990).

The arylamine N-acetyltransferase was purified from the housefly (*Musca domestica*) by Whittaker and coworkers in 1993. The purification steps followed were ammonium sulfate precipitation, gel filtration on Sephadex G-25, affinity chromatography on Blue Sepharose 6B, ion exchange chromatography and gel filtration on Superose 12 fast-protein liquid chromatography. The molecular weight was estimated as 27,600 by gel filtration and 26,000 by SDS-PAGE disc gel electrophoresis. The enzyme was found to be a monomer. The isoelectric point was determined as 5.8.

Based on the information gained from characterization of NATs in those studies, the sensitivity of NATs to changes in ionic strength was realized (Mattano et al., 1989). The activity of arylamine N-acetyltransferase was found to exhibit broad pH optima (Andres et al., 1983, Mattano et al., 1989, Whitaker et al., 1993). The purified enzyme was found to be quite stable in several buffer systems e.g. KHPO₄, Tris-HCl, Mes/NaOH, MOPS/NaOH from pH 6 to 8.6 at 4°C, for several days. Addition of protease inhibitor; phenylmethyl sulfonyl fluoride (PMSF), the chelating agent ethylenediamine tetraacetic acid (EDTA), and the reducing agent DL-dithiothreitol (DTT) and β-mercaptoethanol to the buffers, greatly increased the overall recovery of NAT activity (Andres et al., 1983, Mattano et al., 1989).

The experiments were carried on to determine the relative stability of arylamine N-acetyltransferases (Andres et al., 1983, Whittaker et al., 1993, Mattano et al., 1989). Whittaker and his group reported that the storage of the enzyme at -20°C for 6 months did not result in loss of activity. The activity of arylamine N-acetyltransferase was found to be heat-stable (Ozawa et al., 1990, Guray T and Guvenc T, 1997, Geylan YS, M.Sc. Thesis, 1999). The enzyme solution at neutral pH could be stored at -70°C without loss of activity for at least one year with addition of 5% (v/v) glycerol (Andres et al., 1983, Mattano et al., 1989).

1.2 Genetics of NATs

1.2.1 Gene Family Encoding Cytosolic NATs

To date, 26 NATlike genes have been identified in 18 different prokaryotic and eukaryotic species, although it is likely that additional genes will be discovered as more genomes become sequenced. The genes invariably have an intronless coding sequence that encodes for a protein between 254 and 332 amino acids in length. The highest conserved regions occur at the amino terminus, whereas the carboxyl terminus shows very little conservation between species. Consistent with the recently published crystal structure of the *S. typhimurium* NAT (Sinclair et al., 2000), all NATs possess a conserved cysteine, histidine and aspartate that have been implicated to form a catalytic triad. Inhibitor studies (Andres et al., 1988, Guray and Guvenc, 1997) and site directed mutagenesis studies (Dupret et al., 1992) have confirmed that the cysteine (Cys68 in the human proteins) is crucial for NAT activity.

A phylogenetic tree for the NAT proteins is shown in Figure 5. It indicates the separate clustering of the prokaryotic and eukaryotic and fungi sequences, with the exception of *Amycolatopsis mediterranei* NAT which is distant from both groups. This enzyme is part of the rifamycin B synthesis and catalyses the final amide bond formation reaction (Floss et al., 1999). The NAT1 and NAT2 sequences for rat, mouse and hamster cluster together suggesting that the two proteins are encoded by genes that were present before the divergence of the three rodent species. By

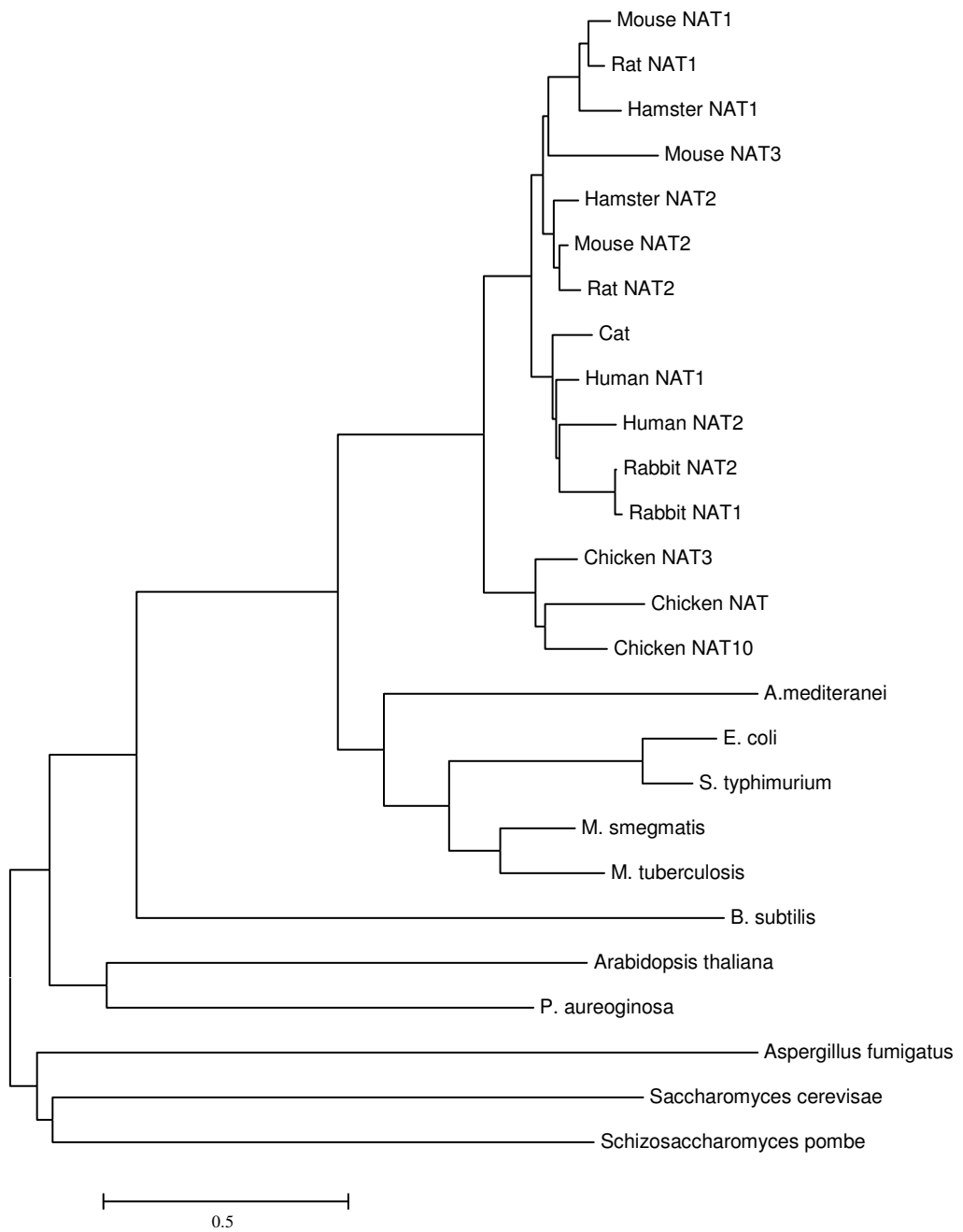


Figure 5. Phylogenetic tree for the NATs (Adapted from Butcher et al., 2000)

contrast, the two human proteins are more closely related to each other, perhaps the genes duplicated later in evolution.

1.2.2 Localization, Structure and Expression of NATs genes

Two NAT isoforms have been identified in humans, namely NAT1 and NAT2, which are the products of distinct genetic loci, designated NAT1 and NAT2, respectively (Blum et al., 1990). A related pseudogene, NATP1, has also been identified (Blum et al., 1990), which contains multiple frameshift and nonsense mutations. The two functional NAT genes share an 87% nucleotide identity, which translates to an 81% homology at the amino acid level. While the entire transcript of NAT1 is derived from a single exon that of the NAT2 is derived from the protein encoding exon together with a second non-coding exon of 100 bp located 8 kb upstream of the translation start site (Blum et al., 1990, Ebisawa et al., 1991). Human NAT1 and NAT2, as well as NATP1, have been localized on the short arm of chromosome 8, more specifically in region 8p22 (Hickman et al., 1994, Matas et al., 1997). The NAT loci are separated by only 170-360 kb and are in the orientation NAT1→NATP1→NAT2, with NAT1 being on the centromeric side of marker D8S261 and NAT2 coinciding with marker D8S21 (Matas et al., 1997). Both NAT1 and NAT2 genes display pronounced allelic variation, with 26 different human NAT1 and 29 different human NAT2 alleles identified to date (Hein et al., 2000).

A similar situation is present in the mouse where three functional genes, designated Nat1, Nat2 and Nat3, have been identified to encode for NAT isoforms (Martell et al., 1991). Mouse NAT2 shows similar substrate specificity with human NAT1, while mouse NAT1 is capable of metabolising the human NAT2 specific substrate isoniazid (Martell et al., 1992). To date, no specific substrate has been identified for NAT3, although the encoding locus appears to be functional (Estrada-Rodgers et al., 1998). The localization and genomic expression of the mouse Nat genes is similar to their human counter parts. The three genes are clustered together in a 130kb genomic region on mouse chromosome 8, cytogenetic band B3.1-B3.3 and within a genetic distance of about 31 cM from the centromere (Fakis et al., 2000). This chromosomal region is syntenic with the region harbouring the genes for

human NAT on chromosome 8p. Polymorphism has been detected only in the Nat2 gene of both A/J37 and A/HeJ43 inbred mice, in the form of missense a A→T mutation at position 296 of the open reading frame, causing the slow acetylator phenotype. It is of interest that mouse Nat2 also possesses a short noncoding exon, located about 6 kb upstream of the intronless open reading frame (Fakis et al., 2000). This raises the possibility that mouse Nat2 may be the genetic orthologue of the human NAT2 gene, although mouse NAT2 and human NAT1 proteins appear to be functionally equivalent.

Information about the localization and genomic organization of the Nat genes in other eukaryotic species has been limited. All genes have an intronless open reading frame and polymorphism in NAT activity has been described in strains of rabbit (Blum et al., 1989), hamsters (Ferguson et al., 1996), and rat (Hein et al., 1991), all of which possess two Nat genes. Upstream non-coding exons have also been described for the rabbit Nat genes (Blum et al., 1989). Cats and other felids have only one gene for NAT (Trepanier et al., 1998), while dogs lack NAT activity due to absence of Nat genes in their genome (Trepanier et al., 1997).

1.2.3 NAT1 Allelic Variants

Historically, NAT1 was thought to be genetically invariant or monomorphic in nature. However, wide interindividual variability in NAT1 activity towards p-amino benzoic acid (PABA) or p-amino salicylate (PAS) (Grant et al., 1991, Weber et al., 1993) was suggestive of a genetic polymorphism, but NAT1 activities were generally unimodally distributed. It wasn't until 1993 when Vatsis and Weber first reported the existence of several allelic variations at the NAT1 locus, that interest in the NAT1 gene aroused, marking the beginning of a systematic survey of NAT1 genotypes.

To date, 26 different NAT1 alleles have been detected in human populations (Table 1), however, only a small number have been shown to alter phenotype *in vivo* (Vatsis et al., 1995, Grant et al., 1997, Hein et al., 2000). Hughes and coworkers used PAS as a probe drug to phenotype a population for NAT1 activity by measuring

Table 1: Human NAT1 Alleles (Butcher et al., 2002)

<i>Allele</i>	<i>Phenotype</i>	<i>Nucleotide change(s)</i>	<i>Amino acid change(s)</i>
NAT1*4	Normal	None	None
NAT1*3	Normal	C ¹⁰⁹⁵ A	None
NAT1*5	Normal	G ^{350,351} C, G ⁴⁹⁷ - 499C, A ⁸⁸⁴ G, Δ ⁹⁷⁶ , Δ ¹¹⁰⁵	Arg ¹¹⁷ → Thr, Arg ¹⁶⁶ → Thr, Glu ¹⁶⁷ → Gln
NAT1*10	Rapid?	T ¹⁰⁸⁸ A, C ¹⁰⁹⁵ A	None
NAT1*11A	Normal	C ⁻³⁴⁴ T, A ⁻⁴⁰ T, G ⁴⁴⁵ A, G ⁴⁵⁹ A, T ⁶⁴⁰ G, Δ ⁹⁽¹⁰⁶⁵⁻¹⁰⁹⁰⁾ , C ¹⁰⁹⁵ A	Val ¹⁴⁹ → Ile, Ser ²¹⁴ → Ala
NAT1*11B	Normal	C ⁻³⁴⁴ T, A ⁻⁴⁰ T, G ⁴⁴⁵ A, G ⁴⁵⁹ A, T ⁶⁴⁰ G, Δ ⁹⁽¹⁰⁶⁵⁻¹⁰⁹⁰⁾	Val ¹⁴⁹ → Ile, Ser ²¹⁴ → Ala
NAT1*11C	Normal	C ⁻³⁴⁴ T, A ⁻⁴⁰ T, G ⁴⁵⁹ A, T ⁶⁴⁰ G, T ⁶⁴⁰ G, Δ ⁹⁽¹⁰⁶⁵⁻¹⁰⁹⁰⁾	
NAT1*14A	Slow	G ⁵⁶⁰ A, T ¹⁰⁸⁸ A, C ¹⁰⁹⁵ A	Arg ¹⁸⁷ → Gln
NAT1*14B	Slow	G ⁵⁶⁰ A	Arg ¹⁸⁷ → Gln
NAT1*15	Slow	C ⁵⁵⁹ A	Arg ¹⁸⁷ → Stop
NAT1*16	Slow	AAA insertion after ¹⁰⁹¹ , C ¹⁰⁹⁵ A	None
NAT1*17	Slow	C ¹⁹⁰ T	Arg ⁶⁴ → Trp
NAT1*18A	Unknown	Δ ³⁽¹⁰⁶⁴⁻¹⁰⁸⁷⁾ , T ¹⁰⁸⁸ A, C ¹⁰⁹⁵ A	None
NAT1*18B	Unknown	Δ ³⁽¹⁰⁶⁴⁻¹⁰⁸⁷⁾	None
NAT1*19	Slow	C ⁹⁷ T	Arg ³³ → Stop
NAT1*20	Unknown	T ⁴⁰² C	None
NAT1*21	Rapid	A ⁶¹³ G	Met ²⁰⁵ → Val
NAT1*22	Slow	A ⁷⁵² T	Asp ²⁵¹ → Val
NAT1*23	Unknown	T ⁷⁷⁷ C	None
NAT1*24	Rapid	G ⁷⁸¹ A	Glu ²⁶¹ → Lys
NAT1*25	Rapid	A ⁷⁸⁷ G	Ile ²⁶³ → Val
NAT1*26A	Unknown	TAA insertion ⁽¹⁰⁶⁶⁻¹⁰⁹¹⁾ , C ¹⁰⁹⁵ A	None
NAT1*26B	Unknown	TAA insertion ⁽¹⁰⁶⁶⁻¹⁰⁹¹⁾	None
NAT1*27	Unknown	T ²¹ G, T ⁷⁷⁷ C	None
NAT1*28	Unknown	TAATAA deletion ⁽¹⁰⁸⁵⁻¹⁰⁹⁰⁾	None
NAT1*29	Unknown	T ¹⁰⁸⁸ A, C ¹⁰⁹⁵ A, Δ ¹⁰²⁵	None

urinary metabolite ratios, they were able to detect individuals with marked impairments of NAT function (Hughes et al., 1998).

However, there was only a moderate correlation between phenotypes determined by *in vivo* and *in vitro* methods, and the authors themselves suggested that less than 50% of the phenotypic variation observed *in vivo* was related to variation in NAT1 function.

It appears that the measurement of NAT1 activity of blood cells is the most reliable method of phenotyping for NAT1. While little is known about the relative expression of NAT1 in various human tissues, studies in the rabbit model suggest that NAT1 activity is comparable in most tissues, including blood cells (Hughes et al., 1998).

The first report of a correlation between NAT1 genotype and phenotype was by Bell and coworkers in 1995 (Bell et al., 1995). They showed that the NAT1*10 allele was associated with activity two fold higher than that of the wild type allele in bladder and colon tissue samples (Bell et al., 1995). In the bladder, higher levels of DNA adducts were detected in NAT1*10 heterozygotes compared with NAT1*4 homozygotes (Badawi et al., 1995). The NAT1*10 allele also has been associated with a marginally elevated activity in erythrocytes (Payton and Sim, 1998). NAT1*10 has no mutations in the protein encoding region of the gene, but contains two nucleotide substitutions (T¹⁰⁸⁸A and C¹⁰⁹⁵A) in its 3' untranslated region. The T¹⁰⁸⁸A base change was found to alter the consensus polyadenylation signal (AATAAA→AAAAAA) leading to the suggestion that increased activity may be due to enhanced mRNA stability (Bell et al., 1995). However, several recent studies do not support the idea that NAT1*10 allele is associated with elevated NAT1 activity (Butcher et al., 1998, Hughes et al., 1998, Lin et al., 1998). As a result, the functional significance of this allele remains unclear at present.

A population study showed a distribution of NAT1 activity that was clearly bimodal in nature and reported a correlation between NAT1 genotype and phenotype involving the slow acetylator alleles NAT1*14 and NAT1*17 (Butcher et al., 1998).

Individuals that were heterozygous for either polymorphism had approximately half the activity of individuals that lacked these base changes. Furthermore, Western blots for NAT1 showed that low activity was due to a parallel decrease in NAT1 protein content, indicating that slow acetylator status was a result of a decrease in the amount of a functionally normal rather than the presence of a protein with altered acetylation capacity.

A later study, found that individuals who possessed a NAT1*11 allele had slightly lower activities compared with individuals who were homozygous for NAT1*4, NAT1*10, or NAT1*3, all of which had similar activities (Bruhn et al., 1999). In the same study, an individual who was homozygous for the NAT1*15 allele had no measurable NAT1 activity. The NAT1*15 allele was found to have a base substitution (C⁵⁵⁹T) in the protein encoding region of the NAT1 gene that introduces a stop codon, leading to the production of a truncated, inactive protein (Hughes et al., 1998). Hughes and coworkers also identified an individual who possessed two low activity alleles, namely, NAT1*14B/NAT1*15, and who subsequently had very low acetylation capacity. There appears to be a gene-dosage effect for the low activity NAT1 alleles. The frequency of slow acetylator alleles for NAT1 is low. The most common low activity allele NAT1*14, has been identified in Caucasian populations ranging from 1.3 to 3.7% (Butcher et al., 1998, Hughes et al., 1998, Lin et al., 1998, Bruhn et al., 1999). Interestingly, a much higher frequency of NAT1*14 allele (25%) was reported for a Lebanese population (Dhaini et al., 2000). This indicates that NAT1 shows considerable interethnic variability.

Some of the more common variant NAT1 alleles have been characterized in bacterial and/or mammalian expression systems. The effects of coding and 3'-noncoding polymorphisms in the NAT1*11 allele were characterized by de Leon and coworkers, recently (de Leon et al., 2000). Using recombinant expression of NAT1*11 in both bacterial and mammalian systems, they showed that no major differences existed in catalytic or other properties of NAT1 11 protein compared with wild-type NAT1 4. This is in agreement with an earlier study (Hughes et al., 1998), which showed that the activity of recombinant NAT1 4 and NAT1 11 were similar, but is in contrast to another study which reported a slightly reduced activity

of blood cells from individuals who carried the NAT1*11 allele (Bruhn et al., 1999). NAT1*16 phenotype was shown to be caused by polymorphism in the 3' untranslated region that leads to a decrease in protein expression (de Leon et al., 2000). NAT1*16 had a triple adenosine insertion on the 3' side of the polyadenylation signal (AATAAA) which significantly altered the secondary structure of the pre-mRNA, leading to a two fold reduction in the amount of NAT1 16 protein and activity, compared with NAT1 4 and NAT1 10.

Some NAT1 alleles was shown to produce proteins with activities that are higher than that of the wild-type protein NAT1 4. Recombinant expression of NAT1*21, NAT1*24, and NAT1*25 in bacterial systems produced allozymes with activities 2- to 3-fold higher than NAT1 4 (Lin et al., 1998). The functional significance of the other NAT1 variants remain unclear at present.

1.2.4 NAT2 Allelic Variants

Since the human NAT2 locus was established as the site of the classical acetylation polymorphism (Blum et al., 1991, Grant et al., 1991) the study of NAT2 allelic variation has been an area of intensive investigation. To date, 29 different NAT2 variables have been detected in human populations (Table 2) (Butcher et al., 2002). Each of the variant alleles is comprised of between one and four nucleotide substitutions, of which 13 have been identified, located in the protein encoding region of the gene. Nine of these lead to a change in the encoded amino acid (C¹⁹⁰T, G¹⁹¹A, T³⁴¹C, A⁴³⁴C, G⁴⁹⁹A, G⁵⁹⁰A, A⁸⁰³G, A⁸⁴⁵C, and G⁸⁵⁷A), while the remaining four are silent (T¹¹¹C, C²⁸²T, C⁴⁸¹T, and C⁷⁵⁹T).

Several studies have been performed that show clear correlations between NAT2 genotype and phenotype (Bell et al., 1993, Cascorbi et al., 1995). Early genotyping studies screened for the presence of the C⁴⁸¹T, the G⁵⁹⁰A, the G⁸⁵⁷A and sometimes the G¹⁹¹A nucleotide changes, all of which were shown to cause a slow acetylation phenotype. Moreover, there was a gene-dosage effect. Individuals who were homozygous for NAT2 polymorphisms had a slow acetylator phenotype, individuals heterozygous for NAT2 polymorphisms had an intermediate acetylator

Table 2: Human NAT2 Allelic Variants (Butcher et al., 2002)

<i>Allele</i>	<i>Phenotype</i>	<i>Nucleotide change(s)</i>	<i>Amino acid change(s)</i>
NAT2*4	Rapid	None	None
NAT2*5A	Slow	T ³⁴¹ C, C ⁴⁸¹ T	Ile ¹¹⁴ → Thr
NAT2*5B	Slow	T ³⁴¹ C, C ⁴⁸¹ T, A ⁸⁰³ G	Ile ¹¹⁴ → Thr, Lys ²⁶⁸ → Arg
NAT2*5C	Slow	T ³⁴¹ C, A ⁸⁰³ G	Ile ¹¹⁴ → Thr, Lys ²⁶⁸ → Arg
NAT2*5D	Slow	T ³⁴¹ C	Ile ¹¹⁴ → Thr
NAT2*5E	Slow	T ³⁴¹ C, G ⁵⁹⁰ A	Ile ¹¹⁴ → Thr, Arg ¹⁹⁷ → Gln
NAT2*5F	Slow	T ³⁴¹ C, C ⁴⁸¹ T, T ⁷⁵⁹ T, A ⁸⁰³ G	Ile ¹¹⁴ → Thr, Lys ²⁶⁸ → Arg
NAT2*6A	Slow	C ²⁸² T, G ⁵⁹⁰ A	Arg ¹⁹⁷ → Gln
NAT2*6B	Slow	G ⁵⁹⁰ A	Arg ¹⁹⁷ → Gln
NAT2*6C	Slow	C ²⁸² T, G ⁵⁹⁰ A, A ⁸⁰³ G	Arg ¹⁹⁷ → Gln, Lys ²⁶⁸ → Arg
NAT2*6D	Slow	T ¹¹¹ C, C ²⁸² T, G ⁵⁹⁰ A	Arg ¹⁹⁷ → Gln
NAT2*7A	Slow	G ⁸⁵⁷ A	Lys ²⁸⁶ → Glu
NAT2*7B	Slow	C ²⁸² T, G ⁸⁵⁷ A	Lys ²⁸⁶ → Glu
NAT2*10	Unknown	G ⁴⁹⁹ A	Glu ¹⁶⁷ → Lys
NAT2*11	Unknown	C ⁴⁸¹ T	None
NAT2*12A	Rapid	A ⁸⁰³ G	Lys ²⁶⁸ → Arg
NAT2*12B	Rapid	C ²⁸² T, A ⁸⁰³ G	Lys ²⁶⁸ → Arg
NAT2*12C	Rapid	C ⁴⁸¹ T, A ⁸⁰³ G	Lys ²⁶⁸ → Arg
NAT2*13	Rapid	C ²⁸² T	None
NAT2*14A	Slow	G ¹⁹¹ A	Arg ⁶⁴ → Gln
NAT2*14B	Slow	G ¹⁹¹ A, C ²⁸² T	Arg ⁶⁴ → Gln
NAT2*14C	Slow	G ¹⁹¹ A, T ³⁴¹ C, C ⁴⁸¹ T, A ⁸⁰³ G	Arg ⁶⁴ → Gln, Ile ¹¹⁴ → Thr, Lys ²⁶⁸ → Arg
NAT2*14D	Slow	G ¹⁹¹ A, C ²⁸² T, G ⁵⁹⁰ A	Arg ⁶⁴ → Gln, Arg ¹⁹⁷ → Gln
NAT2*14E	Slow	G ¹⁹¹ A, A ⁸⁰³ G	Arg ⁶⁴ → Gln, Lys ²⁶⁸ → Arg
NAT2*14F	Slow	G ¹⁹¹ A, T ³⁴¹ C, A ⁸⁰³ G	Arg ⁶⁴ → Gln, Arg ¹¹⁴ → Thr, Lys ²⁶⁸ → Arg
NAT2*14G	Slow	G ¹⁹¹ A, C ²⁸² T, A ⁸⁰³ G	Arg ⁶⁴ → Gln, Lys ²⁶⁸ → Arg
NAT2*17	Slow	A ⁴³⁴ C	Gln ¹⁴⁵ → Pro
NAT2*18	Unknown	A ⁸⁴⁵ C	Lys ²⁸² → Thr
NAT2*19	Slow	C ¹⁹⁰ T	Arg ⁶⁴ → Trp

phenotype, and individuals who lacked NAT2 polymorphism had a rapid acetylator phenotype. Initial studies suggested that the slow acetylator phenotype associated with the presence of certain nucleotide substitution in the protein encoding region of the NAT2 gene was due to a marked decrease in the protein content, while NAT2 mRNA levels remain unchanged (Grant et al., 1990). Several studies have since investigated the mechanism by which the nucleotide substitutions in the NAT2 gene

affect acetylation capacity by the use of the recombinant expression systems (Dupret et al., 1994, Hein et al., 1994, Delomonie et al., 1997). In a study, acetylation capacity of 16 different NAT2 alleles was assessed in a bacterial expression system. Of the seven specific NAT2 substitutions examined, the T³⁴¹C, G⁵⁹⁰A, G⁸⁵⁷A and G¹⁹¹A substitutions produced recombinant NAT2 allozymes with reduced acetylation capacities, while C²⁸²T, C⁴⁸¹T and A⁸⁰³G substitutions produced recombinant NAT2 allozymes with acetylation capacities similar to the wild-type NAT2 4 protein. As a result, NAT2 alleles that contain any of the specific substitutions that produced recombinant NAT2 allozymes with reduced acetylation capacities are associated with a slow acetylator phenotype, and include the NAT2 5, NAT2 6, NAT2 7, NAT2 14, and NAT2 17 clusters (Table 2).

The molecular mechanisms responsible for the production of the slow acetylator phenotypes are not well understood at present. Some base changes appeared to cause a slow acetylation by producing an unstable protein. NAT2 allozymes encoded by alleles with base substitutions at positions 191, 590, or 857 were found to be significantly more unstable in bacterial expression systems than the wild-type protein (Grant et al., 1997, Delomonie et al., 1997). However, in these studies the amount of immunodetectable NAT2 protein was not different upon expression of the variant and wild-type alleles. This is in contrast to the earlier observations by Grant and coworkers who showed that liver NAT content was markedly reduced in slow acetylators, suggesting that the artificial environment of bacterial expression systems may not accurately reflect what occurs in mammalian cells with regard to protein degradation.

The frequency of the slow acetylator phenotype varies considerably among ethnic groups (Evans, 1989), and this is due to the differing frequencies of the polymorphisms that correspond to the slow acetylator alleles. In Caucasian and African populations, the frequency of the slow acetylation phenotype varies between 40 and 70%, while that of Asian populations, such as Japanese, Chinese, Korean and Thai, range from 10 to 30% (Meyer et al., 1997). Caucasian and African populations have high frequencies of NAT2*5 alleles (>28%) and low frequencies of NAT2*7 alleles (<5%), while Asian populations have low incidences of NAT2*5 alleles

(<7%) and higher incidences of NAT2*7 alleles (>10%). Also, NAT2*14 alleles are almost absent from Caucasian and Asian populations (<1%), but are present in African populations at comparably higher frequencies (>8%).

1.2.5 Nomenclature and Classification of NATs

The first attempt to devise a consensus nomenclature for the NATs was published in 1995 and included genes from six species and a total of 39 alleles (Vatsis et al., 1995). Since then, many new alleles have been identified and the nomenclature for these was updated in 2000 (Hein et al., 2000). The Human Gene Nomenclature Committee has agreed that the symbol NAT be assigned to the arylamine N-acetyltransferase genes. Currently, NAT also is used for unrelated genes such as yeast protein N-terminal acetyltransferase, human noradrenalin transporter, eukaryotic translation initiation factor, translation repressor protein and death associated protein 5.

The classification of the eukaryotic genes into NAT1 and NAT2 subfamilies has been done largely on a historical basis of the research area and is a consensus nomenclature (Hein et al., 2000). While this has been appropriate for most members of the genes for NAT, it has raised some confusion with the mouse, hamster and rat NAT2 genes, which encode for proteins with substrate specificity to human NAT1 (acetylate PABA) (Hein et al., 1994, de Leon et al., 1995, Ware et al., 1996). At this stage, mouse is the only species to have three genes for NAT, pseudogenes excepted. Classification of different alleles to different clusters is based on the most significant nucleotide substitution present (Hein et al., 2000).

The prokaryotic genes are sufficiently dissimilar to the eukaryotic genes for NAT to preclude subclassification. Consequently, the prokaryotic genes are referred to as NAT only. An international committee has been established to oversee the nomenclature of the N-acetyltransferases. The committee is responsible for nomenclature updates and assignment of new alleles. This has been found to be essential to ensure consistence of allelic names in literature. A web site that provides

information about the naming of existing and new alleles can be found at <http://www.louisville.edu/medschool/pharmacology/NAT.html>.

1.3 Breast Cancer and NATs

1.3.1 General Anatomy of Human Breast Tissue

The mammary glands are modified sweat glands located within the subcutaneous tissue. Each mammary gland is divided into 15-20 lobes separated and surrounded by the connective tissue composed primarily of adipose cells. Each lobe is an independent gland with its own duct that opens at the apex of the nipple. Each lobe is further divided into many lobules separated by connective and adipose tissue. Intralobular ducts from lobules drain into the interlobular ducts of the lobes. The interlobular duct from each lobe joins and forms a single duct, the lactiferous duct, which traverse through the nipple and dilates into a lactiferous sinus just before it terminates in the summit of the nipple (Figure 6).

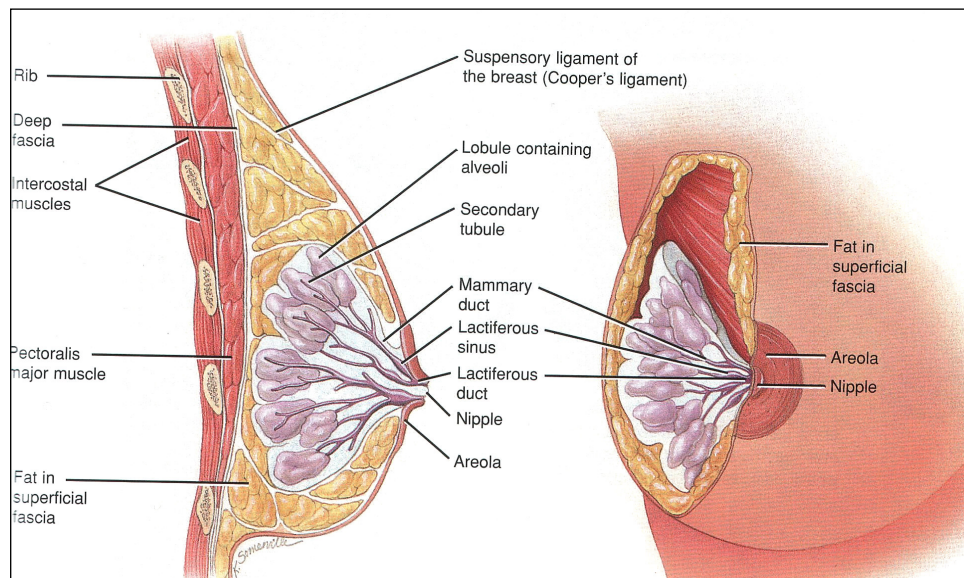


Figure 6. General anatomy of the breast (Strete, D, 2000)

1.3.2 Breast Cancer

Breast cancer is the most common malignancy among women, with an incidence rate varying between 70 and 100 per 100,000 women (Ambrosone et al., 1995). In our population breast cancer takes the first place among the 10 most common malignancies encountered with an incidence of 7.32 per hundred thousand (Ministry of Health, Turkey/ Statistics/1999).

1.3.2.1 Classification of Breast Cancer

The two key determinations to make in the morphologic study of breast cancer are

1. Whether the tumor is confined to the glandular components of the organ (in situ) or whether it invades the stroma (invasive cancer) of the ducts or glands.
2. Whether it is of ductal or lobular type.

1.3.2.2 Non-invasive Cancers of the Breast

Virtually, all breast cancers are adenocancers derived from the epithelial cells. The term “non-invasive” means that the malignant cells are confined to either the ducts or acini of the lobules, with no evidence of penetration of the tumor cells through the basement membranes around these two types of structures into the surrounding fibrous tissue.

There are two forms of non-invasive cancer:

- ductal cancer in situ
- lobular cancer in situ

1.3.2.3 Invasive Cancers of the Breast

Cancer of the breast originates from the epithelium of mammary ducts and acini; however, the studies by Wellings and colleagues (1974) have shown that a

large percentage of breast cancers, both ductal and lobular, take origin in the terminal duct lobular unit rather than from larger ducts.

An “invasive” tumor is one whose cells have broken through the basement membrane around the breast structure in which they have arisen, and spread into the surrounding tissue. The histological types of invasive cancer and their relative incidence for palpable tumors are:

- invasive ductal no special type (NST) (70-80%)
- invasive lobular (5-10%)
- mucinous (1-6%)
- tubular (2%)
- medullary (1-5%)
- papillary (<1%)
- others (<1%)

1.3.2.3.1 Invasive Ductal Cancer (NST)

Invasive duct or ductal cancers comprise the majority (upto 85%) of infiltrating breast cancers (Fisher et al., 1975; Azzopardi et al., 1982; Page and Anderson, 1987; and Rosen and Oberman, 1992). The size of the tumors varies between patients (average 1-2 cm in diameter). They can occur in both pre and postmenopausal women.

On palpation, they may have an infiltrative attachment to the surrounding structures with fixation to the underlying chestwall, dimpling of the skin, and the retraction of the nipple. Histologically, tumor cells are arranged in groups, cords and glandlike structures.

1.3.2.3.2 Invasive Lobular Cancer

This is a distinct morphologic form of mammary cancer that probably arises from the terminal ductules of the breast lobule. Although making up only 5 to 10 %

of breast cancers (Donegan and Perez-Mesa, 1972; Martinez and Azzopardi, 1979; and Dixon et al., 1983), invasive lobular cancers are of particular interest for at least two reasons: (1) They tend to be bilateral far more frequently than those arising in ducts and (2) while invasive ductal cancers usually form at one focus in the breast, they tend to be multifocal within the same breast. Invasive lobular cancers have abundant fibrous stroma, so that macroscopically they are always schirrous. They occur in postmenopausal women.

Histologically, the cells are small and uniform and are dispersed singly or in columns one cell wide in dense stroma. The cells infiltrate around pre-existing breast ducts and acini, rather than destroying them as occurs with invasive cancers. Tumors not detected by mammography often belong to this category because calcifications frequently are not present and the pattern of invasion is diffuse, without margination (LeGal et al., 1992).

The prognosis, according to various studies, is not different from that for infiltrating ductal cancer of no specific type when tumors of similar stage are compared.

1.3.3 General Risk Factors for Breast Cancer

Many risk factors for breast cancer have been identified, and these, together with advances in the analysis of genetic and hormonal factors, have resulted in several etiological hypotheses.

Breast cancer is common, thus a history of a relative having breast cancer can be found in at least 10% of new cases. However, a proportion of these will be sporadic cancers and not due to familial (inherited genetic) factors. The risk of developing breast cancer is increased in first degree relatives (e.g. sister, daughter) of breast cancer cases, particularly if that person is premenopausal. For example, the risk increases to 9 fold for first degree relatives of premenopausal women with bilateral breast cancer. Up to 5 fold increases in risk have been found for women with multiple first degree relatives with breast cancer.

Less than 1 % of all breast cancers occur in men, so being female is an important risk factor. As with all cancers, increasing age is another significant factor. Up to the age of 40-45 years, the rate of increase is steep; it then slows down, although the incidence of breast cancer continues to increase into old age.

There is significantly higher risk of developing breast cancer amongst women with an early age at menarche. At the other end of the reproductive life, women whose natural menopause before 45 years have only half the breast cancer risk of those whose menopause occurs after 55 years. Therefore, women with 40 or more years of active menstruation have twice the breast cancer risk of those with fewer than 30 years of menstrual activity. In some series there has been two to nine-fold increased risk was observed for the woman who had exogenous estrogen therapy. Various epidemiological studies have shown no or very low increase among long term users.

Nulliparous women have an increased risk of developing breast cancer. However, among parous women protection is related to early age for the first full-term pregnancy. If the first birth is delayed to the mid or late thirties, the woman is at a greater risk of developing breast cancer than is a nulliparous woman.

Diet, obviously, can be a determinant for weight. In rodents, a high fat diet increases the incidence of breast tumors, and the international breast cancer incidence rates correlate with the consumption of fat.

There is a marked variation in breast cancer rates between different countries. The highest rates are in North America, North-west Europe, Australia and New Zealand, with the lowest rates in South-east Asia and Africa. Several factors probably contribute to this difference: age at menarche, age at first full-term pregnancy, age at menopause and postmenopausal weight. The length of time between age at menarche and first pregnancy may be quite short in some of these low incidence countries (Oguztuzun S, Ph.D. Thesis, 2000).

Known risk factors mentioned above like higher than average life-time exposure to estrogens and family history of the disease account for only ~30% of the cases (Kelsey et al., 1988) and etiology still remains largely unknown.

1.3.4 Role of NATs in Breast Cancer

Potent carcinogens like aromatic and heterocyclic amines present in the diet, occupational and environmental exposures are commonly lipophilic in nature, so they can be stored and concentrated in the breast fat pad. Those carcinogens are thought to induce tumors in the mammary gland, after metabolic activation to reactive derivatives that form DNA adducts (Li et al., 1996).

Aromatic and heterocyclic amines activated by hydroxylation are either directly detoxified by N-acetylation or transformed to more potent carcinogens by O-acetylation activity of N-acetyltransferases (NAT1 and NAT2) (Sadrieh et al., 1996, Stone et al., 1998). Both NAT1 and NAT2 have genetic variants which have been correlated with biochemical phenotypes ranging from slow to fast acetylators (Hein et al., 1993). The role of NATs in heterocyclic amine activation within human breast and development of breast cancer were investigated in several studies. We had detected a higher mean activity of NAT2 in human breast cancerous tissues compared to their controls (Geylan et al., 2001, Su-Geylan et al., 2006). Similarly, Ambrosone et al, had suggested that extensive acetylation may be related to lobular breast cancer (Ambrosone et al., 1995). Lee et al have demonstrated that tamoxifen (antiestrogen drug) decreases NATs activities in human cancerous breast tissue (Lee et al., 1997). Williams et al suggested an association of NAT1 but not NAT2 with DNA adduct formation (Williams et al., 2001). Recent studies have focused on the potential association of NATs in breast cancer initiation, but the outcomes have been inconsistent. In this regard, Firozi et al. found that polymorphism of NAT2 significantly affected either the frequency or the level of DNA adducts in normal breast tissues of women having breast cancer, especially in smokers (Firozi et al., 2002). Further, in a genotype study conducted on French-Canadian population suggest an increased risk among women who consume well-done meat with

NAT1*10 allele and increased frequency of NAT2 rapid acetylators among smokers (Krajinovic et al., 2000).

1.4 Scope of the Work

AcCoA-dependent arylamine N-acetyltransferases are important polymorphic participants in conjugation reactions which are involved in detoxication/toxication of various arylamines including potential carcinogens. In this respect, the possible role of N-acetyltransferase in the initiation of certain cancers including that of the breast was investigated in humans. Although, some studies had provided evidence for such associations, the results of other studies were contradictory to each other. These contradictions could be explained by the fact that the data at hand was still limited.

It is known that humans are exposed to cooked food mutagens and carcinogens (Mauthe et al., 1998). As mammary epithelial cells also have the ability to metabolize those carcinogens into DNA-binding species (Li et al., 1996), metabolic activation of carcinogens can take place in the breast as well. This indicates that diet is an important contributing factor in the initiation of breast cancer and thus, the risk is expected to vary among different populations. N-acetylation polymorphism and the association to breast cancer is a new research area which has drawn attention. Further studies should be carried on to improve the present understanding of the basis of the association.

The aim of this study is to purify N-acetyltransferases from human breast tumor tissues and characterize some of its properties. Further studies will be carried out in order to investigate the role of N-acetylation polymorphism in human normal and tumor breast tissues by determining tissue-specific acetylations and genotype of NATs. Also, immunohistochemical staining of NAT1 within normal and tumor human breast tissues is going to be carried out in order to explore the differences in NAT1 expression.

CHAPTER 2

MATERIALS AND METHODS

2.1 Materials

Bovine serum albumin (BSA), p-aminobenzoic acid (PABA), sulfamethazine (SMZ), acetylcarnitine, carnitine acetyl transferase (CAT), dithiothreitol (DTT), ethylenediamine tetraacetic acid (EDTA), acetyl coenzyme A (AcCoA), trichloroacetic acid (TCA), dimethylaminobenzaldehyde (DMAB), sodium dodecyl sulphate (SDS), SDS-PAGE molecular weight markers, ammonium persulphate (APS), bromophenol blue, Blue Sepharose, Coomassie brilliant blue R-250, Coomassie brilliant blue G, glycerol, sucrose, N,N'-methylene-bisacrylamide (Bis), hydroxymethyl aminomethane (Tris), N,N,N',N'-tetramethylethylenediamine (TEMED), acrylamide, silver nitrate, glycine, glycerol, sodium carbonate, sodium thiosulfate, Tween-20, formaldehyde, phenylmethanesulphonyl fluoride (PMSF), sodium azide, ampholytes nitrocellulose membrane, microcentrifuge filtration units and cellulose membrane dialysis tubing were purchased from Sigma Chemical Company, St. Louis, MO, U.S.A. Diethyl-aminoethyl-cellulose (DE-52) was from Whatman, Kent, England. Immunohistochemical staining kit was from DAKO, High Wycombe, UK. β -Mercaptoethanol, xylene, ultra pure methanol and glacial acetic acid were from E. Merck, Darmstadt, Germany. Amplified horse radish peroxidase goat anti-rabbit immun-blot assay kit was purchased from Bio-Rad Laboratories, Richmond, CA, U.S.A. Polyclonal antibody against human NAT1 was the kind gift of Dr. E. Sim, Oxford, U.K.

All other chemicals were of analytical grade and were obtained from commercial sources at the highest grade of purity available.

2.2 Methods

2.2.1 Collection of Human Breast Tissue Specimens

Breast tumors and surrounding tumor-free (normal, taken as control; up to 3 cm from the tumor) tissues were obtained from 30 female breast cancer patients with infiltrating ductal cancer aged between 37-76 (49 ± 10 , mean \pm S.D.) who had undergone mastectomy in Ibni Sina Hospital, Sıhhiye, Ankara. A tissue sample was fixed in 10 % formalin for histological examination and the remaining tissue was used for kinetic analysis.

Histopathological examination was undertaken by the pathologists to differentiate normal and malignant tissues. To avoid contamination of surrounding normal tissue, the central parts of the tumors were utilized. All patients completed a questionnaire on factors that might have influenced the expression of NATs, such as medication, smoking and alcohol consumption.

Six of the patients received 2-3 cycles of adjuvant standard combination chemotherapy (cyclophosphamide, methotrexalate, classical CMF, cyclophosphamide, epirubicin, 5-fluorouracil, CEF, Navelbine and Adriablastin) before mastectomy. Three of the patients were current smokers (10-20 cigarettes/day). None of the patients were alcohol drinkers. The menopausal status, estrogen receptor status and grade groupings of the patients were recorded. The study was approved by the regional Ethics Committee.

2.2.2 Preparation of Human Breast Tissue Cytosols

Human breast tumor and tumor-free tissues were minced and suspended in three volumes times its mass of 20 mM Tris-HCl buffer of pH 7.5 containing 0.25 mM PMSF, 1 mM EDTA and 1 mM DTT. The homogenates were centrifuged at 10,000 g for 15 minutes to remove cell debris, nuclei and mitochondria. Cytosols were prepared by subsequent centrifugation at 100,000 g at 4°C for one hour. Supernatants were stored as 3 ml aliquots at -80°C for enzyme assays.

2.2.3 Protein Determinations

The protein concentrations in the prepared cytosols were determined by the method of Bradford (1976) with crystalline bovine serum albumin (BSA) as a standard. Aliquots of 5 to 20 μl of breast cytosols were taken into test tubes and were completed to a final volume of 500 μl with distilled water. Then, 5 ml Bradford reagent was added to test each tube and mixed by vortex. After a ten minute incubation period, the intensity of the color developed in each tube was measured at 595 nm.

The protein concentrations in the cytosols were determined from a standard calibration curve that was constructed from the corresponding $\text{OD}_{595\text{nm}}$ values of BSA standards (0-100 μg). The protein concentrations in the prepared breast cytosols were found to be in the range of 1.4-3.7 mg/ml.

2.2.4 Determination of Human Breast NATs Activities

The spectrophotometric method of Andres (1985) was used with minor modifications (Guray and Guvenc, 1997) to determine AcCoA dependent arylamine N-acetyltransferases' activities. To 150 μl of appropriately diluted enzyme, 60 μl of a solution containing 0.1 mM PABA for NAT1 or 0.1 mM SMZ for NAT2, 15 mM acetylcarnitine, 2.2 u/ml carnitine acetyltransferase (CAT), 2 mM DTT, 2 mM EDTA and 50 mM Tris-HCl buffer of pH 8 was added. The final volume of 750 μl was preincubated for five minutes at 37°C. Then, the reaction was started by the addition of 60 μl 0.1 mM AcCoA. At the end of 5 and 15 minute incubations, the reaction was terminated by addition of 50 μl of 20 % (w/v) trichloroacetic acid (TCA). The precipitated protein was sedimented by centrifugation at 17000g for 25 minutes by using Eppendorf centrifuge.

As the measurement of enzyme activity depends on the depletion of the amine substrate which is reflected by the decrease in Schiff's base formation with dimethylaminobenzaldehyde (DMAB), 100 μl of 5 % (w/v) DMAB was added to

samples, which were then recentrifuged at 17000g for 40 minutes and incubated at least for 10 minutes at room temperature. Blank values were obtained by substituting water for AcCoA which is used to initiate the reaction. The decrease in optical density with time at 450 nm was followed to determine the activities. The absorbance readings were taken in Shimadzu double beam spectrophotometer. The human breast tissue activities were expressed as pmol amine acetylated per minute per ml cytosol.

2.2.5 Purification of NATs from Human Breast Tissue Cytosols

The purification scheme, for obtaining NATs from human breast control and tumor cytosolic fractions, consisted of an anion-exchange (DEAE-Cellulose), and Blue-Sepharose affinity column chromatography using PABA and SMZ as substrates to follow the activity of NAT1 and NAT2, respectively, in the eluted fractions.

Due to the fact that the total protein in the available individual cytosolic fraction is too low, most frequently the purification was started using the mixture of four to eight control or tumor cytosolic fractions and continued as far as the remaining total protein is enough to go for further purification.

2.2.5.1 Ion-Exchange Column Chromatography on DEAE-Cellulose

The column (1.5 cm X 10 cm) packed with DEAE-Cellulose was equilibrated in the cold room with 20 mM Tris-HCl buffer, pH 8.0 containing 2 mM EDTA, 2 mM DTT. Cytosolic fraction (6 ml) was applied to the column at a flow rate of 20 ml/hour. Afterwards, the column was washed with the equilibration buffer at a flow rate of about 30 ml/hour until no absorption of effluent at 280 nm was detected. The bound proteins were eluted from the column with a linear NaCl gradient consisting of 40 ml of the equilibration buffer and 40 ml of the same buffer containing 1.0 M NaCl.

NAT1 activity against PABA and NAT2 activity against SMZ were measured in the fractions collected from the column. The elution fractions with the highest activities against PABA and SMZ were combined and dialysed against 10 mM Tris-HCl buffer containing 2 mM EDTA and 2 mM DTT at pH 7 to get rid of NaCl and also to change the buffer.

The DEAE-Cellulose ion-exchanger was regenerated in the column, without repacking, by washing with 2.0 M NaCl (about 2 bed volumes), to remove the bound substances, and then with 0.1 M NaOH in 0.5 M NaCl (about 2 bed volumes). The column was then washed extensively with distilled water (more than 10 bed volumes) and equilibrated again with the equilibration buffer. The resin is stored at 4°C in 10 mM Tris-HCl buffer of pH 7 containing 20 % ethanol as an antimicrobial agent.

2.2.5.2 Affinity Column Chromatography on Blue-Sepharose

The column (1 cm X 5 cm) packed with Blue Sepharose was equilibrated in the cold room with 10 mM Tris-HCl buffer, pH 7.0 containing 2 mM EDTA, 2 mM DTT. The combined fraction, from the previous step for the breast tumor was applied to the column at a flow rate of 8 ml/hour. Afterwards, the column was washed with the equilibration buffer at a flow rate of about 12 ml/hour until no absorption of effluent at 280 nm was detected. The bound proteins were eluted from the column with a linear NaCl gradient consisting of 10 ml of the equilibration buffer and 10 ml of the same buffer containing 1.0 M NaCl.

NATs activities against PABA and SMZ were measured in the fractions collected from the column. The elution fractions were collected and stored at -80°C.

The Blue-Sepharose affinity gel was regenerated in the column, without repacking, by washing with 0.1 M NaOH (about 4 bed volumes). The column was then washed extensively with 70 % ethanol (3-4 bed volumes) and equilibrated again with the equilibration buffer. The resin is stored at 4°C in 0.1 M Tris-HCl of pH 8 containing 20 % ethanol to avoid microbial growth.

2.2.6 SDS-Polyacrylamide Gel Electrophoresis (SDS- PAGE)

Polyacrylamide slab gel electrophoresis (PAGE), in the presence of the anionic detergent sodium dodecyl sulfate (SDS), was performed on 4 % stacking gel and 12 % separating gel in a discontinuous buffer system as described by Laemmli (1970). The seven proteins given below were used as molecular weight standards (Table 3).

Table 3. Molecular Weight Standards for SDS-PAGE

Molecular Weight Standards	M _r
Bovine Albumin	66000
Egg Albumin	45000
Glyceraldehyde-3-Phosphate Dehydrogenase	36000
Carbonic Anhydrase	29000
Trypsinogen	24000
Trypsin Inhibitor	20100
α-Lactalbumin	14200

2.2.6.1 Electrophoresis Procedure

Vertical slab gel electrophoresis was carried out using the EC120 Mini Vertical Gel System (E-C Apparatus Corp., NY, and USA) that can be used to run two gels simultaneously. The assembly of the glass plate cassettes (8.3 X 7.4 cm) and the process of gel casting were done according to instruction manual provided with the apparatus. Once the cassettes were properly assembled and mounted, the preparation of the separating and stacking gels was started.

The 12 % separating gel and 4 % stacking gel polymerizing solutions were prepared just before use by mixing the given volumes of stock solutions in the written order as given in Table 4. The separating gel solution was first prepared with the TEMED added just before casting the gel into the glass assembly from the edge of one of the spacers until the desired height of the solution (about 5 cm) was obtained. Then, the liquid gel was overlaid with distilled water (about 0.5 ml), without disturbing the gel surface, to obtain an even interface between the separating gel and the stacking gel. The gel was then allowed to polymerize at room temperature for a minimum of 30 minutes. After polymerization, the layer of water was removed completely using filter paper without hurting the gel surface.

The stacking gel was then poured on the top of the resolving gel and the comb was inserted into the layer of the stacking gel without trapping air bubbles under the teeth of the comb. The gel was then allowed to polymerize for a minimum of 30 minutes. After the gel was polymerized, the comb was removed carefully and the wells were washed with distilled water and filled with electrode buffer. At this point, the gel cassettes were removed from the casting stand, mounted and clamped onto the running frame with the notched glass plate of each cassette facing inside. When running only one gel, the blank plastic plate, provided with the system, was mounted in the place of the second cassette in the casting stand and in the running frame.

Aliquots from the protein samples to be analyzed and from the standards mixture were diluted 3:1 with the 4X sample buffer (3 parts sample and 1 part sample buffer), to have the samples in 62.5 mM Tris-HCl buffer, pH 6.8, 2 % SDS, 5 % β -mercaptoethanol, 10 % glycerol and 0.001 % bromophenol blue. Then the samples and standards were placed in a boiling water bath for 3 minutes. Afterwards, protein samples and molecular weight standards (5–25 μ l) were loaded into different wells using a 25 μ l Hamilton syringe with a tipped needle.

Table 4. Formulations for SDS-PAGE separating and stacking gels

Monomer Concentration	12 %	4 %
Acrylamide/bis	12.0 ml	1.3 ml
Distilled water	10.0 ml	6.1 ml
1.5 M Tris-HCl, pH 8.8	7.5 ml	----
0.5 M Tris-HCl, pH 6.8	----	2.5 ml
10% (w/v) SDS	300 μ l	100 μ l
10 % APS	185 μ l	50 μ l
TEMED	15 μ l	10 μ l
Total monomer	30 ml	10 ml

After loading the samples, the running buffer (135 ml) was added to the compartment formed by the running frame and the cassettes (the upper buffer compartment) and the system was checked for leakage. The running buffer (250 ml) was then also added to the outer tank (the lower buffer compartment). Thereafter, the running frame was inserted into the outer tank, the safety cover was replaced and the leads were plugged into the EC250-90 electrophoresis power supply. The power supply was adjusted to give a constant current of 15 mA when the samples were in the stacking gel and 30 mA when the samples passed to the separating gel. Under these conditions, the voltage was about 50V at the beginning and elevated up to 100V at the end of the run that took a total of about 2 hours.

The power supply was switched off, when the dye front is just 0.5 cm from the lower end of the glass plates, the running frame was taken out and the buffer was removed from the upper buffer compartment. Afterwards, the clamps were detached and the cassettes were removed from the running frame. To gain access to the gels in the cassette, the glass plates were pried apart using a spatula taking care not to chip the edges of the glass plates. The left-top corner of each gel was cut to indicate the order of wells. The gels, usually adhered to one of the glass plates, were taken carefully using gloves and placed in the previously prepared appropriate solutions to

stain the samples which have been resolved on the gels, or to prepare the gels for subsequent blotting.

2.2.6.2 Electroblothing of SDS-PAGE Gels

Electroblotting was carried out using EC140 Mini Blot Module of the EC120 Mini Vertical Gel System (E-C Apparatus Corp., NY, U.S.A.), and nitrocellulose was used as a blotting membrane. The gels obtained from the SDS-PAGE were used directly without staining.

Prior to electroblotting, the gels taken from SDS-PAGE were placed for 30 min, in the Towbin transfer buffer (25 mM Tris, 192 mM glycine and 20 % methanol) with shaking (Towbin et al., 1979).

While the gels were incubated in the transfer buffer, the other system components and the transfer membrane were prepared. All of the electroblotting procedure was carried out with gloves. The nitrocellulose membrane, with the dimensions of the gel to be transferred, was soaked in distilled water for 30 seconds with shaking. The membrane should not be allowed to dry, otherwise proteins will not bind to it. Afterwards, two pieces of filter paper, the Scotch Brite sponge pads, and the transfer membrane were soaked in the transfer buffer for 15 min with continuous shaking.

The blotting stack was assembled on the top of stainless steel grid cathode located in the trough of the frame stand of the Mini Blot Module, to which a small amount of transfer buffer was added. The configuration of the assembly was as follows:

Top	Cover with Palladium Wire <u>Anode</u>
	Sponge Pad
	Sponge Pad
	Filter Paper
	PVDF Transfer Membrane

Gel
 Filter Paper
 Sponge Pad

Bottom Frame stand with Stainless steel Grid Cathode

After the above assembly was prepared, the cover of the electroblotting module was pressed onto the blotting stack and fixed with the clamps after turning assembled blotting module upright and then filled with the transfer buffer (about 100 ml). Thereafter, the fully assembled module was inserted into the outer tank and the safety cover with leads was replaced. The red lead was connected to the anode (+) and the black lead to the cathode (-), where the proteins will be transferred as anions to the direction of anode. The transfer process was performed at room temperature for 60 minutes using a constant voltage of 15 – 20 V. When the blotting was finished, the nitrocellulose membrane was immediately removed and placed in the proper solutions, previously prepared for immunostaining.

2.2.6.3 Silver Staining of the SDS-PAGE Gel

The silver staining of the SDS-PAGE gels was carried out according to the rapid silver staining method of the Donelson (2000) as explained in Table 5. The gels previously stained with Coomassie Brilliant Blue may also be silver stained according to the same procedure.

The relative mobility (R_f) of each protein was determined by dividing its migration distance from the top of the separating gel to the center of the protein band by the migration distance of the bromophenol blue tracking dye from the top of the separating gel.

$$R_f = \frac{\text{Distance of protein migration}}{\text{Distance of tracking dye migration}}$$

The R_f values (abscissa) were plotted against the known molecular weights (logarithmic scale ordinate) and standard line was drawn and its slope was used in the calculation of the molecular weight of proteins.

Table 5. Rapid Silver Staining of Proteins in Polyacrylamide Gels

STEPS	SOLUTION	INCUBATION TIME
1) Fix	40 % Methanol; 0.5 ml 37 % HCOH /liter	10 min
2) Wash	Sterile dH ₂ O	2 X 5 min
3) Pretreat	0.2 g/liter, Na ₂ S ₂ O ₃ .5H ₂ O	1 min ^c
4) Rinse	Sterile dH ₂ O	2 X 20 sec ^c
5) Impregnate	2 g/liter, AgNO ₃	10 min
6) Rinse	Sterile dH ₂ O	10 sec
7) Rinse	Developer Solution Na ₂ CO ₃ (60 g/liter); 0.5 ml 37 % HCOH /liter; Na ₂ S ₂ O ₃ .5H ₂ O (4 mg/liter) ^d	10 sec
8) Develop	Developer Solution	Until bands appear
9) Stop	2.5 ml 2.3 M Citric Acid per 50 ml Developer Solution	10 min
10) Wash	Sterile dH ₂ O	10 min
11) Store	40 % Methanol; 0.5 ml 37 % HCOH /liter	At 4°C

^a The solutions are prepared freshly in a quantity that is 10-fold larger than the volume of the gel.

^b Steps 1-10 are carried out at room temperature on a shaker. ^c The times indicated should be followed exactly in order to ensure reproducible image development.

2.2.7. Isoelectric Focusing on Polyacrylamide Gels

Isoelectric focusing (IEF) was carried out on 7.5 % polyacrylamide gels prepared according to the procedures of Robertson *et al.* (1987) and Warlow *et al.* (1988). The Mini Vertical Gel System, used previously in SDS-PAGE was also used for IEF. Accordingly, the process of assembly of the glass plate cassettes and of gel casting were the same as previously described for SDS-PAGE. The glass plates were soaked overnight in ethanolic KOH (188 g KOH in 500 ml 96 % ethanol), then washed in distilled water, and were finally cleaned with 70 % ethanol, prior to cassette assembly. Once the cassettes were properly assembled and mounted, the preparation of the IEF polyacrylamide gel was started. The 7.5 % IEF gel solution was prepared just before use by mixing the given volumes of stock solutions in the written order as given in Table 6.

Table 6. Formulation of the IEF polyacrylamide gel

	pH 3-10
Acrylamide/bis (30%T, 2.67%C)	3.0 ml
Distilled water	6.0 ml
25 % (v/v) glycerol	2.4 ml
Ampholyte 3-10	500 μ l
7.5 % (w/v) APS	95 μ l
TEMED	5 μ l
Total monomer	12 ml

One formulation in the pH range of 3 –10 of the IEF gel were tried using the respective ampholytes. The gel solutions were degassed before the addition of TEMED and then applied to fill the glass assembly. Thereafter, the comb was

inserted into the gel before polymerizing. The gel was then allowed to polymerize at room temperature for a minimum of 45 minutes, after which the comb was removed, the wells were washed with distilled water, and then an overlay solution of 5 % glycerol was applied to all of the wells.

Protein samples and IEF markers were mixed in a 1: 1 ratio with a sample buffer that consisted of 35 % glycerol and 1.4 % ampholytes (3–10) in distilled water. Afterwards, protein samples and IEF markers (5–30 μ l) were loaded into different wells using a 25 μ l Hamilton syringe with a tipped needle. No sample was applied to the first and last two wells to use their respective lanes later in the manual determination of the pH gradient through the gel.

After loading the samples, 50 mM NaOH cold solution (135 ml) was added, after degassing to remove dissolved CO₂ and stabilize the pH, to the compartment formed by the running frame and the cassettes (Cathode) where it is very important to check the system for leakage. Then 25 mM H₃PO₄ (250ml) was added to the outer tank (Anode). Thereafter, the running frame was inserted into the outer tank, the safety cover was replaced and the leads were plugged into the Consort E752 (Consort Corp., Turnhout, Belgium) electrophoresis power supply.

Focusing of two gels per tank was performed at room temperature using a constant initial voltage of 200V for 45 minutes that was increased by 200V every 30 minute until reaching 1000V at which the focusing was allowed to continue for 15 minutes more, to have a total running time of 2.5 hours.

The gels were taken carefully using gloves, as previously described for SDS-PAGE, but before removing the gel from the glass plate at which it adhered, the first and last two lanes were separated vertically from the gel. Then, small pieces of 0.5 cm each were cut by a razor blade and incubated in glass tubes containing 20 mM KCl for 1-2 hours, after which the pH was measured in each tube (Hjelmeland et al., 1979). Standard curve of the pH gradient was constructed and used to determine the isoelectric point (pI) values for the obtained protein bands, which were also confirmed with the IEF pI-markers.

2.2.7.1 Coomassie Blue Staining of IEF Gels

The IEF gel slabs were placed in the previously prepared appropriate solutions to stain the samples, which have been resolved on the gels, or to prepare the gels for subsequent blotting. The IEF gels were stained according to the method of Reisner et al. (1975) that is quick, sensitive and require no destaining (it cannot be used in the presence of detergents). Briefly, the gel was immersed for 1.5 hour in 3.5 % perchloric acid containing 0.025% Coomassie Brilliant Blue G-250 where the blue protein bands started to appear within 10 minutes against a pale orange background. Then, the gel was immersed in 7 % acetic acid to obtain more than 3-fold intensified band against a pale blue background.

2.2.7.2 Electroblotting of IEF-PAGE Gels

The gels obtained from the IEF were electroblotted directly, without staining, using the same procedure used for electroblotting of the gels from the SDS-PAGE with two exceptions. First, a solution of 0.7 % acetic acid was used in the transfer (Chang et al., 1990) instead of Towbin transfer buffer and second, the order of the layers in the blotting stack was reversed because the proteins in the acidic transfer solution will migrate as cations from the anode towards the cathode. The transfer process was performed at room temperature for 60 minutes using a constant voltage of 10 V.

2.2.8 Immunostaining of the Nitrocellulose Membranes

Immunostaining was carried out according to the instruction manual provided with the Horse-Radish Peroxidase (HRP) Western Blotting Kit (Bio-Rad) that was used in the immunostaining of the electroblotted nitrocellulose membranes. All of the incubations were performed in a minimum of 5 ml of solutions in each step with continuous shaking at room temperature.

The electroblotted nitrocellulose membrane was incubated in the blocking solution (5 % non-fat dry milk in TTBS buffer) for 2 hours. Afterwards, the

membrane was incubated with the polyclonal antibody diluted in the blocking solution for 2 hours, where the anti-NAT1 was used at a dilution of 1/200. The peptide sequence used for generation of NAT1 antibody is homologous with the C-terminus of human NAT1. Thus, the antibody recognizes only NAT1 isoform (Stanley et al., 1997).

The membrane was then washed three times, each for 5 min with TTBS and incubated with the secondary antibody (goat anti-rabbit HRP conjugate; 1/1500 diluted in TTBS) for 1 hour. After the incubation with secondary antibody, the membrane was washed again with TTBS (three times, each 5 min). Afterwards the HRP color developing solution (4-chloro-1-naphthol/hydrogen peroxide) was added. The specific protein bands started to appear after 10 - 30 min. Finally, the membranes were carefully dried and the images were obtained using a scanner connected to the computer.

2.2.9 Immunohistochemical Detection of NAT1* in Human Breast Tissues

Primary tumor and normal breast tissue samples were retrieved from the archives of the İbni Sina Hospital, Sıhhiye, Ankara as formalin-fixed paraffin embedded (FFPE) tissue. After sectioning, these samples were dewaxed in citrocLEAR (HD Supplies, United Kingdom), rehydrated through graded ethanols to water, and endogenous alkaline phosphatases were blocked in 20% acetic acid in TBS for 15 minutes. Immunohistochemical analyses were performed using DAKO Envision System, AP (DAKO, CA, USA).

Step by step procedure of immunohistochemical staining for NAT1 procedure in human breast cancer tissues is summarized in Table 7. Nonspecific IgG binding was blocked using 1% BSA for 30 min. Then, antigen retrieval was achieved using a microwave according to the procedure of Oguztuzun, S (Ph.D. Thesis, 2000), and Herpes-Virus Research Laboratory with minor modifications. At the end of the incubations in the microwave, the sections were left for cooling at room temperature for 45 minutes. This was followed by the incubation of sections with the primary antibody against NAT1 in TBS for 2 hours.

Table 7: Immunohistochemical staining protocol for NAT1 in human breast tissues

DEPARAFFINIZATION & REHYDRATION	In rack	Singly	Time (min)
Xylene	+		10
100% Ethanol	+		2
95% Ethanol	+		2
Distilled water	+		1-2
BLOCKING ENDOGENOUS AP ACTIVITY			
20% Acetic acid	+		15
TBST buffer	+		5
ANTIGEN RETRIEVAL WITH MICROWAVE			
Full Power	+		7
550 Watt	+		3x5
TBST buffer	+		5
BLOCKING WITH 1 % BSA			
1 % BSA	+		30
1° ANTIBODY STAINING			
TBST rinse		+	
1° antibody (200µl)		+	120
TBST buffer		+	rinse
2° ANTIBODY STAINING			
Polymer (5 drops)		+	30
TBST buffer		+	rinse
SUBSTRATE INCUBATION			
Fast Red (3 drops)		+	30
TBST buffer		+	-
Distilled water	+		3
DEHYDRATION & COUNTERSTAINING			
Hematoxylin	+		5
Distilled water	+		1
37 mM Ammonia	+		10x
Distilled water	+		2-5

For immunohistochemical detection of NAT1 within human breast tissues, the antiserum 195 for was used. The antiserum 195 was raised against the C-terminal 11 amino acid residues of mouse NAT2 (Stanley et al., 1997). However, the peptide sequence used for generation of these antisera is also homologous with the C-terminus of human NAT1 and recognizes the cognate isoform. The antiserum was used at 1:400 dilution.

In each immunohistochemical assay a negative control was also included to check that all the stages of the reaction are working correctly. The breast tissue was used as a negative control without primary antibody application. TBS was used instead of the primary antibody.

The slides were then, incubated with the secondary antibody for 30 minutes. Finally, for visualization, substrate incubation was carried out for another 30 minutes with the chromogen, Fast Red. As it is a suspected carcinogen, care was taken to avoid ingestion, inhalation or skin contact.

In order to reveal tissue structures, sections were counterstained lightly with hematoxylin, which stains nuclei blue, for 5 minutes. As the colored end-product formed with Fast Red was alcohol soluble, Mayer's hematoxylin, which is a non-alcoholic counterstain, was used. Then, the sections were kept in distilled water for one minute and dipped 10 times in the blueing agent (37 mM Ammonia). Finally, the sections were washed in distilled water for 5 minutes. For mounting of the sections glycerol was preferred as an aqueous mounting medium.

2.2.10 Preparation of Genomic DNA from Human Breast Tissues

Genomic DNA (gDNA) was prepared according to the method of Laird (1991) with minor modifications. A small part of human breast tissue samples weighing 0.025-0.035 g was spared for DNA extraction purposes. It was ground to powder in a mortar with pestle using liquid nitrogen. The powder of the ground tissue was transferred to a sterile eppendorf and 0.5 ml of 10 mM Tris-HCl pH 8.5 lysis buffer containing 5 mM EDTA, 1% SDS, 0.2 M NaCl and 0.1 mg/ml Proteinase K was

added. The sample was then incubated at 55°C for 3-4 hours with agitation for complete lysis. One volume of isopropanol was added to the lysate and the sample was mixed by inversion until the precipitation was complete.

DNA was recovered by lifting the aggregated precipitate from the solution using a disposable yellow tip. Excess liquid was dabbed off, and the DNA was dispersed in a pre-labelled sterile eppendorf containing, 100- 500 µl of 10 mM Tris-HCl buffer at pH 7.5 containing 0.1 mM EDTA (TE). For complete dissolution of DNA, the sample was left overnight at 55 °C. Later UV quantification of DNA was carried on to determine the DNA concentration in the sample and the purity of the DNA at hand was checked. An aliquot of 15 µl was taken from each sample and added to 735 µl of TE. After well mixing, the absorbances at 260nm and 280 nm was read. The concentration of DNA in solution was determined by measuring the absorbance of the solution diluted in TE in a quartz cuvette at 260 nm (A_{260}) where for a path length of 1 cm:

$$A_{260} = 1.00 \Rightarrow 50\mu\text{g/ml double stranded DNA}$$

The ratio of OD260/OD280 was used to assess the purity. Clean DNA solutions have a ratio of 1.8. A value higher than this suggests contamination with RNA, whilst a value lower than this indicates contamination with proteins.

2.2.11 Polymerase Chain Reaction (PCR) for Genotype Determination of NATs

Polymerase Chain Reaction (PCR) amplification was performed in sterile 0.5 µl eppendorf tubes using approximately 1µg gDNA as template, 25 pmoles of each of the appropriate primers, 0.2 mM of each dNTP (A, T, C, G), 1X Thermophilic DNA Polymerase Buffer (10 mM Tris-HCl pH 9.0, 50 mM KCl, 0.1% Triton[®]X-100, and MgCl₂ at a final concentration between 1-3 mM). The reaction volume was completed up to a total volume of either 50 or 100µl with sterile distilled water. A negative control reaction mixture, without template DNA, was always included for each PCR.

The following general PCR cycle was used: denaturation at 95°C for 30 seconds, primer annealing at the appropriate T_m for 30 seconds, extension at 72°C for x minutes, where x equals 1 minute per kilobase of product to be amplified. Amplification was performed over 30-35 cycles and was followed by a final denaturation, annealing, and extension at 72°C for 5-10 minutes. The amplified PCR products were stored at 4°C until analysis.

2.2.11.1 Human NAT1* Alleles

Using the genotyping method of Payton & Sim (1998), the study cohort was screened for the NAT1* alleles, NAT1*4 (wildtype), NAT1*27, NAT1*3, NAT1*10, NAT1*11, NAT1*14A and NAT1*14B according to the stepwise genotyping procedure shown in Figure 7. Genomic DNA from samples was initially amplified using primers N769 and N1113 (Table 8) which amplifies a portion of the NAT1* gene from nucleotides 769 to 1113.

Digestion of this initial product with restriction enzyme Mbo II and subsequent analysis of the size of the resultant DNA fragments allowed determination of the combination of nucleotides occurring at positions 1088 and 1095 of the 3' untranslated region (Figure 8).

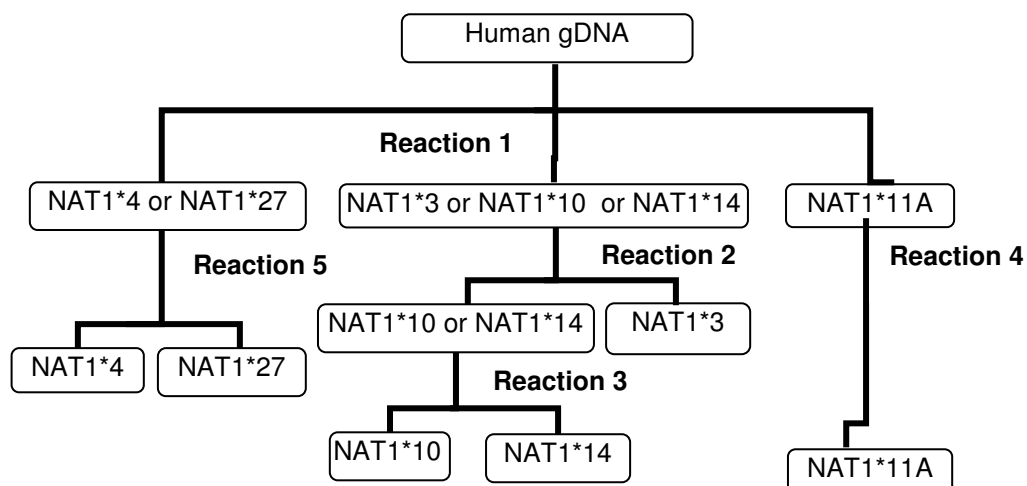


Figure 7. Stepwise genotyping procedure used in identification of the human NAT1* allele

Table 8. Primers used for the amplification of the NAT1* gene

Primer	Sequence (5' to 3') ^a	S/AS ^b	T _m
N-376	_{nt-376} TAT TGC ATG ATT CTC CTG CCT A _{nt-355}	S	58°C
N1177	_{nt1177} GGA ATT CAA CAA TAA ACC AAC AT _{nt 1155}	AS	58°C
N769	_{nt769} ACT CGT AGT GAG GTA GAA ATA _{nt 789}	S	50°C
N1113 ^c	_{nt 1113} ACA GGC CAT CTT TAG AA _{nt 1096}	AS	50°C
N1110a	_{nt 1110} GGC CAT CTT TAA AAT ACA TTT A _{nt 1088}	AS	54°C
N1110b	_{nt 1110} GGC CAT CTT TAA AAT ACA TTT T _{nt 1088}	AS	54°C
N539 ^c	_{nt 539} TCC TAG AAG ACA GCA <u>ACG</u> ACC _{nt 559}	S	52°C
N714	_{nt 714} GTG AAG CCC ACC AAA CAG _{nt 697}	AS	52°C

^aThe subscript numbers give the nucleotide of the NAT1* gene to which the primers anneal, where the adenine of the AUG start codon is labelled 1. ^b S = Sense, AS = antisense ^c Nucleotide substitutions, necessary to create restriction enzyme digest sites, are underlined.

Reaction 1: A 344 bp (335 bp for NAT1*11A) PCR product was amplified

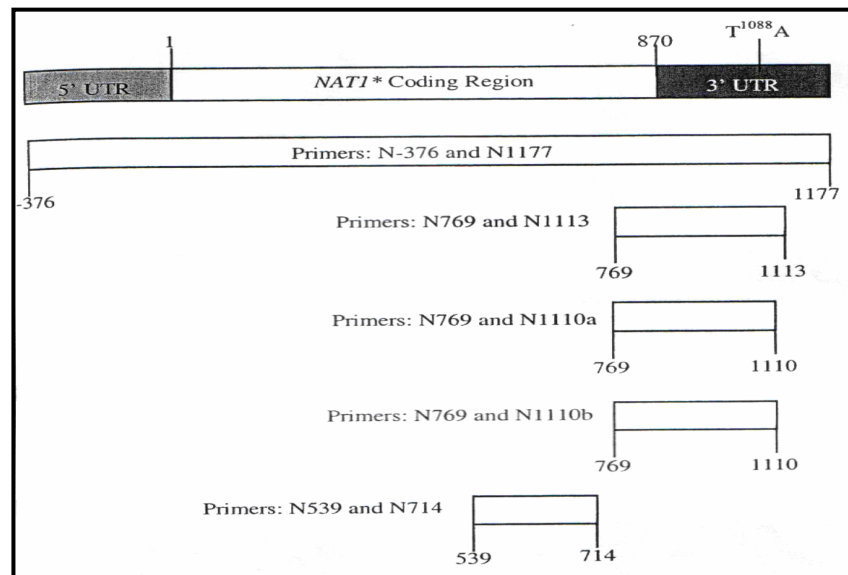


Figure 8: PCR Primers used in the amplification of the NAT1* gene to determine NAT1* genotype

as described from gDNA samples using primers N769 and N1112, 2 mM Mg Cl₂. The annealing temperature of the reaction was 50°C, and product extension was for 45 seconds at 72°C. Thirtyfive cycles were performed with a final extension at 72°C for 5 minutes. The PCR product was digested with MboII, and analysis of the resulting restriction fragments on a 4 % Metaphor agarose/0.5X TBE gel identified the possible alleles present (Table 9).

Table 9. Restriction fragments generated by Mbo II digestion

NAT1* Allele	MboII Restriction Fragments (bp)
NAT1*3	176, 144, 24
NAT1*4	176, 125, 24,19
NAT1*10	176, 144, 24
NAT1*11A	176, 135, 24
NAT1*14A	176, 144, 24
NAT1*27	176, 125, 24,19

Reaction 2: Two AS-PCR amplifications were performed as described from gDNA samples using two sets of primer pairs N769/ N1110a, and N769/ N1110b, 2.5 mM MgCl₂. The annealing temperature of both reactions was 54°C, and product extension was for 45 seconds at 72°C. Thirty cycles were performed with a final extension at 72°C for 5 minutes.

Primer N1110a, which contains an adenine at position 1088 was designed to anneal to and amplify a 341 bp product from NAT1*3, NAT1*4, NAT1*11A and NAT1*27 allele sequences (which contain a thymine at nt 1088), but not from NAT1*10 or NAT1*14A (which contain an adenine at 1088). Primer N1110b, which contains a thymine at position 1088 was designed to anneal to and amplify a 341 bp product from NAT1*10 and NAT1*14A allele sequences only (Table 10)

Table 10. NAT1* Alleles amplified with N769/ N1110a, and N769/ N1110b

NAT1* Allele	Product with N1110b (bp)	Product with N1110b (bp)
NAT1*3	341	
NAT1*4	341	
NAT1*10	-	341
NAT1*11A	341	
NAT1*14A		341
NAT1*27	341	

Reaction 3: A 175 bp was amplified as described from gDNA samples using primers N539 and N713, 2 mM MgCl₂. The annealing temperature of the reaction was 52°C, and product extension was for 30 seconds at 72°C. Thirtyfive cycles were performed with a final extension at 72°C for 5 minutes. The PCR product was digested with BsaO I, and analysis of the resulting restriction fragments on a 4 % Metaphor® agarose/0.5X TBE gel identified the possible alleles present (Table 11).

Table 11. NAT1* Alleles amplified with N539 and N713

NAT1* Allele	BsaO I Restriction Fragments (bp)
NAT1*3	155, 20
NAT1*4	155, 20
NAT1*10	155, 20
NAT1*11A	155, 20
NAT1*14A	175
NAT1*27	155, 20

The presence of mismatched cytosine and guanine at positions 555 and 556 in the N539 primer, generates a BsaO I restriction site in the amplified NAT1*3, NAT1*4, NAT1*10*, NAT1*11A and NAT1*27 allele sequences. NAT1*14A contains a guanine to adenine mutation at 560, therefore no BsaO I site is generated.

Reaction 4: A 1553 bp (1544 bp for NAT1*11A) was amplified as described from gDNA samples using primers N-376 and N 1176, 2 mM MgCl₂. The annealing temperature of the reaction was 52°C, and product extension was for 2 minutes at 72°C. Thirtyfive cycles were performed with a final extension at 72°C for 10 minutes. The PCR product was digested with AlwNI and analysis of the resulting restriction fragments on a 2% agarose/0.5X TBE gel identified the possible alleles present and provided confirmation of the NAT1*11A allele (Table 12).

Table 12. NAT1* Alleles amplified with N-376 and N-1176

NAT1* Allele	AlwN I Restriction Fragments (bp)
NAT1*3	777, 776
NAT1*4	777, 776
NAT1*10	777, 776
NAT1*11A	777, 528, 239
NAT1*14A	777, 776
NAT1*27	777, 776

Reaction 5: An AS-PCR amplification was performed as described from gDNA samples using primers pairs N2 and N850, 2.5 mM MgCl₂. The annealing temperature of both reactions was 58°C, and product extension was for 1 minute at 72°C. Thirtyfive cycles were performed with a final extension at 72°C for 5 minutes. Primer N2, which contains guanine at position 21 was designed to anneal to and amplify a product from the NAT1*27 allele sequence, which contain a guanine at

nucleotide 21, but not from NAT1*3, NAT1*4, NAT1*10*, NAT1*11A or NAT1*14A, which contain a thymine at nucleotide 21 (Table 13).

Table 13. NAT1* Alleles amplified with N2 and N850

NAT1* Allele	Product with N2 (bp)
NAT1*3	-
NAT1*4	-
NAT1*10	-
NAT1*11A	-
NAT1*14A	-
NAT1*27	849

2.2.11.2 Human NAT2* Alleles

Using the genotyping method of Hickman and Sim, (1991) and Hickman et al. (1992) the DNAs isolated from human breast tissue were screened for NAT2* alleles, NAT2*4 (wildtype), NAT2*5A, NAT2*5B, NAT2*5C, NAT2*6A and NAT2*7B. The genotyping procedure scheme is shown in Figure 9. The mutant alleles differ from wildtype by up to three point mutations, which are accompanied by alterations in restriction enzyme digest polymorphisms.

Following PCR amplification of the NAT2* coding region with primers NatHu7 and NatHu8 (Table 14, Figure 10), products were digested with restriction enzymes Kpn I and Taq I.

Following PCR amplification of the NAT2* coding region with primers NatHu14 and NatHu16, products were digested with restriction enzymes Bam HI and Dde I. The combination of restriction fragment patterns with the different enzymes allows determination of the alleles present in a sample.

To verify that PCR amplification was specific for the NAT2* allele, the product of amplification with primers NatHu14 and NatHu16 was digested with restriction enzymes Hind II and Hind III.

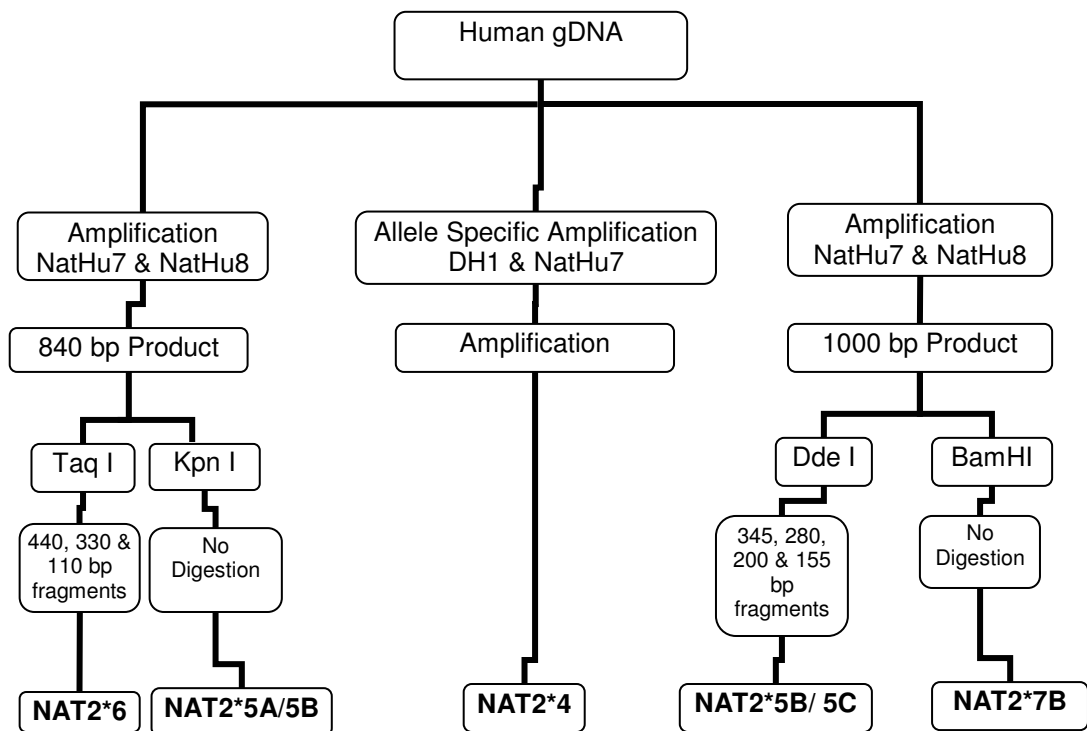


Figure 9. Stepwise genotyping procedure for identification of the human NAT2* alleles

The expected frequency of the NAT2*4 (19.9) and NAT2*5B (44.8) alleles in a Caucasian population is much greater than the expected frequency of the NAT2*5A (1%) and NAT2*5C (3.1%) alleles (Hickman et al., 1992). For this reason, all genotypes of this kind were assigned NAT2*4, 5B combination of alleles.

Table 14. Primers used to amplify the NAT2* gene for determination of NAT*genotype.

Primer	Sequence (5' to 3')^a	S/AS^b	Tm
NatHu7	<u>nt32</u> GGC TAT AAG AAC TCT AGG AAC _{nt52}	S	58°C
NatHu8	<u>nt870</u> AAT AGT AAG GGA TCC ATC ACC _{nt850}	AS	58°C
NatHu14	<u>nt4</u> GAC ATT GAA GCA TAT TTT GAA AG _{nt26}	S	56°C
NatHu16	<u>nt1002</u> GAT GAA AGT ATT TGA TGT TTA GG _{nt980}	AS	56°C
DH1	<u>nt 323</u> TTC TCC TGC AGG TGA CCA _{nt341}	S	56°C

^a The subscript numbers give the nucleotide of the NAT1* gene to which the primers anneal, where the adenine of the AUG start codon is labelled 1. ^b S = Sense, AS = antisense ^c Nucleotide substitutions, necessary to create restriction enzyme digest sites, are underlined.

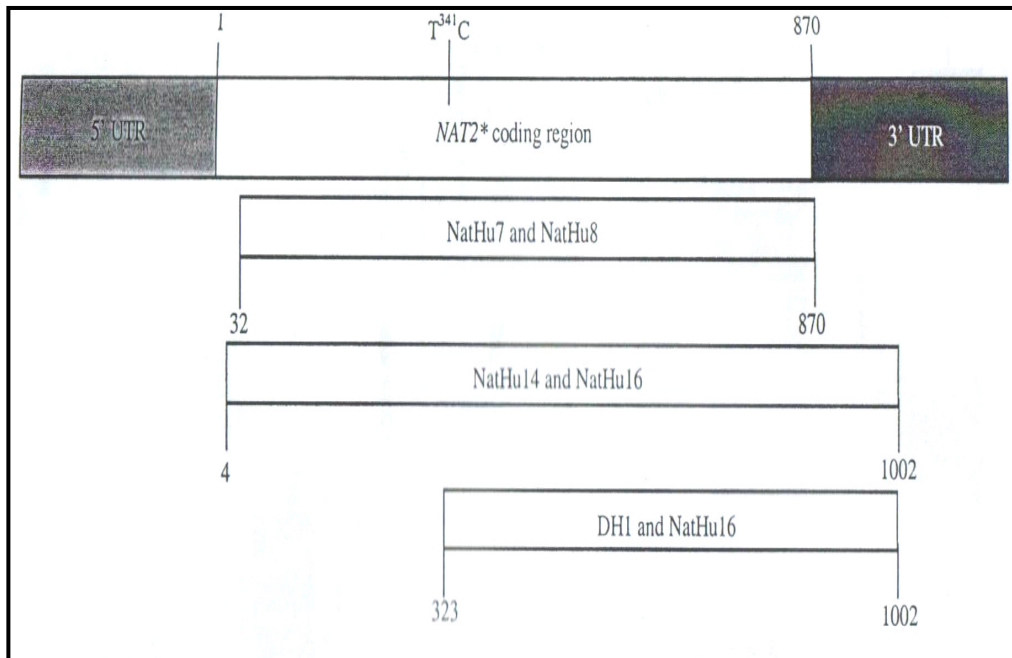


Figure 10: PCR Primers used in the amplification of the NAT2* gene to determine NAT2* genotype

2.2.12 Statistical Analysis

The results were expressed as the mean \pm standard error (SE). Differences between the means were compared with the Wilcoxon rank-sum test. P-value of 0.05 was taken to denote significance.

CHAPTER 3

RESULTS

The purification of the arylamine N-acetyltransferases from human breast tumor cytosolic fractions was carried out following a purification scheme consisting of a sequential anion-exchange (DEAE-Cellulose) and affinity (Blue-Sepharose CL-6B) column chromatography using PABA and SMZ as substrates to follow the activity of NAT1 and NAT2 in the eluted fractions, respectively.

For characterization and comparison of some biochemical properties of NATs, like approximate molecular weight and pI values, SDS-PAGE, isoelectrofocusing and Western blotting analysis was carried out.

Three reduction mammoplasty, three benign and matched controls and five primary tumor and matched normal (tumor-free) breast samples were retrieved from the archives of the İbni Sina Hospital, as formalin-fixed paraffin embedded (FFPE) tissue for immunohistochemical detection and analysis of expression of NATs.

Breast tumors and surrounding tumor-free (normal, taken as control; up to 3 cm from the tumor) tissues were obtained from 30 female breast cancer patients with invasive ductal cancer aged between 37-76 (49 ± 10 , mean \pm S.D.) who had undergone mastectomy in İbni Sina Hospital, Sıhhiye, Ankara. From those patients, NAT1 and NAT2 activities were determined. The possible impacts of grade of malignancy, chemotherapy treatment, estrogen receptor status and menopausal status on NATs enzyme activities were evaluated. All breast tissue samples were collected in ice box and stored at -80°C , until activity studies were carried out. Under these conditions the enzymes were stable at least for three months.

Histopathological examination was undertaken by the pathologists to differentiate normal and malignant tissues. To avoid contamination of surrounding normal tissue, the central parts of the tumors were utilized. All patients completed a questionnaire on factors that might have influenced the expression of NATs, such as medication, smoking and alcohol consumption.

Among the study group, 10 breast samples were selected for determination of NAT1 and NAT2 genotypes based on the sample amount. Further, the possible impacts of grade of malignancy, chemotherapy treatment, estrogen receptor status and menopausal status on NATs genotypes were evaluated.

3.1 Purification of NATs

The purification of the arylamine N-acetyltransferases from human breast tumor cytosolic fractions was carried out basically according to the purification protocols given by Grant et al. (1989) and Whitaker et al. (1993) with some modifications. The purification scheme consisted of a sequential anion-exchange (DEAE-Cellulose) and affinity (Blue-Sepharose CL-6B) column chromatography using PABA and SMZ as substrates to follow the activity of NAT1 and NAT2 in the eluted fractions, respectively.

3.1.1 Ion-Exchange Column Chromatography on DEAE-Cellulose

As described under “Methods”, cytosolic samples from the breast tumor containing a total of 16.7 mg protein with 750 μ U of NAT1 activity toward PABA and 3350 μ U of NAT2 activity toward SMZ or from the breast control tissues containing a total of 6.89 mg protein with 72 μ U of NAT1 activity toward PABA and 275 μ U of NAT2 activity toward SMZ was applied to the column (1.5 X 10 cm) (Table 15).

Afterwards, the column washed with equilibration buffer until no absorption of effluent at 280 nm was detected. Then, the bound proteins were eluted from the

column with a linear NaCl gradient consisting of 50 ml of equilibration buffer and 50 ml of the same buffer containing 1.0 M NaCl.

NATs activities towards PABA and SMZ were measured in the fractions collected from the column. NATs successfully bound to the column as washing fractions did not contain any NATs activities (Figure 11).

The fractions for human breast tumor showing highest activities toward PABA and SMZ eluted in the NaCl gradient at about 0.2 M and 0.4 M NaCl concentrations, respectively.

Table 15. Partial Purification of NATs from Human Breast Tumor Tissues

Purification Step	Protein Total (mg)	NAT1 Activity		NAT2 Activity		Purification Fold	Recovery %
		SA ^a	U Total ^b	SA ^a	U Total ^b		
Crude Extract	16.7	45	750	200	3350	1	100
Ion-Exchanger							
NAT1	2.6	224	577	—	—	5	77
NAT2	3	—	—	600	693	3	21

^a SA: Specific activity given as Ux10⁻⁶/mg protein. ^b U Total: Total units given as Ux10⁻⁶.

As seen from Table 15, anion-exchanger step provided about 5 and 3 purification fold with 77 and 21% recovery of the activities for NAT1 and NAT2, respectively. About 80 % of the NAT2 activity was lost with an unknown reason. Increased ionic strength in the purified fraction for NAT2 might be causing loss of activity of the isoform.

Attempts for the purification of NATs from tumor-free breast tissues were not successful owing either to the comparatively lower amount of NATs within tumor-

free tissues or rapid denaturation of the isoforms. Also, the elution was somehow different, indicating a single protein peak with NaCl gradient.

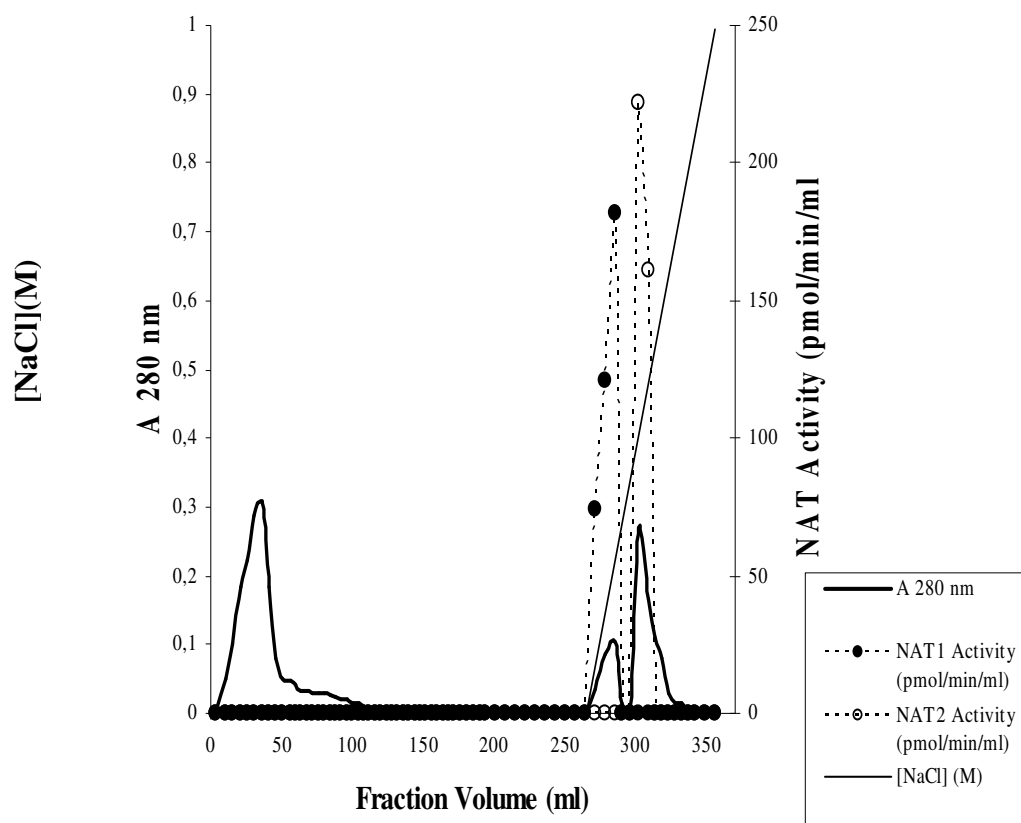


Figure 11. Purification Profile of Human Breast Cytosolic NATs on Ion Exchange Column (1.5 X 10 cm) of DEAE-Cellulose

3.1.2 Affinity Column Chromatography on Blue Sepharose

The eluted fractions with the highest activity for NAT1 and NAT2 were combined in one fraction separately for further purification in Blue-Sepharose affinity column (Figure 12). The combined fractions had a total of 2.6 and 3 mg protein with 577 and 693 μ U of activity toward PABA and SMZ, respectively. The bound proteins were eluted from the column with a linear NaCl gradient consisting of 10 ml of the equilibration buffer and 10 ml of the same buffer containing 1 M NaCl. However, due to the very low protein content of the pooled fractions, NATs' activities were completely lost and could not be detected in washing or elution fractions.

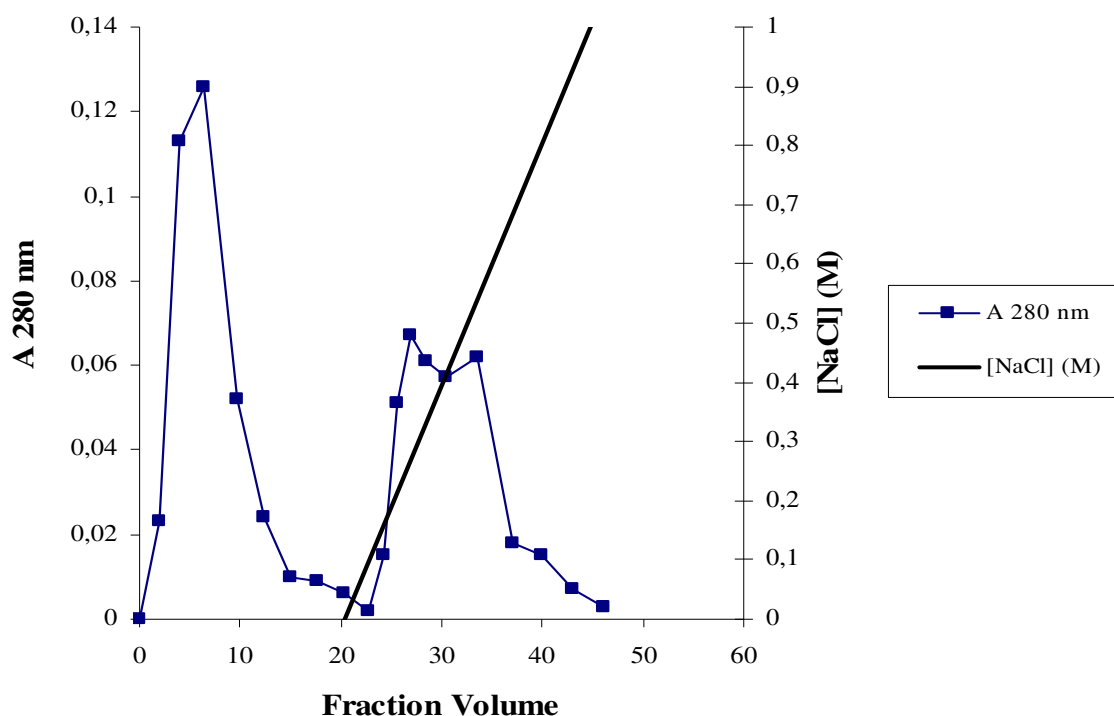


Figure 12. Protein Profile of Human Breast Tumor Cytosolic NAT1 on Blue Sepharose Column Chromatography

3.1.3 SDS-PAGE, Isoelectric Focusing (IEF) and Western Blotting

In order to be able to compare the protein profiles of NATs from human breast tumor and control (tumor-free) tissues, the fractions eluted from DEAE Cellulose anion-exchanger column were analyzed with SDS-PAGE, isoelectrofocusing and Western blotting.

In the purification of NATs from human breast tumor cytosols with anion-exchanger step, NAT1 and NAT2 had eluted as two separate protein peaks. In Figure 13, the silver stained SDS-PAGE gel (12%) of the breast tumor purification fractions is shown. The lanes contained molecular weight markers and different fractions of DEAE-Cellulose ion exchanger column step.

In the first lane, the suspected protein band for NAT1 is indicated with an arrow in a range of molecular weight between 24000-29000 Da. The second protein peak eluted from anion exchanger with NAT2 activity (14 µg) was applied to the second lane. A single protein band was observed within the same molecular weight range (24000-29000 Da).

In the elution profile of NATs with anion exchanger step from human breast control tissues, a single protein peak was observed. However, NATs activities could not be detected. The single peak eluted from this step was analysed with SDS-PAGE. After silver staining, the protein bands, within the 24000-29000 Da range which were suspected to belong to NATs, were observed to be very faint, with poor resolution (Figure 14).

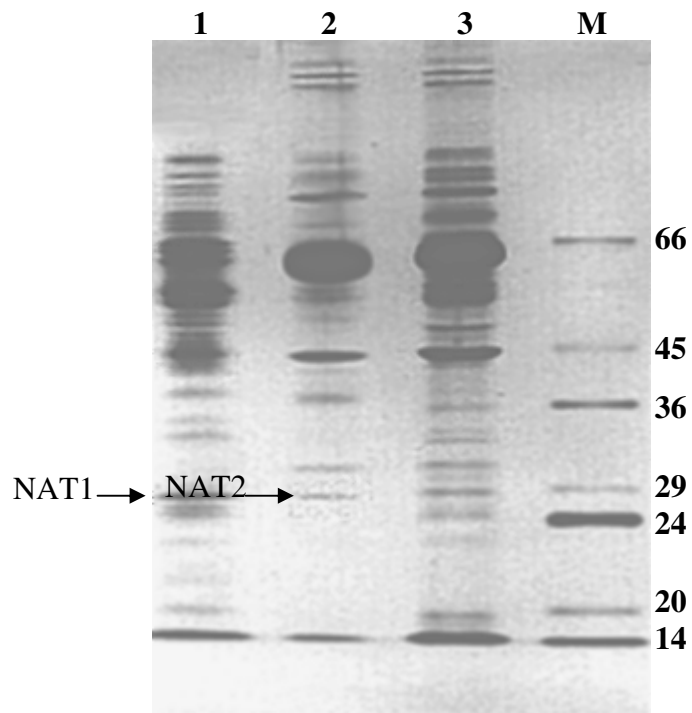
The elution fractions with NATs activities from both breast tumor and tumor-free tissues were analysed with Western blotting (Figure 15). The gel obtained from SDS-PAGE was electroblotted onto nitrocellulose membrane and then immunostained with polyclonal antibodies against NAT1 using the HRP immunblotting kit. The molecular weight of NAT1 was calculated approximately as 27600 Da from the standard curve for molecular weight markers (Figure 16), however, the molecular weight of NAT2 could not be determined, as the polyclonal

antibody only recognized NAT1. Molecular weight calculated for NAT1 was also confirmed with Western blotting.

Cytosolic fractions from human breast control (tumor-free) and tumor tissues were also analyzed by isoelectrofocusing (IEF) using ampholytes with a pH range of 3-10 in order to determine whether there is a change in their isoelectric point (pI) values.

The Coomassie Blue stained isoelectrofocusing gel is shown in Figure 17 (a). Although, approximately equal amount of protein was loaded on the gel for both human breast tumor and tumor-free cytosolic fractions, the number of protein bands observed for breast tumor cytosolic fraction was higher, especially between pI values of 4.6-5.1.

The isoelectric point (pI) value for NAT1 from breast tumor cytosol and elution fraction was calculated approximately as 4.8 from the standard curve blotted from the pH values measured in the gel against the relative distance across the gel which was also confirmed with pI markers and Western blotting analysis (Figure 17 (b)). The gel obtained from the IEF was electroblotted onto nitrocellulose membrane and then immunostained with polyclonal NAT1 antibodies using the amplified Horse Radish Peroxidase immunblotting kit. However, the pI value of NAT1 could not be determined from control breast tissues. Western blotting analysis could not detect NAT1 protein from control breast tissues, most probably due to the lower amount of protein compared to breast tumor tissue.



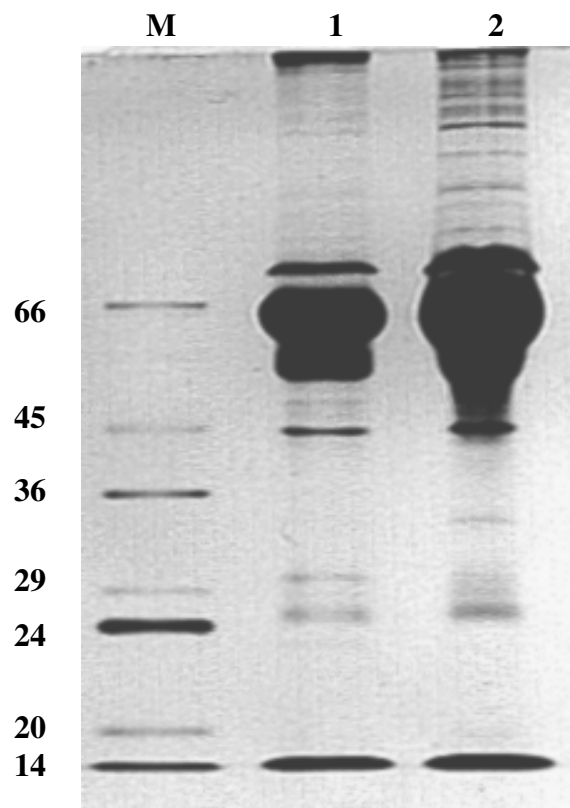
Lane 1: NAT1 Fraction-DEAE-Cellulose (~ 13 µg protein)

Lane 2: NAT2 Fraction-DEAE-Cellulose (~ 14 µg protein)

Lane 3: Breast tumor cytosol (~ 12 µg protein)

Lane M: Low MWT Marker Proteins

Figure 13. SDS-PAGE stained with silver (12 %), of the breast tumor purification fractions and molecular weight markers.

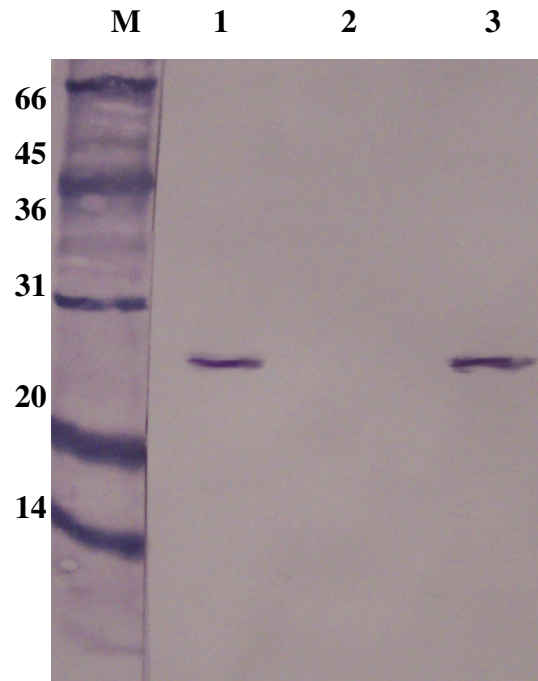


Lane 1: NATs Fraction-DEAE-Cellulose (~ 11 μ g protein)

Lane 2: Breast tumor cytosol (~ 11 μ g protein)

Lane M: Low MWT Marker Proteins

Figure 14. SDS-PAGE stained with silver (12 %), of the breast control purification fraction and molecular weight markers.



Lane M: Low MWT Marker Proteins

Lane 1: NAT1 Fraction-DEAE-Cellulose (~ 13 μ g protein)

Lane 2: NAT2 Fraction-DEAE-Cellulose (~ 14 μ g protein)

Lane 3: Breast tumor cytosols (~ 16 μ g protein)

Figure 15. Western blotting of the purification fraction (Nitrocellulose membrane immunostained with polyclonal anti-NAT1)

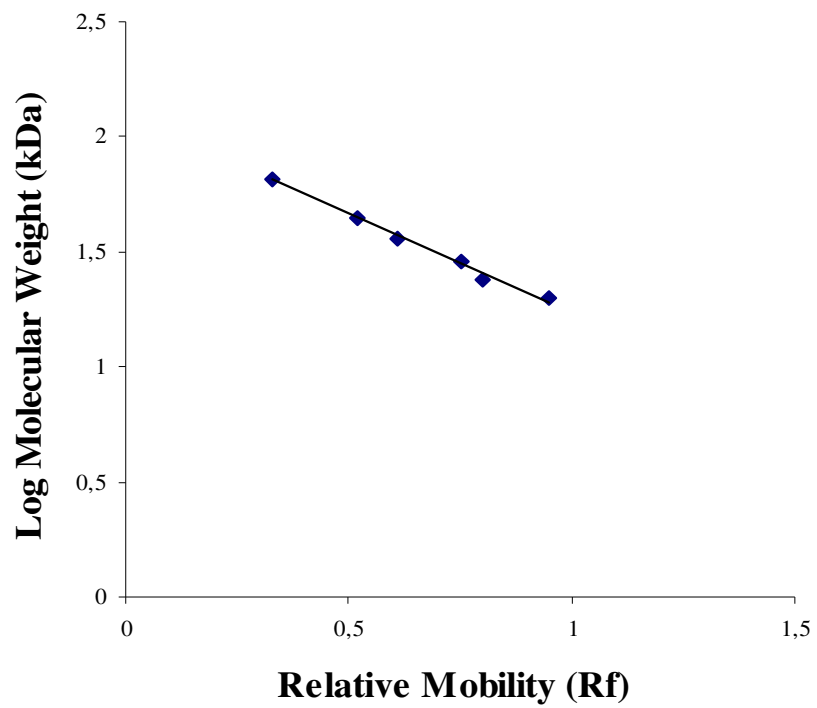
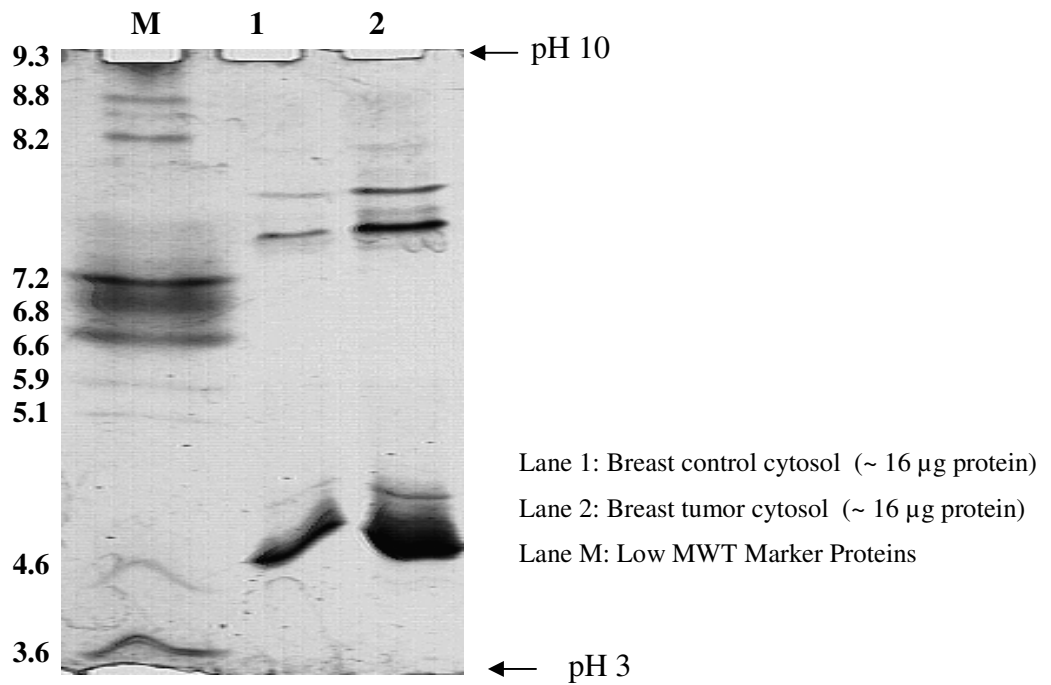


Figure 16. Typical molecular weight standard curve (12 % SDS-PAGE)

(a)



(b)

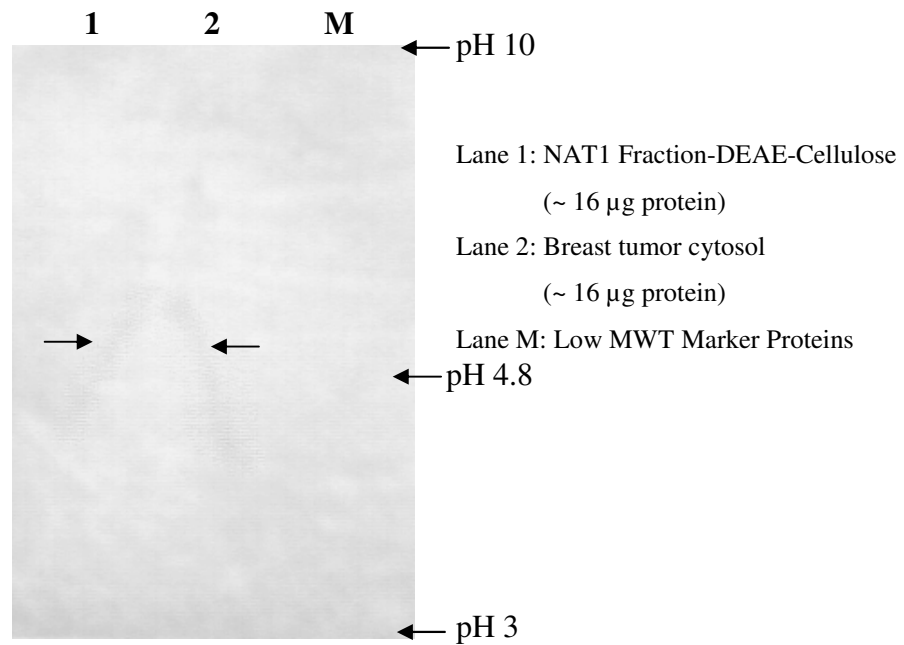


Figure 17. Isoelectric focusing of the cytosolic fractions from breast control and tumor (a) Coomassie Blue stained gel (b) Polyclonal anti-NAT1 immunostained nitrocellulose membrane

3.1.4 Immunohistochemical Detection of NAT1 in Human Breast Tissues

Three reduction mammoplasty, three benign and matched controls, five primary tumor and matched tumor-free breast samples were retrieved from the archives of the İbni Sina Hospital, as Formalin-Fixed Paraffin-Embedded (FFPE) tissue. Optimization of immunohistochemical staining procedure for NAT1 was carried out using human intestine tissues instead of breast tissue specimens which were very few in numbers.

3.1.4.1 Optimization of Immunohistochemical Staining for Human Breast Tissues

To decrease background staining in the specimens, either Guinea Pig serum or BSA was added to the antibody dilution buffer. Further, an incubation step of 20% acetic acid was added, to block endogenous alkaline phosphatase activity which also helped in decreasing background staining. It was observed that BSA was better in decreasing background staining compared to Guinea Pig (Results not shown).

To increase the efficiency of immunohistochemical staining with Ab195, different incubation times for primary antibody, secondary antibody and substrate incubations were tried. For primary antibody incubation, 15, 30, 60, 120 and 180 minute incubations were studied. The slides which were incubated for 15 and 30 minutes were not stained effectively, while 180 minute incubated slides were overstained. Two hour incubation was determined to be optimum for efficient staining. Moreover, increasing the incubation times of secondary antibody and substrate incubations from 15 minutes to 30 improved the overall efficiency of staining.

3.1.4.2 Immunohistochemical Staining of NAT1 from Human Breast Tissues

For immunohistochemical staining of NAT1 reduction mammoplasty (a), benign (b) and malignant (c) breast tissue samples were used (Figure 18). After the breast tissue specimens immunohistochemical staining was completed according to

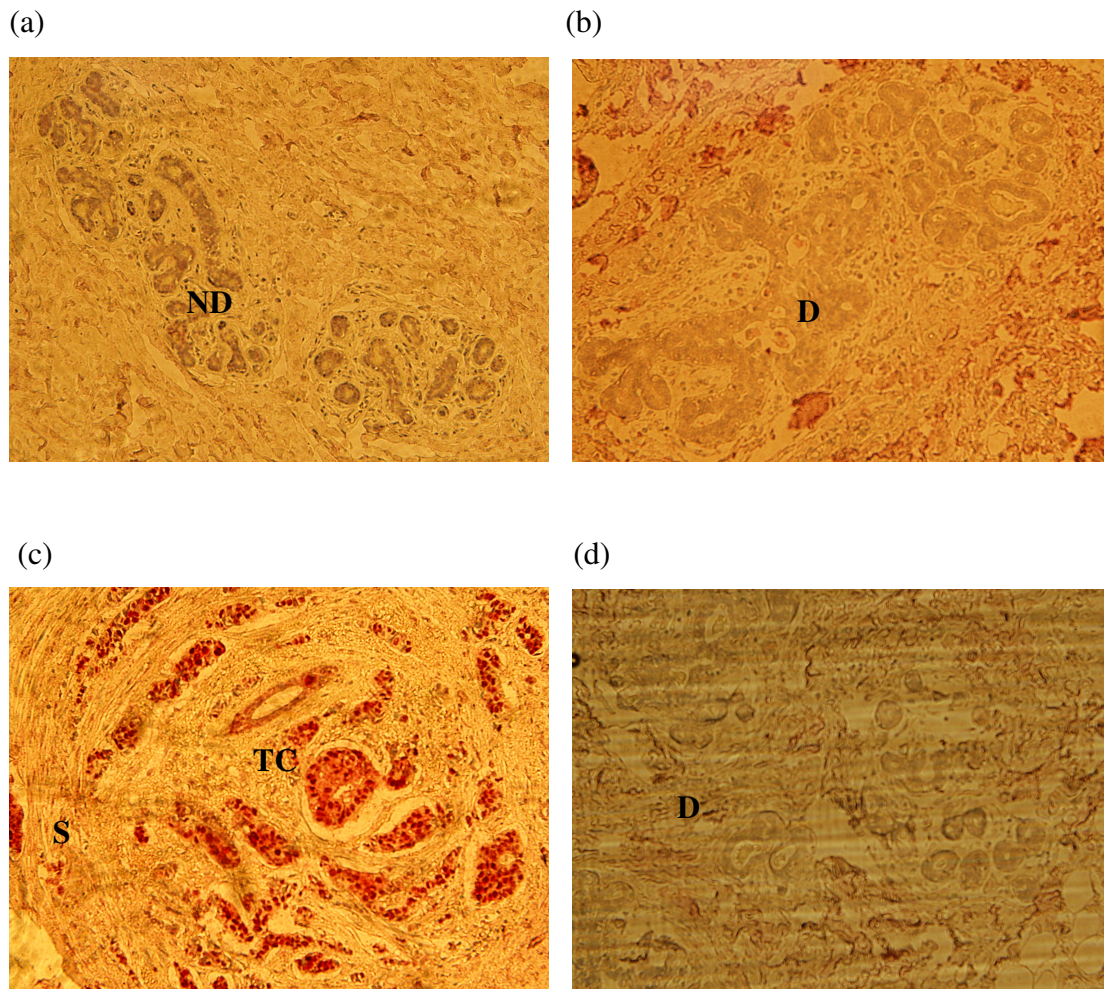


Figure 18. Immunohistochemical staining for NAT1 (X200)

- (a) Reduction mammoplasty (ND: Normal Duct);
- (b) Benign Breast Tissue (D: Ductal);
- (c) Malignant Breast Tissue (TC: Tumor Cells, S: Stroma);
- (d) Negative Control

the optimized procedure, sections were counterstained lightly with hematoxylin, to reveal tissue structures. All the sections were examined by a light microscope (Carl Zeiss Jenamed 2, light microscope) under 200X magnification.

In all specimens diffuse cytoplasmic staining was observed in mammary epithelial cells, while immunoreactivity of NAT1 in stroma was not observed. However, level of intensity of NAT1 immunostaining was observed to be going from weak in reduction mammoplasty samples to strongest in malignant breast tissue.

3.2 Human Breast Tumor and Tumor-Free NAT1 and NAT2 Activities

The distribution of enzyme activities from human breast cancerous (tumor) and matched control (tumor-free) samples for NAT1, NAT2 is given in Table 16. Wide interindividual variations were found in both tumor and tumor-free tissues. Mean enzyme activities in breast tumor tissues were significantly higher than their matched controls.

NAT1 activity of tumors and tumor-free breast tissues ranged from 0-53 pmol/min/mg protein. More than half of the tumor samples (19/30, 63%) had higher NAT1 activity than their corresponding normal tissues and mean NAT1 activity of tumor and matched control samples were significantly different from each other. In three patients (3/30, 10%) tumor and tumor-free breast tissue NAT1 activity was non-detectable.

Smoking did not seem to stimulate the NAT1 activity as for the three patients activities detected in tumor tissue were either indifferent or not changing significantly compared to matched control samples.

Among the study group (n=30), only six patients did receive chemotherapy treatment prior to mastectomy operation. The mean NAT1 activity of tumor tissues in this group was not significantly higher than that of matched controls. On contrary, among the patients who did not receive chemotherapy (24/30, 80%), the mean NAT1 activity of breast tumor tissues was significantly higher. In the treated group, there was a trend for decrease in both tumor and control mean NAT1 activities compared

Table 16: Arylamine NATs activities in tumors and surrounding tumor-free breast tissues of 30 breast cancer patients with invasive ductal cancer^a (Su-Geylan et al., 2006)

	NAT1			NAT2	
	n	Control	Tumor	Control	Tumor
Total	30	13 ± 2 ^b (0-53) ^d	20 ± 3 ^c (0-53)	12 ± 2 (0-35)	34 ± 6 ^c (0-132)
Chemotherapy^e					
+	6	11 ± 3 (0-19)	18 ± 6 (0-42)	9 ± 4 (0-25)	30 ± 15 (0-102)
-	24	14 ± 3 (0-53)	21 ± 3 ^c (0-53)	13 ± 2 (0-35)	36 ± 7 ^c (0-132)
ER Status^f					
+	11	13 ± 4 (0-40)	16 ± 4 (0-45)	15 ± 3 (0-33)	43 ± 13 ^c (0-132)
-	19	12 ± 3 (0-53)	22 ± 4 ^c (0-53)	10 ± 2 (0-63)	30 ± 5 ^c (0-13)
Grade					
1	3	5 ± 3 (0-13)	14 ± 13 (0-42)	19 ± 5 (10-26)	119 ± 9 ^c (102-132)
2	13	11 ± 3 (0-40)	15 ± 4 (0-38)	9 ± 3 (0-25)	27 ± 5 ^c (0-63)
3	14	16 ± 3 (2-53)	25 ± 4 ^c (5-53)	14 ± 3 (0-35)	21 ± 3 (4-46)
Premenopause	17	11 ± 2 (0-26)	20 ± 4 ^c (0-45)	13 ± 3 (0-35)	33 ± 7 ^c (0-122)
Postmenopause	13	16 ± 4 (0-53)	19 ± 4 (0-53)	10 ± 2 (0-25)	37 ± 11 ^c (0-132)

^a Activities are given as pmol/min/mg protein. ^b Mean ± SE. ^c Significantly different from respective control with p<0.05 ^d Minimum and maximum range. ^e + : Chemotherapy received, -: Chemotherapy not received. ^f Estrogen Receptor Status, +: positive, -: negative (Adapted from Su-Geylan et al., 2006)

to mean NAT1 activities in tumor and control breast tissues of patients without chemotherapy treatment, although, it did not reach statistical significance. Similarly, the mean NAT1 activity of tumor tissues in estrogen receptor-positive group (11/30, 37%) was not significantly higher than that of matched controls. The mean NAT1 activity of breast tumor tissues in estrogen receptor-negative group, however, was significantly higher with a $p < 0.05$. A trend for decrease in both breast control and tumor mean NAT1 activities were observed within the estrogen receptor positive group compared to those in estrogen receptor negative group, but it was not significant.

Only in grade 3, there was a significant increase in mean NAT1 activity in breast tumor tissues compared to matched controls. However, there seemed to be a positive correlation between mean NAT1 activities of control and tumor breast tissues and grade of the malignancy. The mean NAT1 activity in both control and tumor tissues was found to be increasing with higher grades.

Menopausal state of the patient does not seem to effect NAT1 activity as control and tumor mean NAT1 activities of postmenopausal patients (13/30, 43%) are not significantly different than premenopausal (17/30, 57%) control and tumor mean NAT1 activities. Within the premenopausal group mean NAT1 activity in tumor tissues was found to significantly higher than the control group.

NAT2 activities of tumor and tumor-free tissues ranged from 0-35 and 0-132 pmol/mg protein/min, respectively (Table 16). NAT2 displayed higher activity in 90 % (27/30) of tumor tissues compared to their respective controls, mean breast tumor NAT2 activity was significantly higher than corresponding tumor-free breast tissues with $p < 0,05$. Among control tissues, the percentage of measurable NAT2 activity was 77% (23/30), while in tumor tissues it increased 91 % (28/30).

Smoking did not seem to stimulate the NAT2 activity as for the three patients' activities detected in tumor tissue were either indifferent or not changing significantly compared to matched control samples.

Among the patients who received chemotherapy treatment, the mean NAT2 activity of tumor tissues was not significantly different than that of matched controls. On contrary, among the patients who did not receive chemotherapy (24/30, 80%), the mean NAT2 activity of breast tumor tissues was significantly higher. In the treated group, there was a trend for decrease in both tumor and control mean NAT2 activities compared to mean NAT2 activities in tumor and control breast tissues of patients without chemotherapy treatment, although, it did not reach statistical significance.

The mean NAT2 activity of breast tumor tissues was significantly higher than that of matched controls irrespective of estrogen receptor status. A trend for increase in both, breast control and tumor tissue mean NAT2 activities were observed in estrogen receptor positive group compared to estrogen receptor negative group, but it was not significant.

A significant increase in the mean NAT2 activity of breast tumor tissues was detected in grades 1 and 2, while in grade 3, mean NAT2 activity of breast tumor tissues was significantly indifferent from matched controls. Grade of the malignancy does not seem to stimulate NAT2 activity, as mean NAT2 activities in both control and tumor tissues were not changing significantly between different grades.

For postmenopausal and premenopausal group, mean breast tumor NAT2 activities were significantly higher than matched controls for both groups. Mean tumor NAT2 activity within postmenopausal group was significantly higher than mean premenopausal NAT2 tumor activity. Menopausal state of the individuals might be affecting NAT2 activity within human breast.

3.3 Genotype Determination of NATs from Human Breast Tissues

Ten breast cancer patients were selected for both genotyping and activity determination of NATs based on the sample tissue size. Among those patients 8 were diagnosed with invasive ductal cancer, which is a more frequently encountered type of breast cancer and 2 with invasive lobular cancer of the breast. The mean (\pm SE)

age for these breast cancer patients was 45 years (± 1.8 ; range 38-58) (Table 15). All had relatively early menarche; increasing lifetime exposure to estrogens, with the mean age being 12.5 ± 0.3 (mean \pm SE). On the other hand, all had at least one child before the age of 30 with a mean age 21 ± 1.2 (mean \pm SE).

Table 17: Variables with the susceptibility of breast cancer among 10 breast cancer patients

Variables	n=10
Age	45.2 ± 1.8
Age at menarche	12.5 ± 0.3
Age at full-term first pregnancy	21.1 ± 1.2
Menopausal Status [†]	
Premenopausal	80
Postmenopausal	20
Estrogen Receptor [†]	
Positive	70
Negative	30

Represented as mean \pm standard error and [†] percent.

Our methodology allowed to detect 7 NAT1 and NAT2 alleles, but only four and five different alleles for NAT1 (NAT1*4, NAT1*3, NAT1*10, NAT1*11) and NAT2 (NAT2*4, NAT1*5A, NAT2*5B, NAT2*5C, NAT2*6A) were found in this small group of breast cancer patients, respectively. Among them, for NAT1, NAT1*4, the wild type allele and for NAT2, slow acetylator, NAT2 6A allele, were the most common alleles (Table 18).

Table 18: NAT1 and NAT2 allele distributions among 10 breast cancer patients

NAT1 alleles		NAT2 alleles	
Putative rapid alleles	n	Rapid alleles	N
NAT1*10	3	NAT2*4	2
NAT1*11	6		
Normal alleles	n	Slow alleles	N
NAT1*4	10	NAT2*5A	6
NAT1*3	1	NAT2*5B	4
		NAT2*5C	1
		NAT2*6A	7
Total	20		20

Examples of PCR amplifications and RFLP patterns for NAT1 and NAT2 are shown in Figure 19 and 20.

NAT1*11, classified as potential high activity allele (Hein et al, 2000), was the second common allele. Previous studies reported that the rare NAT1*11/any genotype was three times more frequent among breast cancer patients compared to controls (Zheng et al., 1999, Lee et al., 2003). The other putative rapid allele, NAT1*10, which was found to be slightly more common in cases than in controls by Hein and coworkers (Hein et al, 2000), was overrepresented compared to NAT1*3 allele within our group.

The slow acetylator alleles were predominating for NAT2. Among them, NAT2*5A was the second most common alleles (Table 18). NAT2*5A was found to be low frequency allele with 1.3 % compared to high frequency NAT2*6A (30.5 %) allele, in a study determining NAT2 genotypes in a group of 303 patients with a broad range of non-malignant diseases from south-east Anatolia (Aynacioglu et al.,

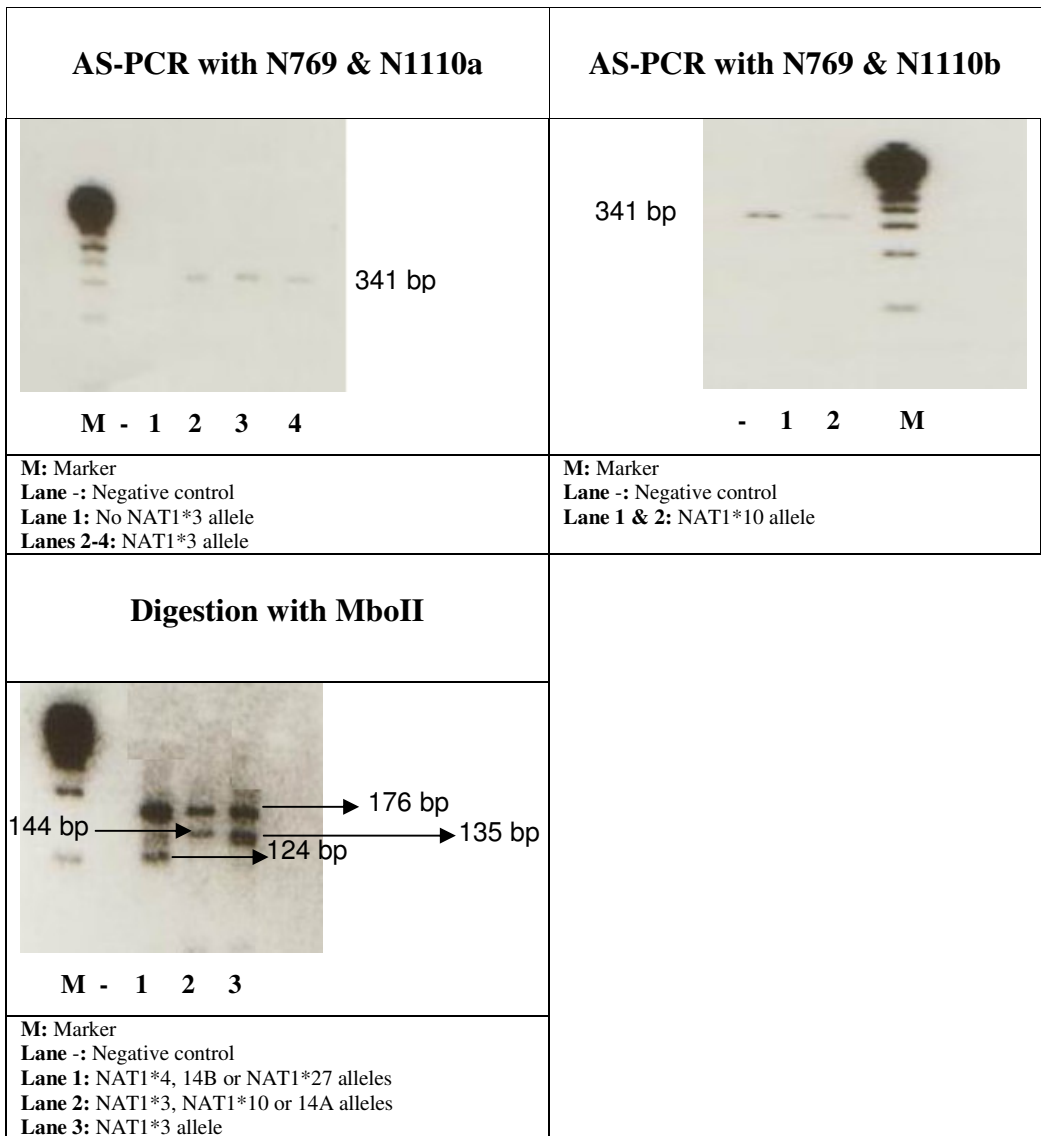


Figure 19: Examples of PCR and RFLP used to determine NAT1* Genotype

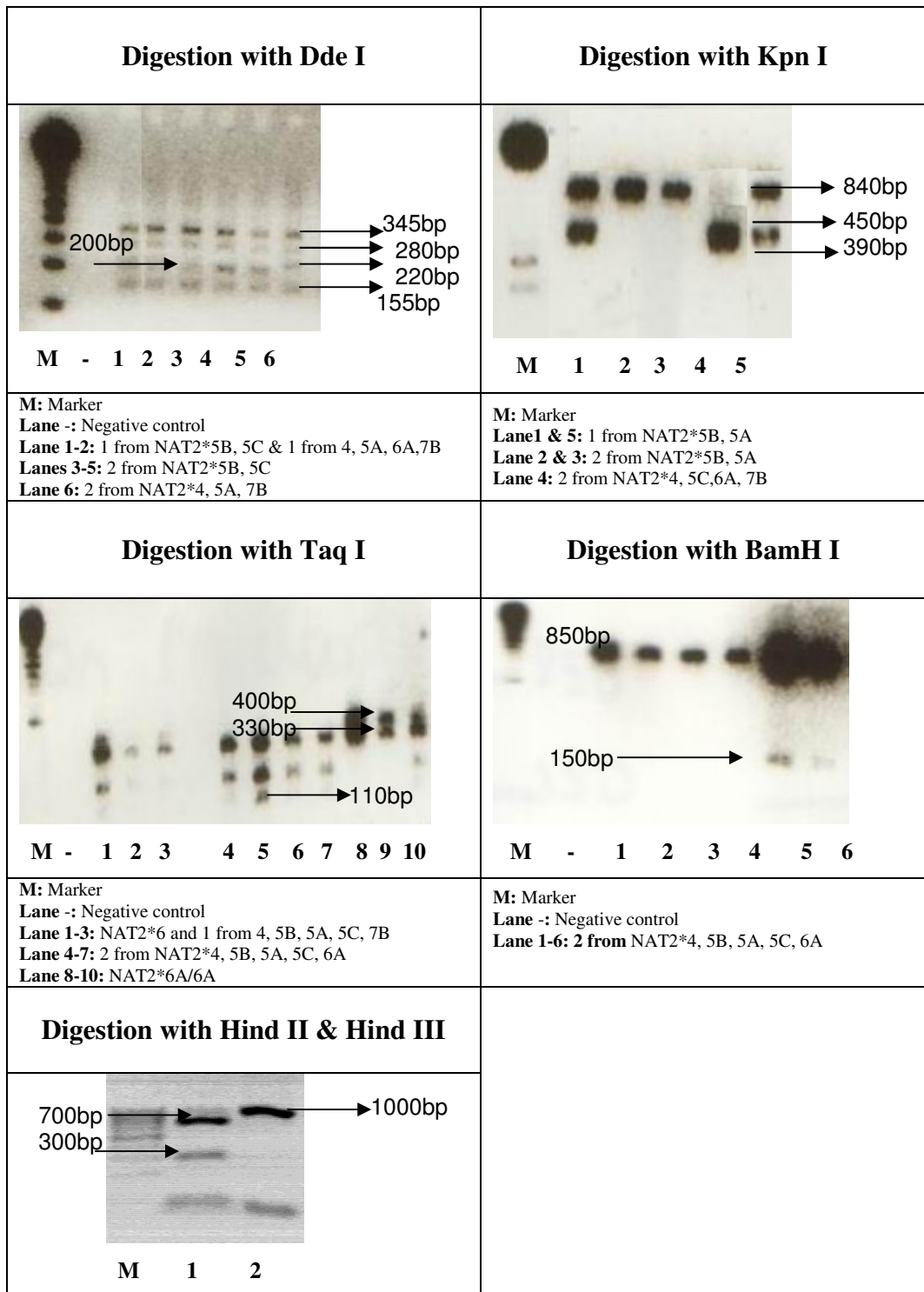


Figure 20: Examples of PCR and RFLP used to determine NAT2* Genotype

1997). The G191A substitution common to the NAT2*14 gene cluster is present in African-American and native Africans, but it is virtually absent in Caucasians, Asians and Turks. Similar to the findings of Aynacioglu and coworkers (1997), we couldn't detect NAT2*14 allele within our group.

Only two patients were postmenopausal and both were found to possess slow NAT2 alleles and putative rapid NAT1 alleles (one being homozygous for NAT1*11).

Genotype distributions of NAT1 and NAT2 for 10 breast cancer patients are shown in Table 19.

In our group, the most prevalent genotype for NAT1 was NAT1*4/ NAT1*4. However, Zheng and colleague reported that the rare NAT1*11/any genotype was three times more frequent among breast cancer patients compared to controls (Zheng et al., 1999). Slow acetylator genotypes NAT2*5A/NAT2*5B and NAT2*5A/NAT2*6A were more prevalent for NAT2. However, in a case control study conducted on 84 breast cancer patients from Ankara, NAT2*5B/NAT2*6A genotype was detected to be slightly more common in cases than in controls (Kocabaş et al., 2004). The only rapid acetylator genotype detected for NAT2 in the group was the NAT2*4/NAT2*6A, Kocabaş and coworkers (2004) also detected this genotype as the highest frequency genotype among cases compared to controls.

Among premenopausal women slow acetylator genotype was predominant for NAT2, while NAT1 genotypes were mostly consisted of normal alleles. The putative rapid and normal acetylator genotypes for NAT1 were nearly equally distributed in the estrogen receptor positive group, while normal genotype seemed to predominate within the estrogen receptor negative group. There was a trend for NAT2 slow acetylator genotypes irrespective of estrogen receptor status.

Table 19. Genotype distributions of NAT1 and NAT2 among 10 breast cancer patients

NAT1 Genotypes	n	NAT2 Genotypes	n
Putative Rapid		Rapid	
*10/*11	2	*4/*6A	2
*11/*11	2		
Sum rapid	4	Sum rapid	2
Normal		Slow	
*4/*4	4	*5A/*5B	3
*4/*3	1	*5A/*5C	1
*4/*10	1	*5A/*6A	2
		*5B/*6A	1
		*6A/*6A	1
Sum normal	6	Sum Slow	8
Total	10	Total	10

NAT1 and NAT2 genotypes of 10 breast cancer patients and their respective phenotypes determined from matched tumor and tumor-free breast tissues are given in Table 20. The distribution of genotypes among those patients was mentioned previously (Table 19). In order to investigate the genotype and phenotype correlations within breast tissue, mean control and tumor NATs activities were compared to respective genotypes in Table 21. There was a trend for significantly increased mean tumor NATs activities irrespective of genotype. However, as only two patients were NAT2 rapid acetylators, the mean tumor NAT2 activity could not be analysed statistically.

In terms of NAT1 genotypes, the patients were divided into two groups as normal and putative rapid acetylators. It was observed that for normal NAT1

Table 20. Genotype and phenotype of NATs from 10 breast cancer patients

	NAT1 Genotype	NAT1 Activity^a	
Patient	Normal	Control	Tumor
KÖ	*4/*4	5.2	27.76
ZA	*4/*4	10.1	29.2
GD	*4/*4	8.6	30.5
HS	*4/*10	14	45
NS	*4/*4	15.3	36.7
SÇ	*4/*3	19.5	24.6
Patient	Putative Rapid	Control	Tumor
MA	*10/*11	6.4	9.7
NM	*11*11	1.2	1.2
DT	*11/*11	9.2	29.4
ZÖ	*10/*11	2.4	5.3
	NAT2 Genotype	NAT2 Activity	
Patient	Slow	Control	Tumor
MA	*5A/*5 B	12.2	19.3
KÖ	*5A/*5 C	28.1	31.6
ZA	*5A/*5 B	6	19.1
GD	*6A/*6A	17.3	21.1
HS	*5A/*6A	33	41
DT	*5B/*6A	16	23
NS	*5A/*5 B	4.5	13
SÇ	*5A/*6A	14	18
Patient	Rapid	Control	Tumor
NM	*4/*6A	26	122
ZÖ	*4/*6A	26.2	33.4

^aNATs activities were given as pmol/min/mg protein.

genotypes, mean tumor NAT1 activities was significantly increased compared to control. However, when the mean control and tumor NAT1 activities in normal NAT1 genotype were compared to putative rapid NAT1 genotypes' respective control and tumor mean NAT1 activities, both control and tumor mean NAT1 activities were observed to be significantly lowered rapid NAT1 genotypes. This finding is in agreement with the findings of Williams and colleagues (Williams et al., 2001), they had also shown that NAT1*10/*any allele and NAT1*11/*any allele

genotype correlated with slow acetylation in breast and rapid acetylation in colon tissues.

Table 21. Comparison of genotype and phenotype of NATs in breast cancer patients

NAT1 Genotype	n	NAT1 Activity ^a		NAT2 Genotype	n	NAT2 Activity	
		Control	Tumor			Control	Tumor
Normal	6	12.1±2.1 ^b	32.3±3 ^c	Rapid	2	26.1±0.1	77.7±44.3
Putative Rapid	4	4.8±1.8	11.4±6.2 ^c	Slow	8	16.4±3.5	23.3±3.1 ^c

^aNATs activities were given as pmol/min/mg protein.

^bMean values are given as Mean ±Standard Error.

^cSignificantly different with p>0.05.

Patients were classified as rapid or slow acetylators in terms of NAT2 genotypes. Among slow NAT2 acetylators, mean tumor NAT2 activities was found to be significantly higher than respective controls. It is known that NAT2 genotype and phenotype correlations are more straight-forward compared to NAT1. Rapid acetylators mean NAT2 control and tumor activities were observed to be higher than slow acetylators, however, statistical analysis could not be carried out as there were only two NAT2 rapid acetylators.

CHAPTER 4

DISCUSSION

AcCoA-dependent arylamine N-acetyltransferases catalyse the acetyl transfer from acetyl coenzyme A to an aromatic amine, heterocyclic amine or hydrazine compound. In humans, acetylation is a major route of biotransformation for many arylamine and hydrazine drugs, as well as for a number of carcinogens present in the diet, cigarette smoke and the environment (Minchin et al., 1992, Hein et al.,1993). Those carcinogens are commonly lipophilic in nature, so they can be stored and concentrated in the breast fat pad. Moreover, mammary epithelial cells were shown to have the ability to metabolize those carcinogens into DNA-binding species (Li et al., 1996).

Arylamine N-acetyltransferases are polymorphic and can detoxify carcinogens by N-acetylation or transform to more potent forms by O-acetylation activity (Sadrieh et al., 1996, Stone et al., 1998). In this respect, the possible role of N-acetyltransferase in the initiation of certain cancers including that of the breast was investigated in humans. Although, some studies had provided evidence for such associations, the results of other studies were contradictory to each other. These contradictions could be explained by the fact that the data at hand was still limited.

Up to date, all the experiments carried on NATs in relation to breast cancer have been conducted on blood, either to determine the NATs genotypes or activities. However, the breast tissue specific acetylation might be more important in terms of initiation of breast cancer. Thus, in this study, purification of arylamine N-acetyltransferases from human breast control (tumor-free) and tumor tissues were carried on in order to compare the protein profiles and to further characterize some biochemical properties of the isoforms.

The purification of the arylamine N-acetyltransferases from human breast tumor cytosolic fractions was carried out basically according to the purification protocols given by Grant et al. (1989) and Whitaker et al. (1993) with some modifications. The purification scheme consisted of a sequential ion-exchange (DEAE-Cellulose) and affinity (Blue-Sepharose CL-6B) column chromatography using PABA and SMZ as substrates to follow the activity of NAT1 and NAT2 in the eluted fractions, respectively.

The ion-exchange step proved to be efficient in separating the NATs isoforms and provided about 5 and 3 purification fold with 77 and 21% recovery of the activities for NAT1 and NAT2, respectively. However, with this step only a partial purification could be achieved. Further purification in Blue-Sepharose could not be pursued successfully as protein amount was not ample and the NATs activities were completely lost.

For biochemical characterization of NATs molecular weight and isoelectric point (pI) determinations were carried out. As, the polyclonal antibody could only recognize NAT1, NAT2 isoform's characterizations could not be performed. SDS-PAGE and Western blotting analysis showed that NAT1 had a molecular weight of about 27600 Da. Analysis have revealed an approximate isoelectric point (pI) of about 4.8 for NAT1. Arylamine N-acetyltransferases purified from human liver had a molecular weight of 31000 Da determined by SDS-PAGE. The isoelectric point was determined as 4.8 for NAT1 and 4.75 for NAT2 from human liver (Grant et al., 1989). The NAT1 in breast tissue seems to be similar to liver isoform, as the approximate molecular weight and the pI values determined are close to the ones determined for liver isoform.

Three reduction mammoplasty, three benign and matched controls, five primary breast tumor tissues and matched five tumor-free samples, were subjected to immunohistochemical staining for analysis of NAT1 expression. In all specimens diffuse cytoplasmic staining was observed in mammary epithelial cells, while immunoreactivity of NAT1 in stroma was not observed. However, level of intensity of NAT1 immunostaining was observed to be going from weak in reduction

mammoplasty samples to strongest in malignant breast tissue. This is similar to the findings of Adam and coworkers who detected an increase in staining intensity of NAT1 in breast tumor tissues (Adam et al., 2003).

Attempts for purification of NATs from normal breast tissues were not successful owing either to the comparatively lower amount of NATs within normal tissues or rapid denaturation of the isoforms, so we could not compare protein profiles of NATs from human tumor and tumor-free breast tissues. In order to understand the molecular basis of the disease, the activity levels of NATs from control and tumor breast tissues were studied.

The differences in the cytosolic NATs enzymes activities within tumor and tumor free tissues were investigated in breast tumors and surrounding tumor-free tissues which were obtained from 30 female breast cancer patients with infiltrating ductal cancer, aged between 37-76, who had undergone mastectomy in İbni Sina Hospital, Sıhhiye, Ankara. Among the study group, 10 breast samples were selected for determination of NAT1 and NAT2 genotypes. Those patients completed a questionnaire on factors that might have influenced the expression of NATs, such as medication, smoking and alcohol consumption.

Six of the patients received 2-3 cycles of adjuvant standard combination chemotherapy (cyclophosphamide, methotrexalate, classical CMF, cyclophosphamide, epirubicin, 5-fluorouracil, CEF, Navelbine and Adriablastin) before mastectomy. Three of the patients were current smokers (10-20 cigarettes/day). None of the patients were alcohol drinkers. The menopausal status, estrogen receptor status and grade groupings of the patients were also recorded. Further, the possible impacts of grade of malignancy, chemotherapy treatment, estrogen receptor status and menopausal status on enzyme activity were evaluated.

Significant differences in both, NAT1 and NAT2 activities between tumors and tumor-free breast tissues were noted. In our previous study which was conducted in a group of breast cancer patients (n=12) with infiltrating ductal cancer,

we could not detect a significant difference in between mean tumor and control NAT1 activities, most probably due to small sample size (Geylan et al., 2001).

Among the patients who had received chemotherapy treatment, mean tumor NAT1 and NAT2 activities were indifferent from their matched controls. However, there was a trend for decrease in mean activities of both control and tumor mean NATs activities in treated group compared mean control and tumor activities among patients who did not receive any chemotherapy. Both, NAT1 and NAT2 were shown to be inhibited by the chemopreventive agent, paclitaxel, in human lung cell-line, the chemotherapeutic agents used in treatment of breast cancer may also have possible inhibitory effects on NATs in human breast cancer tissues (Hsia et al., 2002).

In the estrogen receptor positive group, mean tumor NAT1 and NAT2 activities were indifferent from their matched controls. Mean NAT1 breast control and tumor tissues' activities of estrogen receptor positive group were lower compared to mean NAT1 control and tumor activity within the estrogen receptor negative group. In a recent study, ER-positive cell lines T47D and MCF7 were found to express less NAT1 than the ER-negative cell lines BT20 and MB-MDA-468 (Adam et al., 2003). On the other hand, mean NAT2 breast control and tumor tissues' activities of estrogen receptor positive group were higher compared to mean NAT2 control and tumor activity within the estrogen receptor negative group. The differences in impact of ER status on NAT enzyme activity may be due to independent regulation of NAT1 and NAT2 genes (Grant et al., 1991). Lee, et al. (1997) in his work has shown that estrogen receptor positive patients NAT1 and NAT2 activities are inhibited via the antiestrogenic drug, tamoxifen, more compared to estrogen receptor negative patients. There is no information onto whether those patients who are estrogen receptor positive had usage of antiestrogenic drugs in their treatment and also, the estrogen receptor positive group is small in sample size. Due to these reasons, the changes in NAT1 and NAT2 mean tumor activities might not be reaching significance.

Mean NAT1 activity in both control and tumor tissues was found to be increasing with higher grades which was suggestive of a positive correlation

between mean NAT1 activities of control and tumor breast tissues and grade of the malignancy. The reason why the increase in NAT1 activity is not statistically significant may be due to the small size of the study group. Grade of the malignancy does not seem to stimulate NAT2 activity, as mean NAT2 activities in both control and tumor tissues were not changing significantly between different grades.

Only among premenopausal patients mean NAT1 activity exhibited a significant increase in tumor tissues. As, control and tumor mean NAT1 activities of postmenopausal patients are not significantly different than premenopausal control and tumor mean NAT1 activities, menopausal state of the patient does not seem to effect NAT1 activity. This is the first study investigating the activities of NAT1 in tumor and tumor-free tissues in patients of breast cancer according to menopausal status. On the other hand, the NAT2 mean tumor activity within postmenopausal group was found to be significantly higher than mean premenopausal NAT2 tumor activity. In mouse, the induction of kidney N-acetylation activity by androgens acting on HRE was reported (Estrada-Rodgers et al., 1998). However, there is no information in literature on hormonal regulation of human NATs.

As, 90 % of tumor tissues (27/30) among patients possessed higher NAT2 activities than controls, mean NAT2 activity tumor tissues were significantly higher than mean tumor-free NAT2 activity. This tendency was not changing when estrogen receptor status, menopausal status is considered. Although, Williams et al. (2001) have detected NAT2 mRNA to be two to three-folds lower than NAT1 mRNA in healthy breast tissue obtained from reduction mammoplasty operations, we detected significant increases mostly in NAT2 activities in tumor tissues compared to tumor-free tissues.

Genotype determinations from 10 patients revealed a prevalence of slow acetylator genotypes for NAT2, while normal (wild-type) acetylator genotypes predominated for NAT1. Among them, two patients were postmenopausal possessing slow NAT2 and rapid NAT1 genotypes (one being homozygous for NAT1*11). Some studies report an increased risk for breast cancer among slow acetylator postmenopausal women who smoked (Ambrosone et al., 1996, Huang et al., 1999).

The postmenopausal patients in the group were not smokers; however, they consumed well-done meat on a regular basis. Dose-dependent increases in breast cancer risk were reported for red meat intake and meat doneness level, with the risk being particularly elevated among women possessing NAT1*11 allele (Zheng et al., 1999).

The putative rapid alleles, NAT1*11 and NAT1*10 both of which were found to be more common in cases compared to controls (Zheng et al., 1999, Lee et al., 2003) were also overrepresented in our group compared to NAT1*3 allele. For NAT2, slow acetylator alleles, NAT2*5A and NAT2*6A were the common ones. NAT2*6A was found to be a high frequency allele, but NAT2*5A is a low frequency allele among Turkish population (Aynacioglu, et al., 1997, Kocabas et al., 2004). The possible significance of NAT2*5A and NAT1*11 alleles in breast cancer should be assessed in a case control study where the sample numbers are increased. Among the allelic variants of NAT1* gene, NAT1*10 allele was reported to increase the risk of breast cancer 4-fold among women who consumed well-done meat (Krajinovic et al., 2000). NAT1*10 is an allele with a mutation at 3' polyadenylation site (Hein et al., 1993), resulting in rapid acetylator phenotype, however, its prevalence in our population is not known.

When the genotype and phenotype correlations of NATs within breast tissue were investigated, a trend for significantly increased mean tumor NATs activities irrespective of genotype was observed. The putative rapid NAT1 genotypes, on the contrary, displayed lower control and tumor mean NAT1 activities compared to normal NAT1 genotypes. Patients were classified as rapid or slow acetylators in terms of NAT2 genotypes. Among slow NAT2 acetylators, mean tumor NAT2 activities was found to be significantly higher than respective controls.

In conclusion, NATs were partially purified with complete separation of the isozymes in ion-exchanger step. The partially purified NATs molecular weight was determined as 27600 for NAT1. The isoelectric point was determined approximately as 4.8 for NAT1. With immunohistochemical analysis, level of intensity of NAT1 immunostaining was observed to be going from weak in reduction

mammoplasty samples to strongest in malignant breast tissue. NAT1 and NAT2 display significant differences between tumor and tumor-free breast tissues in a total of 30 female breast cancer patients with infiltrating breast cancer. Chemotherapy treatment was observed to have a slight inhibitory effect on mean NAT1 and NAT2 activities. There was an indication of a possible negative association with mean NAT1 activity and estrogen receptor status, while mean tumor NAT2 activity was observed to increase among estrogen receptor positive patients. Grade of malignancy seems to be positively associated with NAT1, but no such association could be suggested for NAT2 enzyme. Menopausal state of the patient suggested having a significant effect on NAT2 activity. Although, both NAT1 and NAT2 have a trend for increased mean tumor activities, the role of these isozymes in chemical carcinogenesis could not be clearly established in breast cancer irrespective of grade of malignancy, chemotherapy status, menopausal status or estrogen receptor status. NAT2 slow acetylator genotype was predominating among 10 breast cancer patients with NAT2*5A allele being most common. NAT1*11 allele was prevalent among postmenopausal women. When the genotype and phenotype correlations of NATs within breast tissue were investigated, a trend for significantly increased mean tumor NATs activities irrespective of genotype was observed. The putative rapid NAT1 genotypes was found to display lower control and tumor mean NAT1 activities compared to normal NAT1 genotypes. Among slow NAT2 acetylators, mean tumor NAT2 activities was found to be significantly higher than respective controls.

REFERENCES

Adam PJ, Berry J, Loader JA, Tyson KL, Craggs G. Arylamine N-Acetyltransferase-1 Is Highly Expressed in Breast Cancers and Conveys Enhanced Growth and Resistance to Etoposide *in Vitro*. *Mol Cancer Res* 2003;1: 826-835.

Ambrosone CB, Freudenheim JL, Marshall JR, Graham S, Vena JE et al. Extensive acetylation and relation to lobular breast cancer. *Ann NY Acad Sci* 1995; 758: 250-252.

Ambrosone CB, Freudenheim JL, Graham S, Marshall JR, Vena JE, et al. Cigarette smoking, N-acetyltransferase 2 genetic polymorphisms, and breast cancer risk. *J Am Med Assoc* 1996; 276: 1494–1501.

Andres HH, Kolb HJ, Weiss L. Purification and physicochemical characteristics of acetyl CoA: arylamine N-acetyltransferases from pigeon liver. *Biochim Biophys Act* 1983; 746: 182-192.

Andres HH, Klem AJ, Zsabo SM, Weber WW. New Spectrophotometric and radiochemical assays for acetyl-CoA: arylamine N-acetyltransferase applicable to a variety of arylamines. *Anal Chem* 1985; 145: 367-375.

Andres HH, Klem AJ, Schopfer LM, Harrison JK, Weber WW. On the active site of liver acetyl-CoA. Arylamine N-acetyltransferase from rapid acetylator rabbits(III/J). *J Biol Chem* 1988; 263: 7521-7527.

Aynacioglu S, Cascorbi I, Mrozikiewicz PM, Roots I. Arylamine N-acetyltransferase (NAT2) genotypes in a Turkish population. *Pharmacogenetics* 1997; 7: 327-331.

Azzopardi JG, Chepik OF, Hartman WH. Histologic typing of breast tumors. *Am J Clin Pathol* 1982; 78: 806.

Badawi AF, Hirvonen A, Bell DA, Lang NP, Kadlubar FF. Role of aromatic amine N-acetyltransferases, NAT1 and NAT2, in carcinogen DNA adduct formation in the human urinary bladder. *Cancer Res* 1995; 55: 5230-5237.

Bell DA, Taylor JA, Butler MA, Stephens EA, Wiest J et al. Genotype/phenotype discordance for human arylamine N-acetyltransferase (NAT2) reveals a new slow acetylator allele common in African-Americans. *Carcinogenesis* 1993; 14: 1689-1692.

Bell DA, Badawi AF, Lang NP, Kadlubar FF, Hirvonen A. Polymorphism in the N-acetyltransferase (NAT1) polyadenylation signal: association of NAT1*10 allele with higher N-acetylation activity in bladder and colon tissue. *Cancer Res* 1995; 55: 5226-5229.

Blum M, Grant DM, Demierre A, Meyer UA. N-acetylation pharmacogenetics: a gene deletion causes absence of arylamine N-acetyltransferase in liver of slow acetylator rabbits. *Proc Natl Acad Sci USA* 1989; 86: 9554-9557.

Blum M, Grant DM, Demierre A, Meyer UA. Nucleotide sequence of a full-length cDNA for arylamine N-acetyltransferase from rabbit liver. *Nucl Acids Res* 1989; 17: 3589.

Blum M, Grant DM, McBride W, Heim M, Meyer UA. Human arylamine N-acetyltransferase genes: isolation, chromosomal localization, and functional expression. *DNA & Cell Biol* 1990; 9: 193-203.

Blum M, Grant DM, Demierre A, Heim M, Meyer UA. Molecular mechanism of slow acetylation of drugs and carcinogens in humans. *Proc Natl Acad Sci USA* 1991; 88: 5237-5241.

Bova GS, Carter BS, Bussemakers MJ, Emi M, Fujiwara Y et al. Homozygous deletion and frequent allelic loss of chromosome 8p22 loci in human prostate cancer. *Cancer Res* 1993; 53:3869-3873.

Bradford MM. A rapid and sensitive method for the quantitation of microgram quantities of protein utilizing the principle of protein-dye binding. *Anal Biochem* 1976; 72: 248-54.

Bruhn C, Brockmoller J, Cascorbi I, Roots I, Borchert HH. Correlation between genotype and phenotype of the human arylamine N-acetyltransferase type 1 (NAT1). *Biochem Pharmacol* 1999; 58: 1759-1764.

Butcher NJ, Ilett KF, Minchin RF. Functional polymorphism of the human arylamine N-acetyltransferase type 1 gene caused by C190T and G560A mutations. *Pharmacogenetics* 1998; 8: 67-72.

Cascorbi I, Drakoulis N, Brockmoller J, Maurer A, Sperling K et al. Arylamine N-acetyltransferase (NAT2) mutations and their allelic linkage in unrelated Caucasian individuals: correlation with phenotypic activity. *Am J Hum Genet* 1995; 57: 581-592.

Chang LH, Chuang LF, Tasi CP, Tu CPD, Tam MF. Characterization of glutathione S-transferases from day-old chick livers. *Biochemistry* 1990; 29: 744-750.

Chung JG, Lee JH, Ho CC, Lai JM, Chou YC. A survey of arylamine N-acetyltransferase activity in common fruits and vegetables. *J Food Biochem* 1997; 20: 481-490.

Cribb AE, Grant DM, Miller MA, Spielberg SP. Expression of monomorphic Arylamine N-acetyltransferase (NAT1) in human leukocytes. *J Pharmacol Exp Ther* 1991; 259(3): 1241-1246.

De Leon JH, Martell KJ, Vatsis KP, Weber WW. Slow acetylation in mice is caused by a labile and catalytically impaired mutant N-acetyltransferase (NAT2 9). *Drug Metab Dispos* 1995; 23: 1354-1361.

De Leon JH, Vatsis KP, Weber WW. Characterization of naturally occurring and recombinant human N-acetyltransferase variants encoded by NAT1. *Mol Pharmacol* 2000; 58: 288-299.

Delomenie C, Goodfellow GH, Krishnamoorthy R, Grant DM, Dupret JM. Study of the role of the highly conserved residues Arg9 and Arg64 in the catalytic function of human N-acetyltransferases NAT1 and NAT2 by site directed mutagenesis. *Biochem J* 1997; 323: 207-215.

Dhaini HR, Levy GN. Arylamine N-acetyltransferase 1 (NAT1) genotypes in a Lebanese population. *Pharmacogenetics* 2000; 10: 79-83.

Donegon WL and Perez-Mesa CM. Lobular cancer: An indicator for elective biopsy of the second breast. *Ann Surg* 1972; 177: 178-187.

Donelson Laboratory. Rapid Silver Stain of SDS-PAGE Gel

<http://www.biochem.uiowa.edu/donelson/Database%20items/Rapid%20Silver%20Stain.doc> (Last access: 13 January 2006)

Dixon JM, Anderson TJ, Page DL. Infiltrating lobular cancer of the breast. An evaluation of the incidence and consequences of bilateral disease. *Br J Surg* 1983; 70: 513.

Dupret JM, Grant DM. Site directed mutagenesis of recombinant human arylamine N-acetyltransferase expressed in Escherichia coli. Evidence for direct involvement of Cys 68 in the catalytic mechanism of polymorphic human NAT2. *J Biol Chem* 1992; 267: 7381-7385.

Dupret JM, Goodfellow GH, Janezic SA, Grant DM. Structure-function studies of human arylamine N-acetyltransferases NAT1 and NAT2. Functional analysis of recombinant NAT1/NAT2 chimeras expressed in *E. coli*. *J Biol Chem* 1994; 269: 26830-26835.

Ebisawa T, Deguchi T. Structure and restriction length polymorphism of genes for human liver arylamine N-acetyltransferases. *Biochem Biophys Res Commun* 1991; 177: 1252-1257.

Estrada-Rodgers L, Levy GN, Weber WW. Substrate selectivity of mouse N-acetyltransferases 1, 2 and 3 expressed in COS-1 cells. *Drug Metab Dispos* 1998; 26: 502-505.

Evans DA. N-acetyltransferase. *Pharmacol Therapeut* 1989; 42: 157-234.

Fakis G, Boukolova S, Buckle V, Payton M, Denning C et al. Chromosome mapping for the genes for murine N-acetyltransferases (NATs), enzymes involved in the metabolism of carcinogens: identification of a novel upstream noncoding exon for murine Nat2. *Cytogenet Cell Genet* 2000; 90: 134-138.

Ferguson RJ, Doll MA, Rustan TD, Hein DW. Cloning, expression and functional characterization of rapid and slow acetylator polymorphic N-acetyl-transferase encoding genes of the Syrian hamster. *Pharmacogenetics* 1996; 6: 55-66.

Firozi PF, Bondy ML, Şahin AA, Chang P, Lukmanji F et al. Aromatic DNA adducts and polymorphisms of CYP1A1, NAT2 and GSTM1 in breast cancer. *Carcinogenesis* 2002; 23(2): 301-306.

Fisher ER, Gregorio RM, Fisher B. The pathology of invasive breast cancer: A syllabus derived from findings of the National Surgical Adjuvant Breast Project (Protocol No. 4). *Cancer* 1975; 36(1): 1-85.

Floss HG, Yu TW. Lessons from the rifamycin biosynthetic gene cluster. *Curr Opin Chem Biol* 1999; 3: 592-597.

Gaubatz LJ. Cooked food mutagens. *JAMA* 1996; 276: 449-450.

Geylan YS, Güray TN, Sak S: Arylamine N-acetyltransferase activities in human breast cancer tissues. *Neoplasma* 2001; 48 (2): 109-112.

Goodfellow GH, Dupret JM, Grant DM. Identification of amino acids imparting acceptor substrate selectivity to human arylamine acetyltransferases NAT1 and NAT2. *Biochem J* 2000 348(1): 159-166.

Grant DM, Blum M, Demierre A, Meyer UA. Nucleotide sequence of an intronless gene for a human N-acetyltransferase related to polymorphic drug acetylation. *Nucl Acids Res* 1989; 17: 3978.

Grant DM, Lottspeich, Meyer UA. Evidence for two closely related isozymes of arylamine N-acetyltransferase in human liver. *FEBS LETT* 1989; 244(1): 203-207.

Grant DM, Morike K, Eichelbaum M, Meyer UA. Acetylation pharmacogenetics. The slow acetylator phenotype is caused by decreased or absent arylamine N-acetyltransferase in human liver. *J Clin Invest* 1990; 85: 968-972.

Grant DM, Blum M, Beer M, Meyer UA. Monomorphic and polymorphic human arylamine N- acetyltransferases:a comparison of liver isozymes and expressed products of two cloned genes. *Mol Pharmacol* 1991; 39: 184-191.

Grant DM, Hughes NC, Janezic SA, Goodfellow GH, Chen HJ et al. Human acetyltransferase polymorphisms. *Mutat Res* 1997; 376: 61-70.

Guray T and Guvenc T. Characterization of sheep liver N-acetyltransferase. *Biochem Arch* 1997; 13: 107-111.

Hayes RB, Rotman N, Broly E, Caporaso N, Feng P et al. N-acetylation phenotype and genotype and risk of bladder cancer in benzidine exposed workers. *Carcinogenesis* 1993; 14: 675-678.

Henderson IC. Risk factors for breast cancer development. *Cancer (Suppl)* 1993; 71: 2127-2140.

Hein DW, Rustan TD, Bucher KD, Martin WJ, Furman EJ. Acetylator phenotype-dependent and -independent expression of arylamine N-acetyltransferase isozymes in rapid and slow acetylator inbred rat liver. *Drug Metab Dispos* 1991; 19: 933-937.

Hein DW, Doll MA, Rustan TD, Gray K, Feng Y et al. metabolic activation and deactivation of arylamine carcinogens by recombinant human NAT1 and polymorphic NAT2 acetyltransferases. *Carcinogenesis* 1993; 14: 1633-1638.

Hein DW, Rustan TD, Ferguson RJ, Doll MA, Gray K. Metabolic activation of aromatic and heterocyclic N-hydroxyarylamines by wild-type and mutant recombinant human NAT1 and NAT2 acetyltransferases. *Arch Toxicol* 1994; 68: 129-133.

Hein DW, Ferguson RJ, Doll MA, Rustan TD, Gray K. Molecular genetics of human polymorphic N-acetyltransferase: enzymatic analysis of 15 recombinant wild-type, mutant and chimeric NAT2 allozymes. *Hum Mol Genet* 1994; 3: 729-734.

Hein DW, Doll MA, Rustan TD, Gray K, Ferguson RJ et al. Construction of Syrian Hamster lines congenic at the polymorphic N-acetyltransferase locus (NAT2): acetylator genotype-dependent N- and O-acetylation of arylamine carcinogens. *Toxicol Appl Pharmacol* 1994; 124: 16-24.

Hein DW, Grant DM, Sim E. Update on consensus arylamine N-acetyltransferase gene nomenclature. *Pharmacogenetics* 2000; 10: 291-292.

Hein DW, Doll MA, Fretland AJ, Leff MA, Webb SJ et al. Molecular genetics and epidemiology of the NAT1 and NAT2 acetylation polymorphisms. *Cancer Epidemiol, Biomarkers & Prevention* 2000; 9: 29-42.

Herpes-Virus Research Laboratory. Antigen Retrieval for immunohistochemistry <http://herpesvirus.tripod.com/research/protoc.htm#Antigen20Retrieval%20for>
(Revised in June 5, 2000; Last access: 21 Ocak 2006)

Hickman D, Risch A, Buckle V, Spurr NK, Jeremiah SJ et al. Chromosomal localization of human genes for arylamine N-acetyltransferase. *Biochem J* 1994; 297: 441-445.

Hjelmeland LM, Nebert DW, Chrambach A. Electrofocusing of integral membrane proteins in mixtures of zwitterionic and nonionic detergents. *Anal Biochem* 1979; 95: 201-208.

Hsia TC, Chung JG, Lu HF, Ho HC, Yang CC et al. The effect of paclitaxel on 2-aminofluorene-DNA adducts formation and arylamine N-acetyltransferase activity and gene expression in human lung tumor cells (A549). *Food Chem Toxicol* 2002; 40(5): 697-703.

Huang CS, Chern HD, Shen CY, Hsu SM, Chang KJ. Association between N-acetyltransferase 2 (NAT2) genetic polymorphism and development of breast cancer in postmenopausal Chinese women in Taiwan, an area of great increase in breast cancer incidence. *Int J Cancer* 1999; 82: 175-179.

Hughes NC, Janesic SA, McQueen KL, Jeweet MA, Castranio T et al. Identification and characterization of the variant alleles of human acetyltransferase NAT1 with defective function using p-aminosalicylate as an in-vivo and in-vitro probe. *Pharmacogenetics* 1998; 8: 55-66.

Kelsey JL and Berkowitz GS. Breast Cancer Epidemiology. *Cancer Res* 1988; 48: 5615-5623.

Kocabas NA, Şardaş S, Cholerton S, Daly AK, Karakaya AE. N-acetyltransferase polymorphism and breast cancer susceptibility: a lack of association in a case control study of Turkish population. *Int J Toxicol* 2004; 23: 25-31.

Krajcinovic M, Ghadirian P, Richer C, Sinnet H, Gandini S et al. Genetic susceptibility in French-Canadians: Role of carcinogen metabolizing enzymes and gene-environment interactions. *Int J Cancer* 2000; 92(2): 220-225.

Laemmli UK. Cleavage of structural proteins during the assembly of the head of bacteriophage T4. *Nature* 1970; 227: 680-685.

Laird PW. Simplified mammalian DNA isolation protocol. *Nucl Acids Res* 1991; 19: 4293.

Lee JH, Chung JG, Lai JM, Levy GN, and Weber WW. Kinetics of arylamine N-acetyltransferase in tissues from human breast cancer. *Cancer Lett* 1997; 111: 39-50.

Lee KM, Park SK, Kim SU, Doll MA, Yoo KY et al., N-acetyltransferase (NAT1, NAT2) and glutathione S-transferase (GSTM1, GSTT1) polymorphisms in breast cancer. *Cancer Lett* 2003; 196(2): 179-186.

Leff MA, Fretland AJ, Doll MA, Hein DW. Novel human N-acetyltransferase 2 alleles that differ in mechanism for slow acetylator phenotype. *J Biol Chem* 1999; 274: 34519-34522.

LeGal M, Ollivier L, Asselain B. Mammographic features of 455 invasive lobular cancers. *Radiology* 1992; 185: 705.

Li D, Wang M, Dhingra K & Hittelman WN. Aromatic DNA adducts in adjacent tissues of breast cancer patients: Clues to breast cancer etiology. *Cancer Res* 1996; 56: 287-293.

Lin HJ, Probst-Hensch NM, Hughes NC, Sakamoto GT, Louie AD et al. Variants of N-acetyltransferase NAT1 and a case control study of colorectal cancers. *Pharmacogenetics* 1998; 8: 269-281.

Maitra A, Tavassoli FA, Albores-Savaedra J, Behrens C, Wistuba II et al. Molecular abnormalities associated with secretory cancers of the breast. *Hum Pathol* 1999; 30: 1435-1440.

Mannens G, Slegers G, Claeys A. Assay for acetyl-CoA: arylamine N-acetyltransferase by high performance liquid chromatography applied to serotonin N-acetylation. *Biochim Biophys Act* 1990; 1037: 1-6.

Martell KJ, Vatsis KP, Weber WW. Molecular genetic basis of rapid and slow acetylation in mice. *Mol Pharmacol* 1991; 40: 218-227.

Martell KJ, Levy GN, Weber WW. Cloned mouse N-acetyltransferases: enzymatic properties of Nat1 and Nat2 gene products. *Mol Pharmacol* 1992; 42: 265-272.

Martinez V and Azzopardi G. Invasive lobular cancer of the breast: Incidence and variants. *Histopathology* 1979; 3: 467.

Matas N, Thygesen P, Stacey M, Risch A, Sim E. Mapping AAC1, AAC2 and AACp, the genes for arylamine N-acetyltransferases, carcinogen metabolizing enzymes on human chromosome 8p22, a region frequently deleted in tumors. *Cytogenet Cell Genet* 1997; 77: 290-295.

Meyer UA, Zanger UM. Molecular mechanisms of genetic polymorphisms of drug metabolism. *Annu Rev Pharmacol Toxicol* 1997; 37: 269-296.

Minchin RF, Reeves PT, Teitel CH, McManus ME, Mojarrabbi B et al. N- and O-acetylation of aromatic and heterocyclic amine carcinogens by human monomorphic and polymorphic acetyltransferases expressed in COS-1 cells. *Biochem Biophys Res Commun* 1992; 185: 839-844.

Minchin RF, Kadlubar FF, Ilett KF. Role of acetylation in colorectal cancer. *Mutat Res* 1993; 290: 35-42.

The Ministry Health of Turkey. Kadınlarda en çok görülen on kanser türü, 1999. <http://www.saglik.gov.tr/extras/istatistikler/apk2001/092.htm>
(Last access: 10 January 2006)

Oguztuzun S, 2000. Immunohistochemical localization of glutathione S-transferases in normal and cancer human breast tissue. Ph.D. Thesis in Biology, METU-Ankara.

Ohsaka S, Deguchi T. Cloning and expression of cDNAs for polymorphic and monomorphic arylamine N-acetyltransferases from human liver. *J Biol Chem* 1990; 265: 4630-4634.

Ozawa S, Medhat A, Kawabuko Y, Tomaha S, Yamazoe Y et al. Monomorphic and polymorphic isozymes of arylamine N-acetyltransferases in hamster liver: purification of the isozymes and genetic basis of N-acetylation polymorphism. *Carcinogenesis* 1990; 11: 2137-2144.

Page DL and Anderson TJ. Diagnostic Histopathology of the Breast. New York, Churchill Livingstone, 198-205.

Payton MA, Sim E. Genotyping human arylamine N-acetyltransferase Type 1 (NAT1): the identification of two novel allelic variants. *Biochem Pharmacol* 1998; 8: 67-72.

Payton M, Mustaq A, Yu TW, Wu LJ, Sinclair J et al. Eubacterial arylamine N-acetyltransferases- identification and comparison of 18 members of the protein family with conserved active site cysteine, histidine and aspartate residues. *Microbiology* 2001; 147:1137-1147.

Reisner AH, Nemes P, Bucholtz C. The use of Coomassie Brilliant Blue G250 perchloric acid solution for staining in electrophoresis and isoelectric focusing on polyacrylamide gels. *Anal Biochem* 1975; 64(2):509-516.

Riddle B & Jencks WP. Acetyl coenzyme A: arylamine N-acetyltransferase. *J Biol Chem* 1971; 216: 3250-3258.

Risch A, Wallace DMA, Bathers S, Sim E. Slow N-acetylation genotype is a susceptibility factor in occupational and smoking related breast cancer. *Hum Molec Gen* 1995; 4: 231-236.

Robertson EF, Dannelly HK, Malloy PJ, Reeves HC. Rapid isoelectric focusing in a vertical polyacrylamide minigel system. *Anal Biochem* 1987;167: 290-294.

Rodrigues-Lima F, Delomenie C, Goodfellow GH, Grant DM, Dupret JM. 3D Model of human arylamine N-acetyltransferase 2: Homology modelling and structural analysis of human arylamine N-acetyltransferase NAT1: evidence for conservation of a cysteine protease catalytic domain and an active-site loop. *Biochem J* 2001; 356: 327-334.

Rodrigues-Lima F, Dupret JM. 3D Model of human arylamine N-acetyltransferase2: Structural basis of the slow acetylator phenotype of the R64Q variant and analysis of the active site loop. *Biochem Biophys Res Commun* 2002; 291: 116-123.

Rodrigues-Lima F, Cooper RN, Goudeau B, Atmane N, Chamagne A et al. Skeletal muscles express the xenobiotic-metabolizing enzyme arylamine N-acetyltransferase. *J Histochem Cytochem* 2003; 51(6): 789-796.

Rosen PP and Oberman HA. Atlas of Tumor Pathology. *Tumors of the Mammary Gland* 1992. Washington, DC Armed Forces Institute of Pathology.

Sadrieh N, Davis CD and Synderwine EG. N-acetyltransferase expression and metabolism of the food-derived heterocyclic amines in the human mammary gland. *Cancer Res* 1996; 56, 2683-87.

Sandy J, Mustaq A, Kawamura A, Sim E, Noble M. The structure of arylamine N-acetyltransferase from *Mycobacterium smegmatis*--an enzyme which inactivates the anti-tubercular drug, isoniazid. *J Mol Biol* 2002;

Sinclair JC & Sim E. A fragment consisting of the first 204 amino-terminal amino acids of human arylamine N-acetyltransferase 1 (NAT1) and the first transacetylation step of catalysis. *Biochem Pharmacol* 1997; 53: 11-16.

Sinclair JC, Sandy J, Delgoda R, Sim E, Noble ME. Structure of arylamine N-acetyltransferase reveals a catalytic triad. *Nat Struct Biol* 2000; 7: 560-564.

Stanley LA, Mills IG, Sim E. Localization of polymorphic N-acetyltransferase (NAT2) in tissues of inbred mice. *Pharmacogenetics* 1997; 7: 121-130.

Stone EM, Williams JA, Grover PL, Gusterson BA, Phillips DH. Interindividual variation in the metabolic activation of heterocyclic amines and their N-hydroxy derivatives in primary cultures of human mammary epithelial cells. *Carcinogenesis* 1998; 19(5): 873-879.

Strete D. *A Color Atlas of Histology*, 1st Ed., HarperCollins College Publishers, 1995.

Su (Geylan) YS, Isgor B, Coban T, Kapucuoglu N, Aydıntug S, Iscan M, Iscan M a Guray T. Comparison of NAT1, NAT2 & GSTT1-1 activities in normal and neoplastic human breast tissues. *Neoplasma*, 2006; 53: 73-78.

Towbin H, Staehelin T, Gordon J. Electrophoretic transfer of proteins from polyacrylamide gels to nitrocellulose sheets: Procedure and some applications. *Proc Natl Acad Sci USA* 1979; 76: 4350-4354.

Trepanier LA, Ray K, Winand NJ, Spielberg SP, Cribb AE. Cytosolic arylamine N-acetyltransferase (NAT) deficiency in the dog and other canids due to an absence of NAT genes. *Biochem Pharmacol* 1997; 54: 73-80.

Trepanier LA, Cribb AE, Spielberg SP, Ray K. Deficiency of cytosolic arylamine N-acetylation in the domestic cat and wild felids caused by the presence of a single NAT1-like gene. *Pharmacogenetics* 1998; 8: 169-179.

Upton A, Johnson N, Sandy J, Sim E. Arylamine N-acetyltransferases of mice, men and microorganisms. *Trends Pharmacol Sci* 2001; 22: 140-146.

Vatsis KP, Weber WW, Bell DA, Dupret JM et al. Nomenclature for N-acetyltransferases. *Pharmacogenetics* 1995; 5:1-17.

Wagner ED, Gentle JM, Plewa MJ. Effects of specific monooxygenase and oxidase inhibitors on the activation of 2-aminofluorene by plant cells. *Mutat Res* 1990; 216: 163-167.

Ware JA, Svensson CK. Longitudinal distribution of arylamine N-acetyltransferases in the intestine of hamster, mouse, and rat. Evidence for multiplicity of N-acetyltransferases in the intestine. *Biochem Pharmacol* 1996; 52: 1613-1620.

Ward A, Hickman D, Gordon JW, Sim E. Arylamine N-acetyltransferase in human red blood cells. *Biochem Pharmacol* 1992; 44: 1099-1104.

Warlow RS, Morgan J, Nicola N, Bernard CCA. A non-denaturing vertical isoelectric focusing polyacrylamide slab gel system suitable for silver staining and electrophoretic blotting. *Anal Biochem* 1988;175: 474-481.

Watanabe M, Sofuni T, Nohmi T. Involvement of Cys69 residue in the catalytic mechanism of N-hydroxyarylamine O-acetyltransferase of *Salmonella typhimurium*. Sequence similarity at the amino acid level suggests a common catalytic mechanism of acetyltransferase for *S. typhimurium* and higher organisms. *J Biol Chem* 1992; 267: 8329-8436.

Weber WW, Cohen SN. N-acetylation of drugs: isolation and properties of N-acetyltransferase from rabbit liver. *Mol Pharmacol* 1967; 3: 266-273.

Weber WW, Cohen SN, Steinberg MS. Purification and properties of N-acetyltransferase from mammalian liver. *Annals NY Acad Sci* 1968; 151: 734-741.

Weber WW. N-Acetyltransferase (Mammalian Liver). *Methods Enzymol* 1971; 17: 805-811.

Weber WW. "Acetylation of Drugs" in *Metabolic Conjugation and Metabolic Hydrolysis*, Fishman WH, New York, 1973.

Weber WW, Levy GN, Hein DW. "Acetylation" in *Conjugation Reactions in Drug Metabolism*, Taylor & Francis MGJ, London, 1990.

Weber WW, Vatsis KP. Individual variability in p-aminobenzoic acid N-acetylation by human N-acetyltransferase (NAT1) of peripheral blood. *Pharmacogenetics* 1993; 3: 209-212.

Wellings SR, Jensen HM and Marcum RG. Atlas of subgross pathology of the human breast with special reference to possible precancerous lesions. *J Natl Cancer Inst* 1974; 55: 231.

Whitaker DP and Goosey ME. Purification and properties of the enzyme arylamine N-acetyltransferase from the housefly *Musca Domestica*. *Biochem J* 1993; 295: 149-154.

Williams AJ, Stone EM, Fakis G, Johnson N, Cordell JA et al. N-acetyltransferases, Sulfotransferases, and heterocyclic amine activation in the breast. *Pharmacogenetics* 2001, 11: 373-388.

Zenser TV, Lakshmi VM, Rustan TD, Doll MA, Deitz AC et al. Human N-acetylation of benzidine: role of NAT1 and NAT2. *Cancer Res* 1996; 56: 3941-3947.

Zheng W, Deitz AC, Campbell DR, Wen WQ, Cerhan JR et al. N-acetyltransferase 1 genetic polymorphism, cigarette smoking, well-done meat intake, and breast cancer risk. *Cancer Epidemiol Biomarker Prev* 1999; 8: 223-239.

APPENDIX A

Preparation of Reagents for SDS-PAGE

1) Stock Separating Gel Buffer (1.5 M Tris-HCl, pH 8.8)

36.3 gm Tris base were dissolved in about 100 ml distilled water and pH 8.8 was adjusted with 1 M HCl. Finally, volume is completed to 200 ml.

2) Stock Stacking Gel Buffer (0.5 M Tris-HCl, pH 6.8)

12.1 gm Tris base were dissolved in about 100 ml distilled water and pH 6.8 was adjusted with 1 M HCl. Finally, volume is completed to 200 ml.

3) Stock Gel Solution (Acrylamide-BIS, 30 % T, 2.67 % C)

60 gm acrylamide were dissolved in about 175 ml distilled water and then 1.6 gm BIS (Bis-acrylamide) were added and solution was completed to 200 ml with distilled water. Finally, the solution was filtered through course filter paper.

Note: % T represents acrylamide monomer percent concentration and % C indicates the cross-linking monomer concentration, which was calculated as below:

$$\% T = [(gm \text{ acrylamide} + gm \text{ bisacrylamide}) / \text{total volume}] \times 100$$

$$\% C = [gm \text{ BIS} / (gm \text{ acrylamide} + gm \text{ BIS})] \times 100$$

4) 10 % SDS Solution

10 gm SDS were dissolved in water with gentle stirring and completed to a final volume of 100 ml.

5) Catalyst (10 % Ammonium Persulfate “APS”)

It is prepared freshly by dissolving 100 mg APS in a final volume of 1 ml distilled water.

6) Tracking Dye (0.05 % Bromophenol Blue)

Tracking dye solution was prepared by dissolving 5 mg solid bromophenol blue in a final volume of 10 ml.

7) 5 X Electrode (Running) Buffer (25 mM Tris, 192 mM Glycine, pH 8.3)

Stock running buffer solution was prepared by dissolving and completing 15 gm Tris base, 72 gm glycine to 1 liter distilled water. The pH of the buffer was not adjusted with acid or with base. This buffer was diluted 1:5 and 1 gm solid SDS was added to 1 liter of buffer before use.

8) 4 X Sample Dilution Buffer (SDS Reducing Buffer)

0.25 M Tris-HCl buffer, pH 6.8 containing 8 % SDS, 40 % glycerol, 20 % β -mercaptoethanol, 0.004 % bromophenol blue. It was prepared by mixing the following volumes of given solutions:

2.5 ml	1 M Tris-HCl, pH 6.8
4.0 ml	Glycerol
2.0 ml	2-Mercaptoethanol
0.4 ml	Tracking Dye
0.8 gm	10 % SDS
Distilled water to 10.0 ml	

APPENDIX B

Questionnaire on Breast Cancer Risk Factors

Name of the patient:					
Age:					
Sex: F M					
Occupation:					
Place of Birth:					
Accommodation:					
Education:					
Primary School		High School		University	Graduate Studies
Family History of Cancer					
Yes		None		1. degree relatives	2. degree relatives
Type of Cancer:					
Cigarette Smoking					
Yes		None		1-10 /day	1 pack/day 1 pack/day<
Alcohol Consumption					
Yes		No ne		1 cup/year	1 cup/month 1 cup/day
Red Meat Consumption					
Yes		No ne		Well-done	Medium Half Baked
Consumption: Every /		Day		Week	Month Year
Age of Menarche:					
Age at First Full Term Pregnancy:					
Number of children:					
Miscarriage:					
Breast Feeding:					
Yes		None		3 months	6 months 1 year 1 year<
Doğum kontrol yöntemi:					
Yes		No ne		Birth Control Pill (BCP) Other	
Duration of BCP Usage:			Name of the pill:		
Menopausal State :					
Hormone Treatment:					
Yes		None		Duration of Treatment:	Name of the drug :
Grade of the malignancy:					
Chemotherapy					
Yes		None		Duration of Treatment :	Drugs:
Estrogen Receptor:					
Progesterone Receptor:					

CURRICULUM VITAE

PERSONAL INFORMATION

Surname, Name: Su (Geylan), Y. Senem
Nationality: Turkish (TC)
Date and Place of Birth: 21 December 1974, İstanbul
Marital Status: Married
Phone: +90 216 545 59 97
Fax: +90 312 210 12 89
email: senemsu7@yahoo.com

EDUCATION

Degree	Institution	Year of Graduation
MS	METU Biochemistry	1999
BS	METU Biological Sciences	1996
High School	Doğuş Koleji, İstanbul	1992

WORK EXPERIENCE

Year	Place	Enrollment
1996-2004	METU Biological Sciences	Teaching Assistant

FOREIGN LANGUAGES

Advanced English

PUBLICATIONS

1. Su (Geylan) YS, Isgor B, Coban T, Kapucuoglu N, Aydıntug S, İscan M, İscan M and Guray T. "Comparison of NAT1, NAT2 & GSTT1-1 activities in normal and neoplastic human breast tissues" *Neoplasma* 2006; 53: 73-78.
2. Su (Geylan) YS and Güray TN. *2nd International NAT Workshop*, "Human Breast Arylamine N-acetyltransferases Activities", T9, 2001.
3. Geylan, Y.S., Güray, T.N. and Sak, S., "Arylamine N-acetyltransferase activities in human breast cancer tissues", *Neoplasma*, 48(2), 109-12, 2001.
4. Geylan, Y.S. and Güray, T.N., *4th Xenobiotic Metabolism and Toxicity Workshop of Balkan Countries*, "Characterization of arylamine N-acetyltransferases in tissues from breast cancer", 50, 2000.